2013

Wind farm layout optimization under uncertainty with landowners' financial and noise concerns

Le Chen
Iowa State University

Wind farm layout optimization under uncertainty with landowners' financial and noise concerns

by

Le Chen

A dissertation submitted to the graduate faculty

in partial fulfillment of the requirements for the degree of

DOCTOR OF PHILOSOPHY

Major: Mechanical Engineering

Program of Study Committee:
Erin MacDonald, Major Professor
W. Robert Stephenson
Judy Vance
Baskar Ganapathysubramanian
Eugene S. Takle

Iowa State University

Ames, Iowa

2013

TABLE OF CONTENTS

LIST OF TABLES

LIST OF FIGURES

LIST OF NOMENCLATURE

a	Entrainment constant
a_c	Atmospheric attenuation coefficient
A	Octave-band attenuation
A_{atm}	Attenuation due to atmospheric absorption
A_{bar}	Attenuation due to barriers
A_{div}	Attenuation due to the geometrical divergence
$A_f(j)$	Standard A-weighting
A_{gr}	Attenuation due to the ground effect
A_{misc}	Attenuation due to miscellaneous
$AEP_{tot}(X)$	Farm's total annual energy in MWh
$AEP_i(X)$	Annual energy for turbine i in MWh
c	Cell label, $c \in \{1,144\}$
c_r	Cost-reduction coefficient
C_{a1}	Assembly & installation cost for a single turbine in $
C_{ac}	Annual compensation per MW in 2002 dollars
C_{aot}	Annual operating expenses for a farm in $
C_{b1}	Balance of station cost for a single turbine in $
C_{e1}	Electrical interface/connections cost for a single turbine in $

C_{f1}	Foundation cost for a single turbine in $
C_{ict}	Initial capital cost for a farm in $
C_{ic1}	Initial capital cost for a single turbine in $
C_{llt}	Total land lease cost per year in $
C_{omt}	Levelized operations and maintenance cost for a farm in $
C_{p1}	Engineering $ permits cost for a single turbine in $
C_{r1}	Road & civil work cost for a single turbine in $
C_{rot}	Levelized replacement/overhaul cost for a farm in $
C_{t1}	Transportation cost for a single turbine in $
C_{ts1}	Turbine system cost for a single turbine in $
$C(X)$	Levelized cost per year of a wind farm in $
$COE(X)$	Cost of Energy in $/MWh
COE_i	Cost of Energy for sample i, $i = 1,2,\ldots,n_s$
d	Distance from the source to receiver
d_0	The reference distance
D	Rotor diameter
D_C	Directivity correction
f_i	Objective function i
f_i^*	Optimal value when minimizing objective function i individually
$h_c(X)$	Equality constraint c

h_h	Hub height of a turbine, $h_h = 80m$
h_r	Reference height
$h_0(X)$	Equality constraint
i	Turbine index, $i \in \{1, N\}$
j	An index representing the eight standard octave-band midband frequencies
k	Shaper factor for Weibull distribution
$L(X)$	Total number of landowners who say yes
$L_{fT}(ij)$	Sound pressure level at a receiver location for noise source i and octave-band j
L_{AT}	A-weighted downwind sound power level at a receiver location
L_W	Octave-band sound pressure level for the noise source
L_1	Manhattan metric
L_2	Euclidean metric
L_∞	Chebyshev metric
m_0	Person's initial wealth
$N(X)$	Total number of turbines
n	Number of noise sources
n_s	Number of samples
n_{yes}	Preset number of landowners who say yes, $n_{yes} = 4,5,or6$
N_{LO}	Total number of landowners

$p(u_0, \theta)$	Probability of occurrence for ambient wind speed u_0 in direction θ \
P	Environmental parameters
$P_i(u_i(u_0, \theta))$	Power output of turbine i as a function of effective wind speed of turbine i
P_r	Machine rating of the turbine in KW
P_{tot}	Total power production of the farm
P_{MWi}	Total megawatts installed on the land of landowner i
$PDF(v)$	Probability density function for Weibull distribution
q	Magnitude of the penalty
r_1	Effective downstream radius of the wake
r_{fc}	Fixed charge rate
r_r	Rotor radius
R^2	Correlation coefficient
t	Landowner index, $t \in \{1,9\}$
u_0	Ambient wind speed for turbine i
$u_{0\max}$	Maximum ambient wind speed for turbine i
u_i	Effective wind speed of turbine i in the wake of n upstream turbines
$u_i(u_0, \theta)$	Effective wind speed of turbine i for an ambient wind speed u_0 and a wind direction θ
u_{ij}	Effective downstream wind speed for turbine i affected by the wake of upstream turbine j

u_r	Wind speed at a reference height h_r
U	Landowner's utility function
w_i	Weight assigned to each individual objective
WTA	Minimum annual compensation amount per MW installed that a landowner is willing to accept for signing the lease agreement
WTA_i	Willingness to accept for landowner i
WTA_n	Willingness to accept for noise
$WTA_{n,43}$	Willingness to accept for a landowner at noise level of 43dB
WTA_p	Willingness to accept for participation
X	153 bits binary string design variable
z_0	Surface roughness of ground, $z_0 = 0.25mm$
α	Wind shear exponent
μ_{COE}	Mean value of Cost of Energy
μ_{COE}^*	Optimal mean value if optimize μ_{COE} individually
σ_{COE}	Standard deviation of Cost of Energy
σ_{COE}^*	Optimal mean value if optimize σ_{COE} individually
θ	Wind direction
λ	Scale factor for Weibull distribution
$\varphi(X,c)$	Constraint that a turbine can only be placed in the land cell of an owner who says yes
$\phi(X)$	Penalty function

$\|\cdot\|$ Metric of choice

ACKNOWLEDGEMENTS

I am incredibly fortunate to have Dr. Erin MacDonald as my advisor. She has been making me feel warm and peaceful since my first day at IRIS lab. The endless support and guidance from her have transformed me from a student to a researcher. She taught me the right way to conduct research and write papers, directed me when I got lost, corrected me when I made mistake, and encouraged me when I had progress. Her enthusiasm and ethics for academic research ignited my desires to be an outstanding researcher, and her kindness and patience gave me the feelings of family warmth. I will never forget the warm concerns she expressed when my apartment was flooded in. She cared about my life and allowed me to work remotely so that I can stay with my family. Without her kindness and endless help, my Ph.D. journey cannot be that smooth.

I would like to thank all my committee members: Dr. W. Robert Stephenson, Dr. Judy Vance, Dr. Baskar Ganapathysubramanian and Dr. Eugene S. Takle. They are all supportive and resourceful advisors. The suggestions and directions they provided are vital to my research process.

Also, I would like to thank Dr. Ross Morrow for helping me improve my programming skills. I learned a lot from him on how to formulate an efficient optimization problem and how to write efficient codes.

Thank you, Dr. Anupam Sharma and Dr. Chris Harding, for being the co-authors on the noise model paper. You both actively contributed to the work in Chapter 5. Also, Matthew Galeano contributed to the analysis of agricultural impact of wind farms in Appendix. Thank you for your hard work during the REU program. In addition, thank you,

Drew Robinson, Jacob Uptain, and Sarah Woolf, for your hard work on our project. You conducted great interviews with landowners and developers, and provided me great insights to further my research.

Jinjuan She and Ping Du, I am so lucky to have you as my colleagues in IRIS. Your advices are instrumental for my research process. Our friendship is cherished.

Mom and dad, thank you for your endless love. Thank you, Zhenhua, for being the one and only. Thank you, Evan and little Ethan, for making my life so colorful.

This work was partially support at the Ames Laboratory under contract number DE-AC02-07CH11358 with the U.S. Department of Energy. The document number assigned to this thesis/dissertation is IS-T 3111.

ABSTRACT

Current wind farm layout research focuses on advancing optimization methods. The research includes the assumption that a continuous piece of land is readily available. In reality, landowners' decisions and concerns play a crucial role in wind projects, and some land parcels are more important to project success than others. During early farm development stages, developers must model many important factors, such as wind resource, land availability, topography, and etc. These factors are associated with great uncertainties. In this dissertation, three system-level optimization models, which include landowners' concerns and optimization-under-uncertainty formulation, are developed progressively.

System Model 1 applies a realistic cost model, including landowner remittances, to determine optimal turbine placement under three landowner participation scenarios and two land-plot shapes. The formulation represents landowner participation scenarios as a binary string variable, along with number of turbines. The optimal Cost-of-Energy results are compared to actual Cost-of-Energy data and found to be realistic. System Model 2 advances Model 1 with an optimization-under-uncertainty formulation. A farm layout is optimized under multiple sources of uncertainty including wind shear and farm cost. Landowner participation is represented as uncertain with a novel model of willingness-to-accept compensation. System Model 3 advances Model 2 by modeling landowners' noise concerns and associated compensation. This uncertain model, together with a noise propagation model is then incorporated into the optimization-under-uncertainty system model.

Including uncertain parameters and compensation models leads to a total farm cost estimate that is more accurate than the most current publicly-available model used by the National Renewable Energy Laboratory, which requires the addition of an arbitrary term to match industry-reported Cost-of-Energy data. Additionally, the framework presented here can help developers identify land plots that are worth the extra investment during early farm development. It can provide developers with a robust farm design that is not only profitable but also has minimal noise disturbance for landowners. It can also give landowners an idea of where turbines are likely to be placed, and the likely auditory impacts. This improved transparency-of-information can potentially facilitate the negotiation process between developers and landowners during early farm planning and ultimately improve the success rate of projects.

CHAPTER 1. OVERVIEW

Energy costs, supply uncertainty, and environmental concerns are motivating the United States to develop sources of clean and renewable energy, such as wind energy. The U.S. Department of Energy initiated a collaborative project to investigate a modeled scenario in which wind provides 20% of U.S. electricity by 2030 [1], and identified significant challenges such as reducing the cost of wind energy. This can be addressed, in part, with wind farm layout optimization (WFLO).

To transform wind power to electrical power efficiently, the placement of wind turbines in a wind farm is optimized to maximize capture of wind resource and minimize wake loss and turbulence interactions from multiple turbines [2]. WFLO research has addressed these conflicting goals; for a literature review, see Section 2.1. This research aims to address the WFLO problem using an optimization-under-uncertainty approach with landowners' financial and noise concerns.

1.1. Landowners' Role in Wind Farm Layout Optimization

When the wind farm is being placed on an area of land owned by individual landowners, developers must negotiate with all landowners to get their permission to build turbines on their land. Typically, developers approach landowners communally with an invitation postcard and a public dinner and presentation, for an example see [3]. Next, landowners are approached individually for contract negotiations to lease their land, typically in exchange for monetary compensation. The compensation, also termed remittance fees and land least costs in this dissertation, typically ranges from $1000 to $5000 with an average of $2757 annually per MW installed, as discussed in Section 3.1.3.

Assuming a 1.5MW turbine is placed on the land of a landowner, the landowner can expect to receive an average compensation amount of $4136 annually. The contract permits building on the entire plot of land, within zoning regulations, but with no guarantees on turbine placement. Developers also offer contract riders for specific unfavorable impacts of the project and additional construction, e.g. crop damage, noise disturbance outside of negotiated limits, and road-building. However, the riders have no predictions on the amount of damage or disturbance that will occur. Therefore, landowners must decide whether or not to participate in the project without knowing the exact location of turbines and the associated impacts.

One possible community response to a wind farm is NIMBY (Not In My Backyard), an emotionally complex response. As Wüstenhagen et al. [4] discuss, at first, landowners are excited about the project. As they learn more about the potential downsides of participating in the project, such as impacts on crops and potentially obstructed views, the support for the project decreases. As the project proceeds and the details are finalized, support increases again. This trend is reflected in the associated property values. Hoen et al. [5] find that during the development stages of the wind facility, the value of nearby property decreases. However, when all the construction is completed, the property value increases again. Figure 1.1 illustratively shows the congruent trends identified in these two studies: a dip in acceptance in the time when developers most need acceptance to proceed with project planning. Negotiations between wind developers and landowners can be difficult during this time. Wind developers are unsure of the final design of the farm, and understandably want to keep all options for development available. The contracts they offer landowners are for access to the entire plot of land, with no guarantee on the noise impact,

visual impact, construction impact on crops, or inconvenience during turbine installation and maintenance (beyond what is regulated by applicable zoning laws). Landowners are offered a compensation package that is very difficult to value, as they are given incomplete information on how the turbines will impact their lifestyle and land.

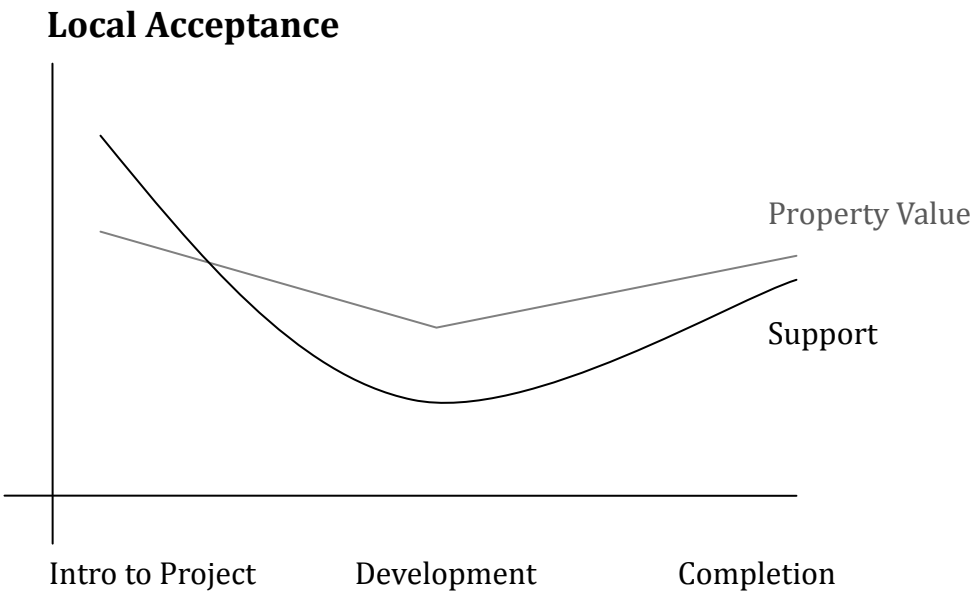

Figure 1.1 Property value and support for wind farm projects have congruent trends [4, 5].

However, landowners must make participation decisions during the early-development stage of a wind farm project. Their decisions and concerns have a great impact on the implementation of the wind farm project, and can lead to project failure [6-10]. Unfortunately, none of the current wind farm layout optimization research has incorporated the participation decisions of landowners. To address this limitation, this dissertation develops a novel Willingness-to-Accept (WTA) utility model with heterogeneous and uncertain parameters to represent the participation decisions of landowners. WTA is typically defined as the minimum monetary amount a decision maker is willing to accept in return for giving up a good or putting up with something unfavorable.

In wind projects, landowners are sellers and developers are buyers. In order for the landowner to be willing to accept the developer's monetary lease agreement, the utility of having turbines plus their associated monetary compensation must be greater than or equal to the utility of not having turbines and not having monetary compensation. The background for the WTA utility theory can be found in Section 2.5.

Due to the confidential nature of the wind industry, the negotiation process and compensation information are not often disclosed to public [11]. According to the Wind Turbine Design Cost and Scaling Model (WTDC&S) from National Renewable Energy Laboratory (NREL) [12], no model is available to predict land lease costs. Therefore, NREL's model only uses a single number to represent the land least costs, as discussed in literature review Section 2.3.1. To address this limitation, this dissertation develops a more realistic cost model, as detailed in Section 3.1.3 of Chapter 3.

1.2. **The Uncertain Characteristics of Wind Farm Layout Optimization**

Researchers typically use Cost-of-Energy (COE) as an objective function to extract the maximum energy for the minimum cost in wind farm layout optimization problem; for a detailed literature review, see Section 2.1. The COE formulation, in which the cost of running the farm is estimated on a yearly basis and divided by the predicted annual energy output of the farm, can estimate the real cost in dollar per unit energy produced. The estimated COE can then be compared with the actual collected market COE data to evaluate the viability of the project. It acts as a universal metric and has various applications. For example, it has been used by Department of Energy (DOE) and research institutes to evaluate the total system impact of any change in turbine design [12] and compare costs

and profitability of different conventional and alternative energy technologies on an equal standing [13]. It has also been used by developers to compare the viability of possible projects.

When placing wind turbines within an available land area, developers must model many important factors, such as wind resource, availability of land, topography, access of roads and transmission lines, and others to predict the COE of a farm. During the early stages of a farm development, i.e. pre-feasibility and feasibility analysis [14], these factors are associated with great uncertainties. Their accuracy is limited by cost and accessibility. For example, developers cannot conduct a full site survey until they have obtained the permission from landowners to access their land.

Although they have limited and uncertain information, developers must make important and expensive decisions, such as placing equipment orders or obtaining funding from potential project backers. Likewise, landowners must decide on their participation in the project without knowing exactly, or even roughly, where turbines will be placed on their land. These decisions have high levels of risk. Therefore, it is important to help wind farm developers and landowners mitigate risk during the early development stages of a wind farm project.

1.3. **Modeling Noise Impact in Wind Farm Layout Optimization**

When deciding whether or not to participate in a wind project, the biggest concerns of landowners are the environmental impacts of the project, e.g. noise disturbance, shadow flicker interference, and visual impact. Among all the environmental impacts, noise disturbance gets most attention due to its annoyance and perceived detrimental impacts on

health. It is believed that noise disturbance could impair people's ability of recovering from daily stress [15], which will ultimately have adverse impacts on health [16-18]. Sometimes, people just simply do not like noise disturbance or think it will reduce their property values, even though the noise is hardly perceivable. In wind farm practices, developers receive complaints or lawsuits about excessive noise and its associated adverse health impacts [19], for an example see [20].

The source noise of a modern wind turbine, which emits from the rotor blades, can range from 98 to 104 dB at a wind speed of 8 m/s [21]. When the turbine noise is propagated into the surrounding environment, the receiver noise level at a location 500 meters away can range from 30 to 40 dB. According to a study conducted by Ambrose and Rand, a community would have a strong desire to stop noise if the noise level they receive is above 43 dB, and have vigorous community action if the noise level is above 49.5 dB [19]. Therefore, it is important to model noise impact in wind farm layout optimization research, especially for the wind farm that is placed on land where individuals are living.

1.4. **Contributions**

This dissertation aims to help wind farm developers and landowners make wise decisions during early development stages of a wind farm project. Figure 1.2 illustrates the major contributions of this work. The first contribution is modeling landowner decisions in the WFLO problem, as detailed in Chapters 3-5, while the second contribution is the development of an optimization-under-uncertainty system model, as introduced in Chapters 4 and 5. The final contribution is the incorporation of realism into the WFLO problem, e.g. developing a realistic COE model (Chapter 3), taking into account realistic

wind scenarios (Chapter 4), and applying the proposed system model to real piece of land with landowners (Chapter 5).

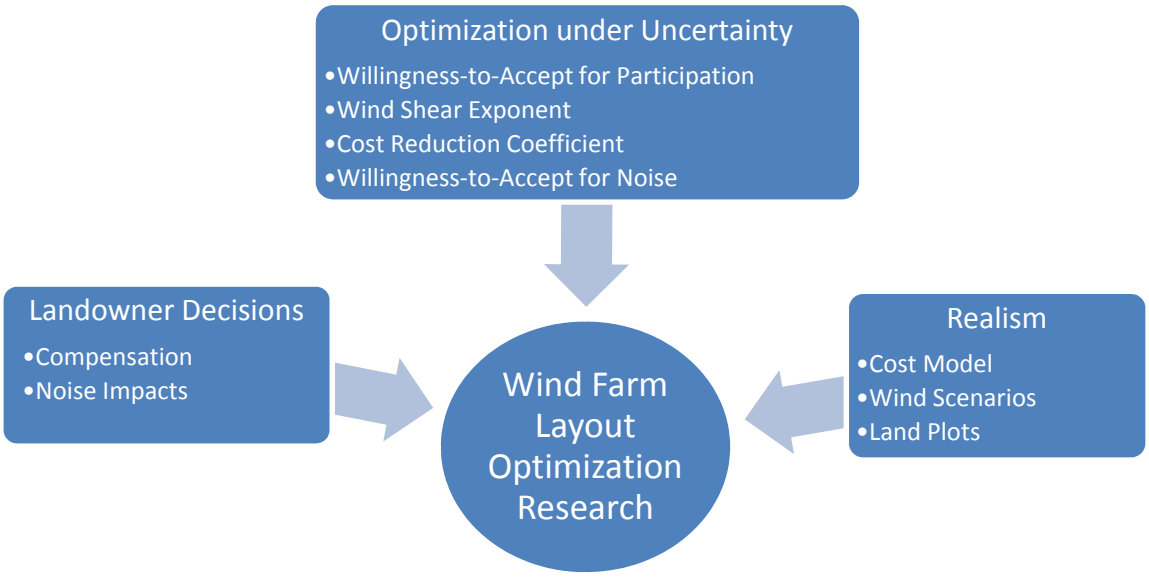

Figure 1.2 Major contributions of this work.

Instead of assuming a continuous piece of land is available for the wind farm construction, as in most layout optimizations, Chapter 3 develops a novel approach that represents landowner participation scenarios as a binary string variable. In addition, unlike other research which uses a pseudo-COE formulation, Chapter 3 develops a realistic COE model and incorporates it into a wind farm layout optimization system model. The system model is tested under two land-plot shapes: equally-sized square land plots and unequal rectangle land plots. The proposed system model can help site developers identify the most crucial land plots for project success and the optimal position of turbines, with realistic estimates of costs and profitability.

Chapter 4 advances the model using an optimization-under-uncertainty approach. An optimization-under-uncertainty system model is developed in this chapter to assist in early-stage wind farm development. A wind farm layout is optimized under multiple sources of uncertainty. Yearly wind data is modeled as aleatory uncertainty using a Weibull distribution. Landowner participation is represented with a novel uncertain model of willingness-to-accept monetary compensation. An uncertain wind shear parameter and economies-of-scale cost reduction parameter are also included. The proposed optimization-under-uncertainty system model can mitigate risks for both wind farm developers and landowners. It demonstrates that even in the uncertain development environment, the work can still help the developer predict the viability of the project with an estimated COE and give landowners an idea of where turbines are likely to be placed on their land.

Chapter 5 further advances the optimization-under-uncertainty system model with landowners' noise concern. Unlike previous research which typically sets farm noise as a constraint or an objective function, Chapter 5 models monetary compensation for noise disturbance with an uncertain willingness-to-accept model for noise, which represents the amount of annual payment in dollar that a landowner is willing to accept to compensate for a certain noise level. The uncertain willingness-to-accept model, together with a noise propagation model and two other important sources of uncertainty, is then incorporated into the optimization-under-uncertainty system model. The advanced system model is tested on a real piece of land in Iowa with 22 landowners and 12 noise receivers (houses). It proves that even in the uncertain development environment, the work can still provide

developers a robust wind farm design that is not only profitable but also has minimal noise disturbance for landowners.

The document proceeds as follows: Chapter 2 provides the literature review and relevant background for this dissertation. Chapter 3 introduces the first system-level COE wind farm layout optimization model with landowner remittances and participation rates, while Chapter 4 details the second system model—an advanced optimization-under-uncertainty model with a realistic model of landowner decisions. The third enhanced optimization-under-uncertainty system model with landowners' noise concern is presented in Chapter 5, and Chapter 6 provides the conclusion.

CHAPTER 2. LITERATURE REVIEW AND RELEVANT BACKGROUND

This chapter provides the literature review and relevant background for this dissertation. Section 2.1 reviews the previous research on Wind Farm Layout Optimization (WFLO) problem and finds out the neglect of landowner issues in the literature. A comprehensive literature review on uncertainty research related to wind energy is provided in Section 2.2, which finds out the lack of uncertainty research on the WFLO problem. Sections 2.3, 2.4, and 2.5 provide the key background for the WFLO problem, optimization under uncertainty, and Willingness-to-Accept utility theory.

2.1. Previous Research on Wind Farm Layout Optimization and the Neglect of Landowner Issues

For a large wind farm project, turbines are always placed in close proximity due to economic considerations, such as the cost of wiring required to transport the generated electricity to the grid. When a turbine in a wind farm is extracting energy from wind, it will develop a turbulent wake that reduces the downstream wind speed [22]. Placing turbines too close together reduces the total energy output. Researchers have studied these conflicting goals, minimizing cost and maximizing energy, in the WFLO problem.

Mosetti et al. are the first to apply computational optimization algorithms to the WFLO problem [23]. They model the wind farm as a discrete 10×10 square grid, where the center of each cell is a potential turbine location. The side length of each cell is set to be 5 rotor diameters (D). The layout of wind turbines is optimized using a genetic algorithm (GA) in order to extract the maximum energy for the minimum installation cost.

Grady et al. replicate Mosetti et al.'s experiments and improve the GA [24]. In their experiment, 600 individuals distributed among 20 subpopulations are set to evolve more than 3000 generations. The optimization results of Grady's work are quite different from those of Mosetti's. As Grady explains, the reason for this difference is that Mosetti et al. only allow 200 individuals to evolve 400 generations; therefore, Grady believes, Mosetti et al.'s work does not run enough individuals for a sufficient number of generations to achieve convergence.

Sisbot et al. use a multi-objective GA approach to obtain an optimal layout of wind turbines by maximizing the power production capacity while constraining the budget of installed turbines [25]. They use an irregular solution space with 100 equal rectangular cells.

Wang et al. investigate the effects of computation grids (e.g. shape of the grids, the arrangement direction of the grids, and the density of grids) on optimization results using GA for a fixed size of wind farm [26]. They find out that the appropriate computational grids are vital to the success of the optimization work, and the optimized layout is firmly restricted by the rationality and accuracy of the computational grids.

A number of researchers introduce other heuristic approaches into the WFLO problem, such as Particle Swarm Optimization [27], Simulated Annealing [28], Greedy Heuristic [29], and Monte Carlo Simulation [30]. However, these approaches have a common shortcoming: the design space is discrete and the turbines can only be placed in the center of each cell [31].

DuPont and Cagan overcome the limitation of the discrete solution space and apply an extended pattern search approach to a continuous solution space [22]. They apply the

pattern search algorithm to develop a two-dimensional layout for a given number of turbines. They have a similar objective function as Mosetti et al.'s, which minimizes costs while maximizing the total power output. As the number of turbines N needs to be set prior to the optimization process, the optimization process is required to be run over many different preset $N's$ to determine the optimum, which can be time-consuming for a large wind farm.

Chowdhury et al. also use a continuous solution space [32]. They present a new method of placing turbines in a wind farm, called the Unrestricted Wind Farm Layout Optimization (UWFLO), to achieve maximum farm efficiency. Unlike above-mentioned approaches, which only use identical wind turbines, the UWFLO model investigates the benefits of using turbines with different rotor diameters.

All of the above-mentioned approaches, whether discrete or continuous, focus on advancing the optimization technology and assume land availability as a given parameter. However, as discussed in Section 1.1, landowners play a crucial role in the WFLO problem. A continuous piece of land is not readily available until negotiations with landowners have concluded—and potentially never available, depending on which landowners agree to participate in the project. The availability of land controls, in-part, the final layout of the turbines.

Therefore, this dissertation enhances the information gleaned from optimization results by incorporating the participation decisions of resource-owners (landowners) into the optimization. Using this approach, site developers can know in advance which landowners are most crucial to the success of the project. They can focus most of their time, labor, and resources on recruiting these important landowners. This will ultimately reduce

the failure rate of projects and save time and money. Chapter 3 details the approach to incorporating landowner participation scenarios into the WFLO problem, while Chapter 4 develops a novel willingness-to-accept model to represent landowner decisions and incorporates it into an optimization-under-uncertainty system model. Chapter 5 further advances the optimization-under-uncertainty system model with landowners' noise concern. It develops an uncertain willingness-to-accept model for noise, which represents the minimum amount of annual payment in dollar that a landowner is willing to accept to compensate for a certain noise level.

2.2. **Uncertainty Research Related to Wind Energy and Limitations**

A great number of researchers have investigated the uncertain aspects of wind energy. There are generally four categories for the research:

(1) Uncertainty research on power performance of a wind turbine or a wind farm, e.g. power output, annual energy production, and etc.

(2) Uncertainty research on economic aspects of wind energy, e.g. projected costs, farm revenue, bidding or trading wind energy, and etc.

(3) Uncertainty research on specific wind turbine components, e.g. control system, wind turbine loads, airfoil, and etc.

(4) Uncertainty research on other macro-aspects of wind energy, e.g. entire wind power system in electricity market, transmission network, appraisal of wind project, and etc.

First of all, a variety of research investigates the uncertain characteristics of power performance for wind turbines. Frandsen presents the problem of uncertainty related to

power performance evaluation, which proves that the uncertainty of experimental power curve may easily result in an uncertainty of annual power production of 10% or more [33]. His research recommends that the measured power curve should be accompanied by a rigorous evaluation of uncertainty to facilitate commercial usage of experimental power curve. Ravey and Derrick also work on the uncertainty research of power performance [34]. They use site calibration to reduce the uncertainty in power performance verification of wind turbines in complex terrain. Other researchers, such as Kwon introduces a Monte-Carlo based numerical simulation procedure to evaluate the uncertainty of expected annual energy production caused by the variability of natural wind and power performance [35].

Unlike the above-mentioned research, which only focuses on investigating the uncertainty in power performance for a single turbine, Messac et al. and DuPont et al. study the uncertainty of entire farm performance for the WFLO problem [36]. Messac et al. characterize the uncertainty of annual wind condition using both parametric and nonparametric models, and then propagate the uncertainty into local wind power density and finally into power performance evaluation. DuPont et al., on the other hand, take account the effects of wind shear variability in the WFLO [37].

Secondly, some research studies the uncertain economic aspects of wind energy. For example, Veers studies the effect of uncertainty on projected cost [38], while Walford investigates the uncertainty in wind turbine operation and maintenance costs [39]. Veers further classifies uncertainty into two categories: common versus independent, and suggests that engineers should test and evaluate design assumptions carefully to advance a design from the conceptual stages with high uncertainty to a more mature stage with lower uncertainty [40]. Besides that, Friedman investigates the economic uncertainty of

municipal wind turbine projects, and develops a method to determine the economic returns of a wind proposal [41]. Gomez-Quiles investigates the uncertain revenue of a wind farm caused by price and resource uncertainty, and develops an econometric model to estimate the risks of using limited information to estimate annual revenue [42].

Moreover, other researchers take into account the economic uncertainty of entire electricity markets with integration of wind energy. For example, Usaola and Angarita investigate the optimal bidding of wind energy in uncertain environments [43]. Pinson et al. also take into account the trading of wind energy under uncertainty [44]. They develop a general method to obtain optimal bidding strategies based on probabilistic wind power forecasts, and model the sensitivity a wind power producer may have in order to regulate costs.

Thirdly, the uncertainty research on specific wind turbine components is also a popular topic. Among all the turbine components, the uncertain characteristics of control system are most widely studied. Sloth et al. take into account the design of robust LMI-based controller with parametric uncertainty [45], while Guo et al. include the controlling of a variable-speed wind turbine with uncertain aerodynamic and mechanical parameters [46]. Other researchers, such as Luo et al. work on strategies to smooth wind power fluctuations of wind turbine generator due to wind turbulence [47].

Other components of wind turbines are also studied. For example, Saranyasoontorn and Manuel investigate the uncertainty of wind turbine loads due to uncertainty in inflow turbulence, and find out that the variability in turbine load statistics is generally smaller than the variability in inflow parameters [48], while Ju and Zhang study the robust optimization design of wind turbine airfoil under geometric uncertainty [49].

Finally, various uncertainty research is focused on other macro-aspects of wind energy. For example, a variety of researchers take in account the entire wind power system in electricity markets [50-53]. Among them, Karki and Billinton investigate the cost-effective wind energy utilization for reliable power supply, and propose a simulation technique to determine the appropriate wind power penetration in an existing power system from both the reliability and economic aspects [50], while Usaola develops a method for probabilistic load flow in electricity networks with uncertain wind generation [51]. Ruiz et al. propose a combined approach that uses a stochastic and reserve method for the uncertainty management in the unit commitment problem for the power system with great amount of wind power [52].

Other researchers, such as Toh et al., integrate wind power forecast errors into the expected energy not served formulation, and study the effects of wind energy penetration on system reliability, total cost for energy and reserve procurement for a traditional power system [53]. Other than the entire wind power system, some research also takes into account the transmission network. Yu et al. develop a chance constrained formulation to deal with the uncertainty of load and wind turbine generator in transmission network expansion planning [54].

Wind energy forecasting is also a popular research path. Moehrlen discusses the uncertainty in wind energy forecasting in his Ph.D. dissertation with great details [55], while Lange investigates the uncertainty of wind power prediction with a special focus on the important role of nonlinear power curve [56]. Another uncertainty research area is power project appraisal under uncertainty. Venetsanos et al. proposes a framework for the

appraisal of power projects in uncertain environment within a competitive market environment [57].

General speaking, a great number of research investigates the uncertain characteristics of wind energy. The uncertainty research covers a variety of categories, including power performance, economic aspects, wind turbine components, and other macro-aspects of wind energy. However, among the researchers, only Messac et al. and DuPont et al. consider the uncertain characteristics of the WFLO, and they only take into account a single source of uncertainty. None of the previous work has investigated diversified sources of uncertainty in the WFLO, yet it is this interaction that causes the high levels of risk in early-stage wind farm development decisions. Therefore, Chapter 4 and Chapter 5 address this limitation and take account diversified sources of uncertainty into the WFLO problem. An optimization-under-uncertainty system model is developed to assist in early-stage wind farm development.

2.3. **Key Background for Wind Farm Layout Optimization Problem**

This section provides the key background for the WFLO problem, including the cost model, wake loss model, wind scenarios selection, and typically-used land-plot shapes.

2.3.1. Cost model

Various cost models are available in the literature to estimate the annual cost of a wind farm. Most researchers use a pseudo-cost formulation, taking into account only the cost of total number of turbines, as in [22, 23, 58-60], and ignoring other important costs. There do exist more comprehensive cost models. For example, Şişbot et al. use a cost model for Enercon turbines, which is based on the installation cost and the operational cost [25].

González et al. use a comprehensive cost model, including wind turbine cost, tower cost, foundation cost and auxiliary cost [61]. Zhang et al. develop an onshore wind farm cost model based on response surface using extended radial basis functions [62]. The model can estimate the total annual cost of a wind farm based on the rotor diameter of a turbine, number of turbines in a farm, construction labor cost, management labor cost, and technician labor cost.

Unlike the above-mentioned cost models, which neglect the costs related to landowners totally, the Wind Turbine Design Cost and Scaling Model (WTDC&S) from National Renewable Energy Laboratory (NREL) has included a component for land lease costs [12]. This is the model that forms the basis for the modified cost model used in this dissertation. The WTDC&S model aims to provide reliable cost estimates for both land-based and offshore turbines. It is widely used in the WFLO problem, as it provides the most comprehensive model information in the literature. The model takes into account both the initial capital cost and the annual operating expenses of a turbine. Table 2.1 provides a detailed cost estimates for a land-based 1.5MW baseline turbine from the NREL report [12]. Note that all the costs in the table are estimated on a yearly basis in 2002 dollars.

Table 2.1 Costs estimated from the WTDC&S model for a land-based 1.5MW baseline turbine [12].

Component	Component Cost in Thousand Dollars	Cost Percentage
Initial Capitol Cost	166	76%
• Turbine System Cost	123	57%
• Balance of Station Cost	43	20%
Annual Operating Expenses	51	24%
• Operation and Maintenance Cost	30	14%
• Replacement or Overhaul Cost	16	7%
• Land Least Cost	5	2%

In WTDC&S model, the initial capital cost, which is composed of the turbine system cost and the balance of station cost, is modeled under Wind Partnerships for Advanced Component Technology (WindPACT) projects [12]. The cost estimates are based on turbine rating, rotor diameter, hub height, and other key turbine descriptors. However, the annual operating expenses, which are the sum of the operations and maintenance cost, the replacement or overhaul cost, and the land least cost, are not well estimated in the model. The operation and maintenance cost, as defined in WTDC&S model [12], includes the day-to-day scheduled and unscheduled operations and maintenance expenses of running a farm. The replacement or overhaul cost, on the other hand, is defined as the cost to cover long-term replacements and overhaul of major turbines components, including blades, gearboxes, generators, and etc. Work is underway by NREL to build complicated models for these two cost terms. However, in the current WTDC&S model, NREL only uses two factors, which represent the maintenance and replacement costs per unit energy production respectively, to estimate these two terms. The factors are recommended by the Low Wind Speed Technology (LWST) projects, and will be improved in the future [12].

Similar limitation also applies to the land least cost in the WTDC&S model [12]. NREL believes no model is currently available for better representing land least costs in the literature, so they only use a proposed number, which represent the land least costs per unit energy production, to estimate the total land least costs. NREL admits in the report that the usage of this single number is inappropriate in the long run, but does not plan to develop a more complicated model for the land least costs. NREL also admits in [63] that the COE estimated by the WTDC&S model is not line up with industry estimate, and uses a term called “market price adjustment” to present the difference between the modeled cost

and the industry estimate. To address this limitation, this dissertation develops an enhanced cost model with realistic estimations of land lease costs, as detailed in Section 3.1.3 of Chapter 3. Chapter 4 and Chapter 5 further advance the cost model with the incorporation of uncertain willingness-to-accept monetary compensation amounts for landowner participation and noise disturbance respectively.

2.3.2. Wake loss model

When a turbine is transforming wind energy into electricity, it will produce a turbulent wake that decreases the downstream wind speed [22]. A wake loss model is therefore introduced to determine the effective downstream wind speed with known ambient wind speed and wind direction. In order to determine the optimal positioning of turbines, it is necessary to determine the effects of the wake of a turbine on the wind energy collected by any turbines constructed behind it. Figure 2.1 is a representation of multiple wakes for a circular array of 10 turbines developed by Jensen [64].

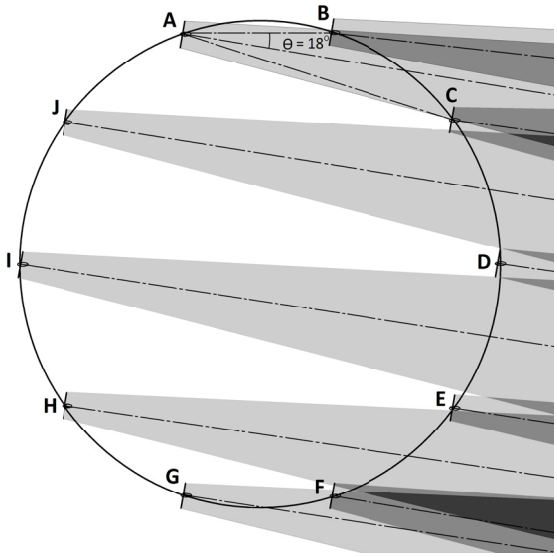

Figure 2.1 Representation of multiple wakes [64].

Note that different wake loss models are available in the literature [61, 65, 66]. Some researchers compared different types of wake models and found out that it was not possible to distinguish any particular model as better than the others in terms of accuracy [67, 68]. For example, Barthelmie et al. evaluated six state-of-the-art wake models against a set of six experiments and found out that although some of the models tended towards high or low prediction, this trend was not consistent among different experimental scenarios [67]. Other researchers, such as Gaumond et al., compared three wake models and found out that the Jensen model might underestimate wake losses for a large wind farm, but would work well for a small wind farm when there are less than 10 turbines in a row [69]. As this problem has a relatively small wind farm and no particular model is proven to be better than others, the author decided to use the Jensen wake model [64] (Figure 2.2), which is frequently used by researchers [2, 22, 23, 58] and straight-forward to implement.

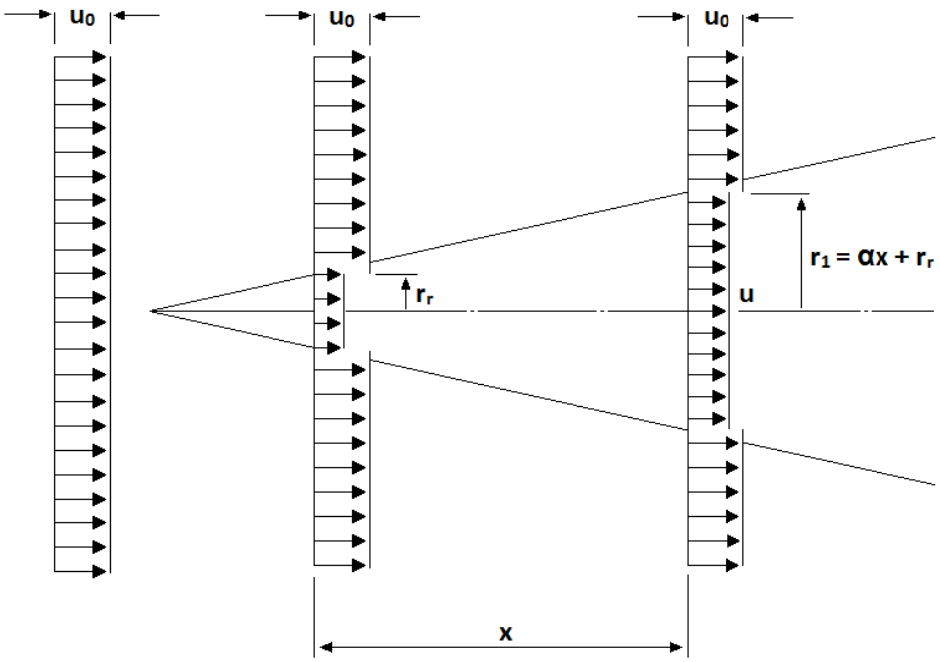

Figure 2.2 Jensen's Wake Loss Model [2, 22, 23, 58].

Figure 2.2 illustrates Jensen's wake loss model [2, 22, 23, 58]. The wind is blowing from left to right with ambient wind speed u_0 -- in Jensen's model, this is the wind speed of a turbine that is not in the wake of any other turbines. Note that some turbines in Figure 2.1 are not in the wake of any other turbine, like H, some are downstream of one turbine, like B, and some are downstream of multiple turbines, like E.

After establishing a momentum balance and assuming that "the wind speed directly behind the rotor is approximately one-third of the oncoming wind speed" [22, 64], the following equation is derived to determine the downstream wind speed u_{ij} of turbine i affected by the wake of upstream turbine j [22, 64]:

$$u_{ij} = u_0\left(1 - \frac{2}{3}\left(\frac{r_r}{r_1}\right)^2\right) \tag{2.1}$$

Where r_r stands for the rotor radius, r_1 refers to the effective downstream radius of the wake, and u_{ij} is the effective downstream wind speed of turbine i in the wake of upstream turbine j at distance x [22]. To solve for u_{ij}, Jensen's wake model further assumes that r_1 and downstream distance x follow a linear relationship as shown by the triangular wake in Figure 2.2 and Equations (2.2) [22, 64], in which h_h is hub height (80m), z_0 is surface roughness, and a is the entrainment constraint.

$$r_1 = r_r + ax \tag{2.2}$$

$$a = \frac{0.5}{\ln(h_h / z_0)} \tag{2.3}$$

Figure 2.3 graphs the wind speed reduction in the wake of a single turbine, following the assumptions of Jensen's model.

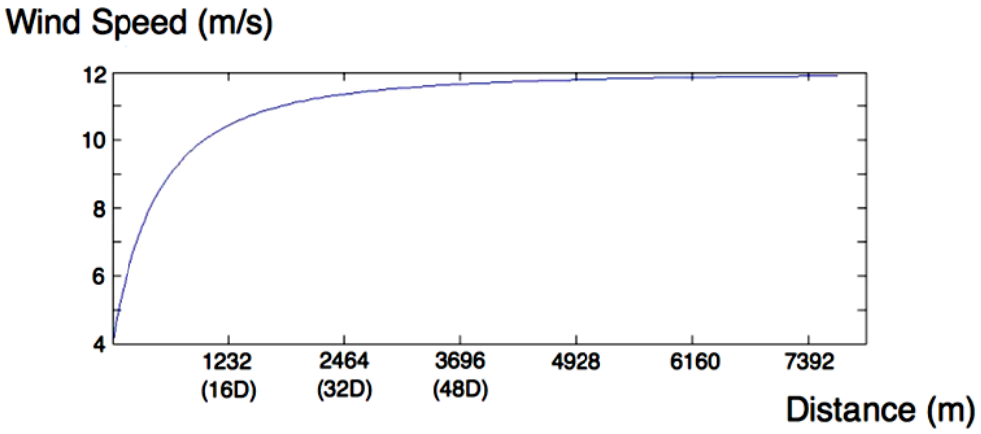

Figure 2.3 Wind speed reduction within a wake [22].

In the case that a downstream turbine is placed in the wakes of several upstream turbines, the kinetic energy deficit of multiple wakes is assumed to be equal to the sum of the energy deficit [22, 23]. The resulting effective downstream wind speed u_i for turbine i in the wake of n upstream turbines can be calculated using the following formula:

$$u_i = u_0\left[1 - \sqrt{\sum_{j=1}^{n}(1-\frac{u_{ij}}{u_0})^2}\right] \tag{2.4}$$

2.3.3. Wind scenarios

Different representations of wind scenarios are available in the literature. Most researchers apply the WFLO problem to two simple wind scenarios: 1) unidirectional uniform wind of 12 m/s, and (2) multidirectional non-uniform wind from 36 angular directions with variable wind speed – 8 m/s, 12 m/s, and 17 m/s [22, 23, 58, 70, 71]. However, the wind speeds in these two scenarios, which range from 8 m/s to 17 m/s, are very optimistic compared to the real world wind data. To address this limitation, the work

uses the wind scenarios with varying wind speed from 6 m/s to 8 m/s in Chapter 3, which is recommended by the NREL report [72].

There are also more complex wind models available. For example, Zhang et al. develop a multivariate and multimodal wind distribution model based on kernel density estimation [73], while Erdem and Shi construct and compare seven bivariate wind models [74]. Morgan et al. and Carta et al. conduct comprehensive reviews on the available wind models, and find out the most-commonly used Weibull distribution can fit most wind data well [75, 76]. Therefore, the author decided to use Weibull distribution to model the real one year data from Iowa Environment Mesonet in Chapter 4 and Chapter 5. The selected wind model provides a realistic estimation of the wind condition in Iowa, as detailed in section 4.2.1. The probability density function (PDF) of Weibull distribution for wind speed v is a function depending on the shape factor k and the scale factor λ [77]:

$$PDF(v)=\frac{k}{\lambda}\left(\frac{v}{\lambda}\right)^{k-1}e^{-\left(\frac{v}{\lambda}\right)^{k}} \tag{2.5}$$

2.3.4. Land-plot shapes

Different land-plot shapes are tested in the literature. Most researchers use a regular square plot of land to implement the optimization model [22, 23, 58, 59, 71, 78, 79], while Sisbot et al. use an irregular plot of land [80]. However, none of the previous research addresses the real land plot with real landowners. In this dissertation, the author first applies the system model to two different land-plot shapes: equally-sized square land plots and unequal rectangle land plots, as detailed in Section 3.1. Then, a real piece of land in Iowa with 22 landowners and 12 noise receivers (houses) is used to test the feasibility of

the proposed optimization-under-uncertainty system model, as detailed in Section 5.5.1 of Chapter 5.

2.4. **Key Background for Optimization under Uncertainty**

Many engineering projects require important decisions during early stages of development with access to limited or uncertain knowledge [81]. One criticism of engineering design optimization is that the optimal solutions are not robust to perturbations in design parameters or other uncertainties [82]. Optimization under uncertainty addresses this criticism.

In engineering decision analysis, uncertainty is regarded as "the state where a decision-maker cannot accurately predict the outcome of an event" [81]. In design optimization, uncertainty can be defined as "the incompleteness in knowledge and the inherent variability of the system and its environment" [83]. Treatment of uncertainty falls under two categories [82, 83]:

(1) Robust design optimization focuses on "making the design inert to the variations of system input through optimizing mean performance of the system and minimizing its variance simultaneously" [84]. It improves the quality of a product by minimizing the consequences of the variations without eliminating the causes [85-88].

(2) Reliability-based design optimization focuses on emphasizing "high reliability of a design by ensuring the probabilistic constraint satisfaction at desired levels" [84]. It maintains the design feasibility for design constraints at expected probabilistic level [86].

Wind farms have many sources of uncertainty. During development, most sources of uncertainty are epistemic due to the lack-of-knowledge of parameters, such as availability of land, wind resource, and topographical conditions. There also is aleatory uncertainty in some parameters due to the inherent variability, such as fluctuating wind conditions, that does not resolve as development progresses. These are all examples of environmental parameters. Chapter 4 and Chapter 5 address both lack-of-knowledge and inherent uncertainty of environmental parameters. Though the focus is on specific incidences of the former, the latter is addressed by modeling wind conditions as a Weibull distribution, see Section 4.2.1. Wind farms also have uncertainty in mechanical engineering system performance, which could be addressed through reliability-based design, but is not addressed in this research.

The overall procedure for optimization under uncertainty is shown in Figure 2.4 [81, 83]. The first step is to mathematically model the deterministic design problem. Then, sensitivity analysis is conducted to identify the most important uncertain variables or parameters. Finally, the important uncertain variables or parameters are classified and quantified. The next step is to model uncertainty propagation, which aims to propagate the input uncertainties through the design problem/system formulation and analyze the resulting uncertainty characteristics of the output(s) [83].

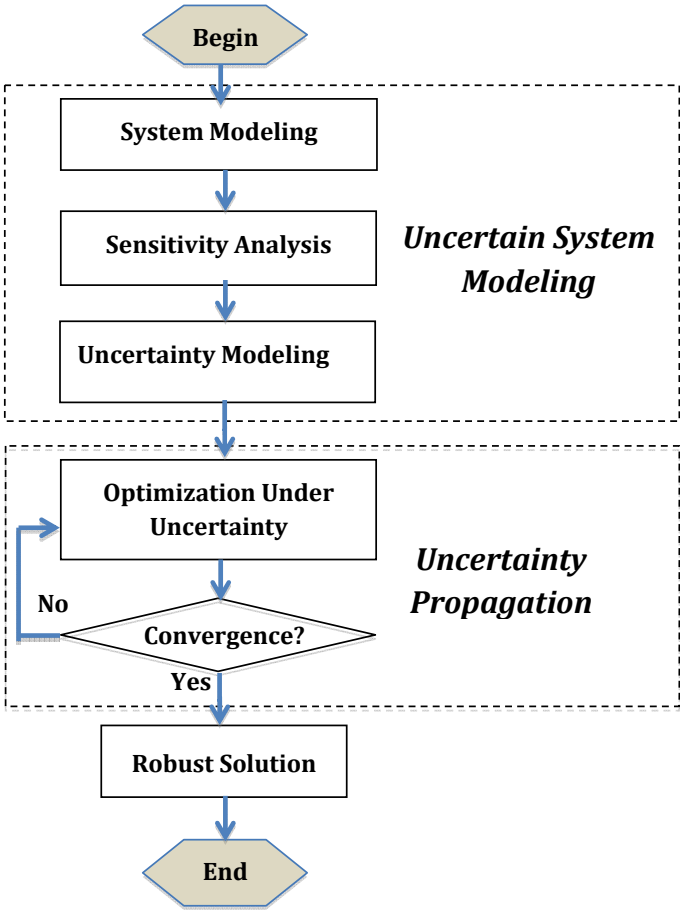

Figure 2.4 Optimization under uncertainty procedure [81, 83].

2.4.1. Modeling Uncertainties

Once uncertainties are identified and classified, sensitivity analysis eliminates unimportant uncertainties and simplifies the optimization problem. Sensitivity analysis expresses uncertainties as simple representations and varies them in intervals, one at a time, to find the resulting intervals of the system output [81]. The results of sensitivity analysis can be represented in a tornado diagram to identify the most important uncertainties [89]. Optimization under uncertainty then concentrates on these important uncertainties. In this dissertation, Probability Theory [83] is used to model the important

uncertain parameters as random variables. Due to lack-of-knowledge in early wind-farm development, sufficient data are not available to quantify the uncertain parameters as probabilistic distributions. Therefore, the reasonable range of each uncertain parameter is divided into several intervals with assigned probabilities (probability distribution uniform within each interval), as discussed in Section 4.2 of Chapter 4.

2.4.2. Uncertainty Propagation

The next challenge is to efficiently represent the effect of uncertainty on the system output [90]. Uncertainty propagation is introduced to quantify uncertainty characteristics of system output due to input uncertainties. There are three typical computational simulation approaches for modeling uncertainty propagation: Taylor Series Approximation, Meta-Model Approach, and Sampling Based Method [83]. Sampling Based Method, which performs repeated sampling and simulation over the uncertain parameters for given design variables, is most widely used [82, 83, 91, 92]. Common sampling methods include: Monte Carlo Method [92], Importance Sampling [93], and Latin Hypercube Sampling [83, 93, 94], the most generalized approach. It can be viewed as a compromise method that incorporates the benefits of Monte Carlo Method and Importance Sampling [93]. It is effective with computationally-demanding models, as its efficient stratification properties can propagate uncertainty with relatively small sample size [83, 93, 94]. This dissertation uses Latin Hypercube Sampling, as detailed in Section 4.3 of Chapter 4.

2.5. **Background for Willingness-to-Accept Utility Model**

In economics, utility theory assumes that a person's preference can be presented in numerically useful ways [95]. The notion of utility, which is a measure of value or welfare,

can represent a person's preferences over a set of choices [96]. Maximum utility theory, which was made famous by Jeremy Bentham [97], assumes the decision makers are rational, e.g. they can make decisions to maximize the subjective utility. In consumer economics, various utility-based theories are available to represent consumer preferences. Among them, the reference-dependent theory, proposed by Tversky and Kahneman [98], is well acknowledged. The theory believes that "individuals understand the options in decision problems as gains or losses relative to a reference point" [99], where the reference point refers to the current position of the individual.

Consider a decision maker who is endowed with two goods i and j. The initial quantities of the two goods are represented by g_i^0 and g_j^0. The Willingness to Pay (WTP) and Willingness to Accept (WTA) are defined as follows in Utility theory [99]:

(1) Willingness to Pay $WTP_{ji}(g_i^0, g_i^{'}, g_j^0)$ is the maximum amount of good j that a decision maker is willing to give up in return for an increase of the quantity of good i from g_i^0 to $g_i^{'}$;

(2) Willingness to Accept $WTA_{ji}(g_i^0, g_i^{'}, g_j^0)$ is the minimum amount of good j that a decision maker is willing to accept in return for a decrease of the quantity of good i from g_i^0 to $g_i^{'}$.

When applying the reference-dependent theory to WTP and WTA measures, the following two utility functions can be obtained [98, 99]:

$$U[g_i^{'}, g_j^0 - WTP_{ji}(g_i^0, g_i^{'}, g_j^0)] = U(g_i^0, g_j^0) \tag{2.6}$$

$$U[g_i^{'}, g_j^0 + WTA_{ji}(g_i^0, g_i^{'}, g_j^0)] = U(g_i^0, g_j^0) \tag{2.7}$$

Here U is a decision maker's utility function. It can be measured relatively in the presence of choices, but has no absolute scale [100].

In wind projects, landowners are sellers and developers are buyers. Landowners are endowed with two "goods": wealth and peaceful living environment. When they decide to sign the lease agreement with developers, their wealth will increase due to the monetary compensation. In return, their living environment will be impaired due to the presence of wind turbines. As the living environment cannot be quantitatively presented, the conventional utility functions, as shown in Equations (2.6) and (2.7), are inappropriate for modeling landowners' decisions. In section 4.2.2, a novel WTA utility model for landowners, which includes a binary variable to represent the change of living environment, is developed.

The WTP and WTA utility models are widely-studied in the literature. Researchers aim to estimate the WTP or WTA measures in various applications, for examples see [101-103]. The difference between WTP and WTA has also been investigated; for a detailed review, see [104]. The WTP and WTA utility models have certain limitations. The models are based on the fundamental assumption that the decision makers are rational, which is not always the case. For example, the WTP for a new piece of land is likely to be lower than the WTA for the sale of an *identical* piece of land already owned, a common phenomenon called the endowment effect [105].

A variety of researchers have investigated the extent to which decision makers behave as predicted by utility models [106], and determined they are frequently violated. In

wind projects, it is not possible for all the landowners to be rational, as these decisions are sometimes emotional and always complex. Sometimes, landowners are not willing to sign the lease agreement, no matter how much compensation they will receive, just because their neighbor or someone they respect decides not to sign. Alternatively, there have been cases of acrimonious neighbors in which one will sign and the other will make the opposite decision, no matter the compensation offered. The flexible model presented in this dissertation allows developers to exclude certain plots of land, or model necessary compensation as unreasonably high, in order to plan with landowners that do not want to have turbines on their land under any circumstance. Additionally, landowners' compensation acceptance values are represented as uncertain and estimated by developers, whereas a purely rational model would represent these quantities as certain and simply equal to the associated cost of crop losses and noise annoyance.

CHAPTER 3. MODEL 1: A SYSTEM-LEVEL COST-OF-ENERGY WIND FARM LAYOUT OPTIMIZATION MODEL WITH LANDOWNER REMITTANCES AND PARTICIPATION RATES

Current wind farm layout optimization research focuses on advancing optimization methods. The research includes the assumption that a continuous piece of land is readily available. In reality, wind farm development projects rely on the permission of landowners for success. When a viable wind farm site location is identified, local residents are approached for permission to build turbines on their land, typically in exchange for monetary compensation. Although "landowner acquisition," as it is called in the industry, plays a crucial role in the development of a wind farm, it has not been analyzed in layout optimization research. The scope of this chapter is focused on incorporating landowner participation scenarios into the Wind Farm Layout Optimization (WFLO) problem. The proposed system model aims to help developers identify the most crucial land plots for project success and the optimal positions of turbines, with realistic estimates of costs and profitability.

Based on interviews with landowners and representatives from small- and large-scale developers, the author found that more information earlier in the development process would lead to smoother negotiations. For example, it would be helpful to developers, and also to landowners, to have an understanding of where turbines will be placed earlier in the wind farm development timeline. This could be done using the WFLO. Yet, one important assumption included in the WFLO research is that all of the land in a given region is readily available for use. In reality, a continuous piece of land is not readily

available until negotiations with landowners have concluded—and potentially never available, depending on which landowners agree to participate in the project. The availability of land controls, in-part, the final layout of the turbines.

Developers also need an accurate prediction of a project's financial viability, or Cost-of-Energy (COE). Minimizing COE, which aims to generate the maximum amount of energy with minimum cost, is often represented in the objective function of a WFLO as a pseudo-COE formulation, taking into account only the cost of total number of turbines, as in [22, 23, 58-60], and ignoring other important costs. To address this limitation, the work uses a more realistic COE formulation, in which the cost of running the farm is estimated on a yearly basis and divided by the predicted annual energy output of the farm, to estimate the real cost in dollar per unit energy produced. The estimated COE can then be compared with the actual collected market COE data to evaluate the viability of the project.

This chapter relaxes the assumption that a continuous piece of land is available, developing a novel approach that includes a model of landowner participation rates. Unlike other research which uses a pseudo-COE formulation, this chapter develops a realistic COE model and tests the system model under two land-plot shapes: equally-sized square land plots and unequal rectangle land plots. Chapter 3 proceeds as follows: Section 3.1 details the formulation of the optimization problem, while Section 3.2 presents the optimization solution and results. Finally, the discussion and conclusion are offered in Section 3.3.

3.1. **Problem formulation**

The problem aims to help a site developer identify which land plots are most crucial to minimizing the COE under certain landowner participation rates. It assumes that wind farm developers can estimate from experience the approximate landowner participation rate. The problem applies to an area of land 3696 by 3696 meters, divided into nine plots. Two land-plot shapes are tested in the problem: (i) nine landowners with equally-sized square plots of land, as shown in Figure 3.1; and (ii) nine landowners with unequal rectangle plots of land, as shown in Figure 3.2.

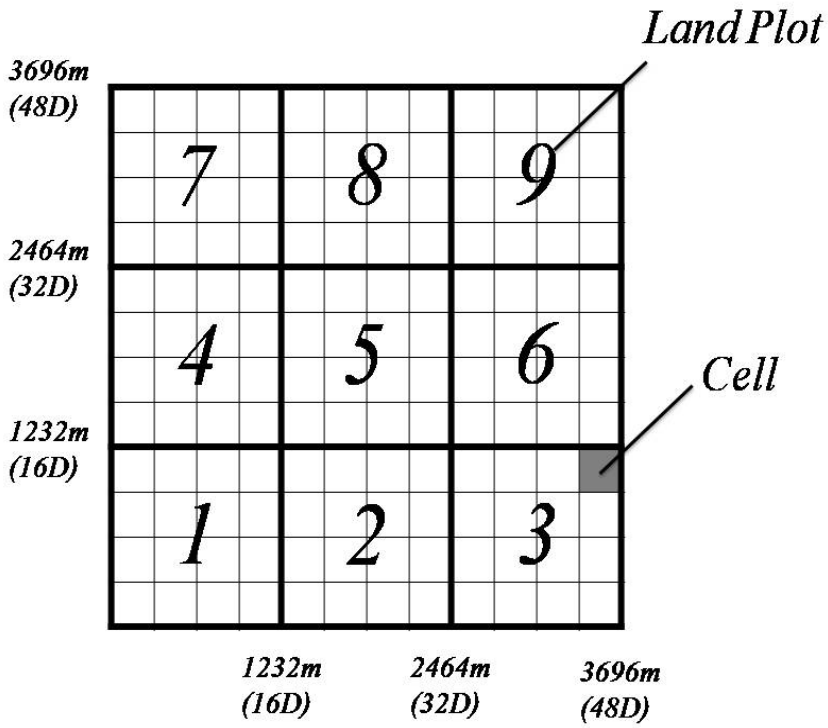

Figure 3.1 The land is divided amongst nine landowners with equally-sized square plots.

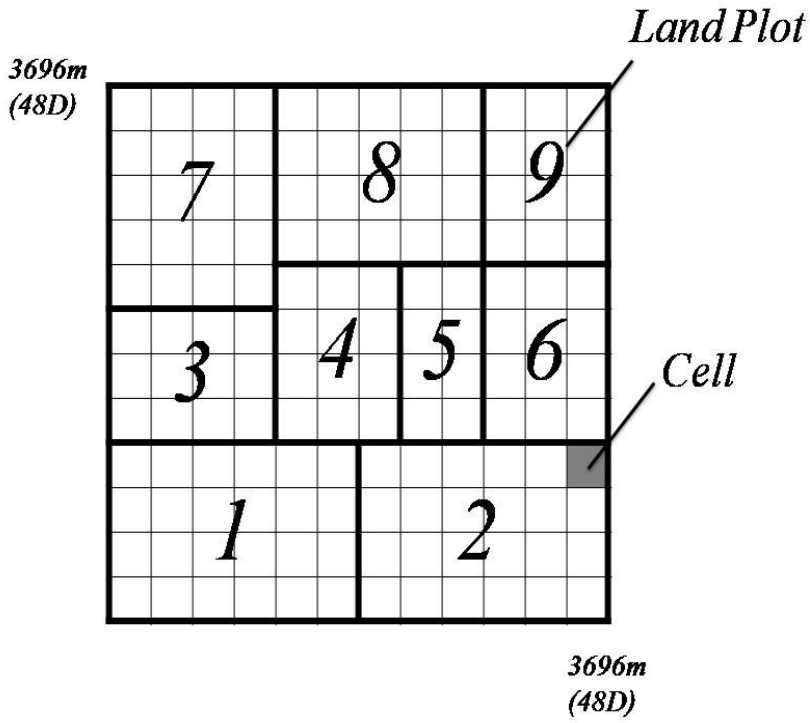

Figure 3.2 The land is divided amongst nine landowners with unequal rectangle plots.

Land-plot shape (i) has equal square plots (1.52 square kilometers). This is reasonable for an Iowa farm, where the average plot is 1.34 square kilometers [107]. Each plot of land is further divided into 16 cells, and wind turbines can only be placed in the center of each cell, the rational for this is discussed in Assumption 2 below. Land-plot shape (ii) has different land-plot shapes and sizes, ranging from 0.76 square kilometers to 2.28 square kilometers.

3.1.1. Assumption explained

Assumption 1: The farm will use GE1.5sle turbines with a rotor diameter of 77m and hub height of 80m.

Assumption 2: At least four rotor diameters (4D, 308m) are required to separate any two turbines in the wind farm to reduce wake interactions [78]. In order to implement

this assumption, the wind farm is divided into 144 square cells with a width of 4D. Turbines can only be placed in the center of each cell.

A variety of spacings can be seen in the literature. Most researchers use square cells ($5D \times 5D$ or $4D \times 4D$) [22, 23, 58, 59, 71, 78, 79], while Sisbot et al. use rectangular cells with $8D$ and $2D$ for prevailing wind and crosswind respectively [80]. Wang et al. investigate the effects of computation grids on optimization results and find that "[t]he shapes of computation grids in the optimization of wind turbines should be determined according to the specific wind condition of the wind farms" [26]. In this study, the author assumes the square cells are adequate.

Assumption 3: Two wind scenarios are tested in this chapter: 1) unidirectional uniform wind: a constant wind 7m/s blowing from west to east; and 2) multidirectional non-uniform wind: wind blowing from 36 angular directions with variable wind speed — 6m/s, 7m/s, and 8m/s, as shown in Figure 3.3.

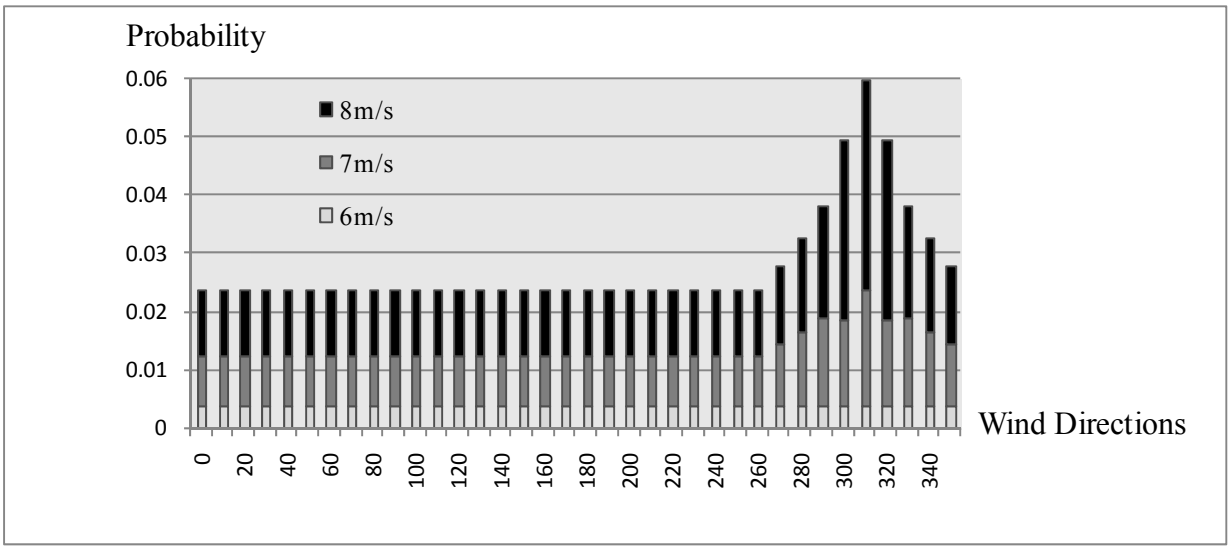

Figure 3.3 Multidirectional Non-uniform Wind Scenario has three wind speeds from 36 angular directions.

The detailed wind distribution for the second wind scenario is shown in Figure 3.3. It is shown that wind speed 6m/s is equally distributed among 36 directions, while wind speeds 7m/s and 8m/s prevail between the directions from 270 to 350 degree.

There are different representations of complex wind scenarios in the literature [22, 23, 58, 61, 71, 73-76]. Here the work varies wind speed from 6 to 8 m/s, as recommended by the NREL report [72]. In implementation, it is straight-forward to modify the formulation with historical wind data, as the author is doing in new research, but is beyond the needs of the demonstration problem presented here.

Assumption 4: The number of landowners who are willing to participate in the project is assumed to be fixed in a given scenario, as estimated from an experienced development company. This study investigates three cases with different landowner participation rates: (a) 4 out of 9 landowners are willing to participate (participation rate of 44%); (b) 5 out of 9 landowners are willing to participate (participation rate of 56%); and (c) 6 out of 9 landowners are willing to participate (participation rate of 67%).

Assumption 5: Land topography is flat with a surface roughness of 0.055m, a reasonable surface roughness for open farmland [108].

3.1.2. Optimization formulation

Figure 3.4 is an overview of optimization formulation. Unlike other research which uses a pseudo-COE formulation, this chapter develops a realistic COE model based on three sub-models: Jensen's wake loss model as introduced in Section 2.3.2 [64], GE turbine's power model as detailed in Section 3.1.4 [109], and the cost model as introduced in Section 3.1.3.

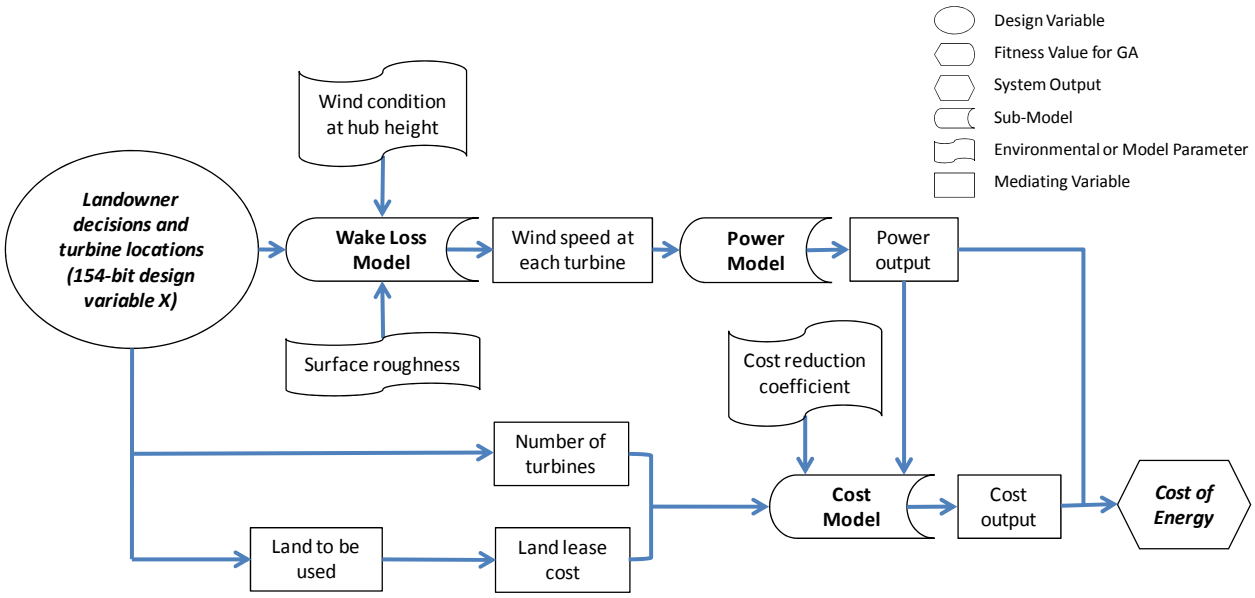

Figure 3.4 Overview of optimization model.

The objective of the optimization model is to identify the most crucial landowners and the optimal positions of turbines for specific wind farm cases in order to minimize costs while maximizing the total energy output. Therefore, instead of using turbine locations and number of turbines as the only design variables, the work also models landowners' decisions as a nine-bit binary string and incorporate it into design variable X. The objective function COE, is defined as:

Minimize:

$$COE(X) = \frac{C(X)}{AEP_{tot}(X)} \tag{3.1}$$

Subject to:

$$h_0(X) = L(X) - n_{yes} = 0 \qquad n_{yes} = 4,5,or,6 \tag{3.2}$$

$$h_c(X) = \varphi(X,c) = 0 \qquad \forall c \in \{1,\ldots,144\} \tag{3.3}$$

Where $COE(X)$ is the cost of energy in \$/MWh; $C(X)$ is the levelized cost per year of a wind farm in dollar, detailed in Section 3.1.3; and $AEP_{tot}(X)$ is the farm's total annual energy in MWh, detailed in Section 3.1.4. X is a 153-bit binary string design variable to indicate landowners' potential decisions for project participation and the potential turbine locations. As shown in Figure 3.5, the first 9 bits of the string indicate the potential decisions of landowners, where "1" represents that the corresponding landowner is willing to participate and "0" represents that they are not. The last 144 bits of the string indicate the potential turbines locations, where "1" represents that the corresponding cell contains a turbine and "0" represents that it does not.

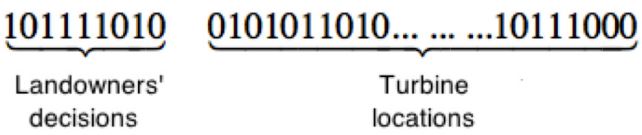

Figure 3.5 Binary string design variable X has 153 bits.

X_k represents the k^{th} bit of binary string X; c is the cell label.

$$\begin{aligned} &For\ 1 \le k \le 9, \\ &\qquad X_k = 0 \quad IFF\ landowner\ k\ says\ no \\ &\qquad X_k = 1 \quad IFF\ landowner\ k\ says\ yes \end{aligned} \tag{3.4}$$

$$\begin{aligned} &For\ 10 \le k \le 153, \\ &\qquad X_k = 0 \quad IFF\ cell\ marked\ c\ does\ not\ contrain\ a\ turbine \\ &\qquad X_k = 1 \quad IFF\ cell\ marked\ c\ contrains\ a\ turbine \end{aligned} \tag{3.5}$$

In Equations (3.2) and (3.3), $h_0(X)$ and $h_c(X)$ are equality constraints, $c \in \{1,\ldots,144\}$. In Equation (3.2), $L(X)$ is a function that depends on the design variable X. It calculates the total number of landowners who say yes that are selected by the optimization program:

$$L(X)=\sum_{k=1}^{9} X_k \tag{3.6}$$

n_{yes} is the parameter representing the number of landowners who agree to participate, which is based on the estimate of landowner participation rates from the wind farm development company.

$\varphi(X,c)$ is a function that depends on the design variable X for a cell marked c. It represents the constraint that a turbine can only be placed in the land cell of an owner who agrees to participate. When a turbine is located in the land cell of a non-participating owner, $\varphi(X,c)=1$; otherwise, $\varphi(X,c)=0$.

Taking the equally-sized square land plots as an example, the detailed problem representation is shown in Figure 3.6.

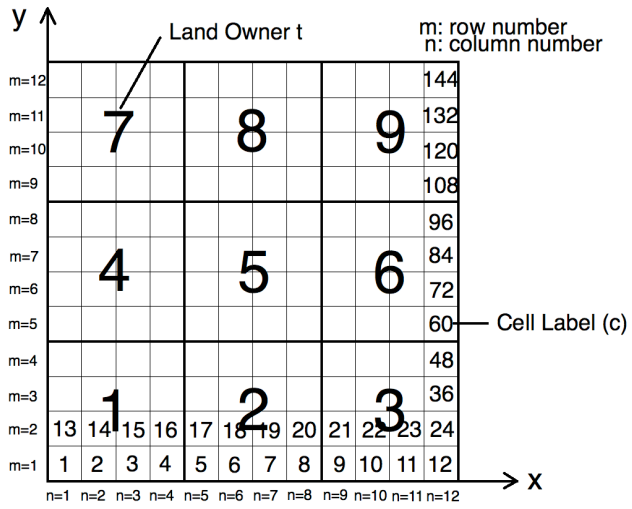

Figure 3.6 Detailed problem representation for equally-sized square land plots.

For the cell marked c, the row number (m) and the column number (n) of cell c can be calculated by:

$$m=\left\lfloor \frac{c-1}{12} \right\rfloor +1 \tag{3.7}$$

$$n = c - (m-1) \times 12 \tag{3.8}$$

Where $\left\lfloor \frac{c-1}{12} \right\rfloor$ refers to the nearest integer less than $\frac{c-1}{12}$. Therefore, the coordinates of a potential turbine in cell c are:

$$(x, y) = (2D + (n-1) \times 4D, 2D + (m-1) \times 4D) \tag{3.9}$$

The landowner who owns cell c can be found by:

$$t = \left\lfloor \frac{n-1}{4} \right\rfloor + 1 + \left\lfloor \frac{m-1}{4} \right\rfloor \times 3 \tag{3.10}$$

Where t is the landowner label as shown in Figure 3.6; m and n are the row number and the column number of cell c which can be calculated using Equations (3.7) and (3.8). Therefore, $\varphi(X, c)$ can be defined as:

$$\varphi(X, c) = \begin{cases} 1 - X_t & when\ X_{c+9} = 1 \\ 0 & when\ X_{c+9} = 0 \end{cases} \tag{3.11}$$

3.1.3. Enhanced cost model

COE is typically calculated on an annual basis using a levelized cost model, the cost to convert the present value of the total cost of building and operating a wind farm over its economic life to equal annual payments [110]. Figure 3.7 presents the overall structure of this model. The annual operating expenses take into account the expenses related to landowner remittance cost, maintenance cost, and levelized replacement and overhaul cost. The initial capital cost, which is levelized over the life of the farm (assumed to be 30 years), includes turbine system cost and the balance-of-station cost. The enhanced cost model is developed based on the NREL WTDC&S model and the Turbine System Cost Report from

Lawrence Berkeley National Laboratory [12, 111], as previously discussed in Section 2.3.1. It includes new model component for a realistic estimation of landowner remittance fees, and incorporates a cost reduction for initial capital costs of a large wind farm.

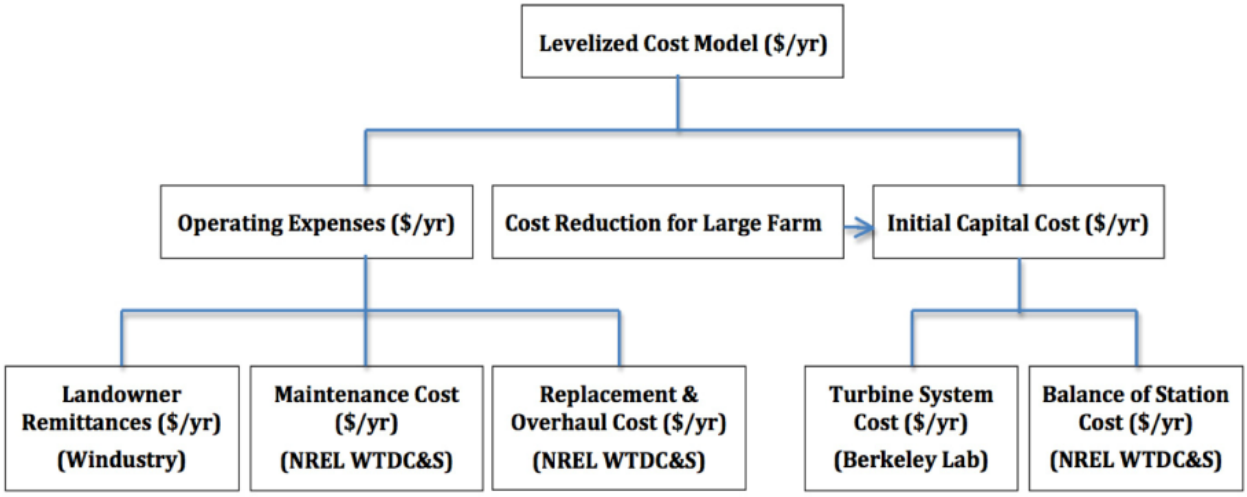

Figure 3.7 Incorporating a realistic estimation of Landowner Remittance Fees into the Levelized Cost Model.

Note that all the costs in this model are based on 2002 dollars. When data from other periods need to be incorporated into the model, they have been escalated or deescalated using the producer price indexes or general inflation index, as indicated in the NREL WTDC&S model [12]. The PPI data, which are sorted by North American Industry Classification System (NAICS) codes, can be obtained through [112]. The general inflation index is based on the Gross Domestic Product (GDP) numbers, which are updated yearly.

The levelized cost per year of a wind farm project is defined as follows:

$$\mathrm{C}(X) = C_{aot}(X) + C_{ict}(X) \tag{3.12}$$

Where $C_{aot}(X)$ is the annual operating expense, $C_{ict}(X)$ is the levelized initial capital cost for the farm, and X is the design variable of the optimization problem, detailed in Section 3.1.2. Each component of this equation will be explained below.

1) Total annual operating expenses including land lease costs

The total annual operating expense for the wind farm, $C_{aot}(X)$, is defined by:

$$C_{aot}(X) = C_{llt}(X) + C_{omt}(X) + C_{rot}(X) \tag{3.13}$$

Where $C_{llt}(X)$ is the total land lease cost per year for a wind farm, $C_{omt}(X)$ is the total maintenance cost per year for a wind farm, and $C_{rot}(X)$ is the total levelized replacement and overhaul cost per year for a wind farm.

2) Land lease cost (remittance fees)

The total annual land lease cost, $C_{llt}(X)$, in dollars, is defined by:

$$C_{llt}(X) = C_{ac} \times P_r \times N(X) \times 10^{-3} \tag{3.14}$$

Where C_{ac} is the annual compensation per MW in 2002 dollars; P_r is the machine rating of the turbine in KW; and $N(X)$ is the total number of turbines, the term $P_r \times N(X) \times 10^{-3}$ calculating the total megawatts installed.

Typically, C_{ac} ranges from \$1000 to \$5000. Table 3.1 summarizes compensation data from twenty-six wind projects from 1998 to 2008. The data comes from Windustry, which gathers wind project easement and lease information from published sources [11]. All of the compensation data are escalated or deescalated to 2002 dollars using the Gross Domestic Product Deflator Inflation Calculator [113]. C_{ac} is set to be \$2757, the average in 2002 dollars of the data in Table 3.1.

Table 3.1 Land Lease Cost in 2002 dollars, adjusted from [11].

Project	Location	Commission Date	Original compensation per MW per year	Compensation per MW per year in 2002 dollars
Iowa Distributed Wind Energy	Iowa	1998	$2400	$2583.6
Lake Benton Ⅰ	Minnesota	1998	$2000	$2153
Delaware Mountain Wind Farm	Texas	1999	$2000	$2125
Storm Lake Ⅰ and Ⅱ	Iowa	1999	$2667	$2833.7
Vancyle Ridge	Oregon	1999	$2272-2667	$2414-2833.7
Waverly Ⅱ	Iowa	1999	$2320	$2465
Madison Windpower	New York	2000	$1212-2424	$1262.3-2524.6
Farmer Project	Minnesota	2001	$2667	$2714.2
Top of Iowa	Iowa	2002	$2667	$2667
Colorado Green	Colorado	2003	$2000-4000	$1967.8-3935.6
High Winds Energy Center	California	2003	$5185	$5101.5
Mendota Hills	Illinois	2003	$2250-2500	$2213.8-2459.8
New Mexico Wind Energy Center	New Mexico	2003	$2700	$2656.5
Woodward	Oklahoma	2003	$2667	$2624.1
Ainsworth Wind Energy Facility	Nebraska	2005	$1515	$1453.2
Crescent Ridge Wind Farm	Illinois	2005	$3030	$2906.4
Trimont Area Wind Farm	Minnesota	2005	$2500-3000	$2398-2877.6
Weatherford Wind Energy Center	Oklahoma	2005	$2040	$1956.8
Big Horn	Washington	2006	$2300	$2173.5
Maple Ridge	New York	2006	$3108	$2937.1
Olive Wind Energy Center Ⅰ and Ⅱ	North Dakota	2006-2007	$3061	$2869.1
Peetz Table Wind Energy Center	Colorado	2007	$3750-4993	$3486-4641.5
Langdon Wind Energy Center	North Dakota	2007-2008	$3144	$2895.2
Ashtabula Wind Energy Center	North Dakota	2008	$5387	$4913.5
Crystal Lake – GE Energy	Iowa	2008	$4000	$3648.4
Smokey Hills Wind Farm	Kansas	2008	$1667	$1520.5

a) Maintenance, and replacement and overhaul costs

The other terms of $C_{aot}(X)$ come from NREL WTDC&S Model [12]. The components include:

$$C_{omt}(X) = 7 \times AEP_{tot}(X) \tag{3.15}$$

$$C_{rot}(X) = 10.7 \times \mathrm{P}_r \times N(X) \tag{3.16}$$

Where $AEP_{tot}(X)$ is the annual energy production for the wind farm in MWh.

3) Levelized initial capital cost for the farm

The levelized initial capital cost for the farm is calculated using Equation (6):

$$\mathrm{C}_{ict}(X) = C_{ic1} \times N(X) \times \left(\frac{2}{3} + \frac{1}{3} e^{-0.00174 N(X)^2}\right) \times r_{fc} \tag{3.17}$$

Where C_{ic1} is the initial capital cost for a single turbine; and r_{fc} is the fixed charge rate.

a) Initial capital cost

The initial capital cost (C_{ic1}) for a single turbine includes the turbine system cost and balance of station cost:

$$\mathrm{C}_{ic1}(X) = C_{ts1} + C_{b1} \tag{3.18}$$

The value of C_{ts1}, turbine system cost, is selected based on a report by Bolinger and Wise at Lawrence Berkeley National Laboratory, which summarizes price data on 81 U.S. wind turbine transactions totaling 23,850 MW announced from 1997 through early 2011 [111]. From this data, the author selects the average turbine price per KW in 2002 (800

\$/KW) to calculate the turbine system cost. The turbine system cost C_{ts1} for a single turbine is defined as:

$$C_{ts1} = 800 \times P_r \tag{3.19}$$

Where C_{ts1} is the cost for one turbine system in dollars and P_r is the machine rating of the turbine in KW.

Note that as the 800 \$/KW comes from large orders and small orders averaged together, the cost of a turbine is potentially underestimated when paired with an economy-of-scale cost-reduction term, detailed below. However, the author chooses this average value as it can present the general turbine price in 2002. It averages the effects of different places of purchase, different market supply and demand situation, for example. To address the limitation of using this value, the author will include an uncertain cost-reduction term to mitigate the risk of underestimation in Chapter 4.

The balance of station cost, C_{b1}, for a single turbine is composed of six parts: foundations C_{f1}, transportation C_{t1}, roads & civil work C_{r1}, assembly & installation C_{a1}, electrical interface/connections C_{e1}, and engineering & permits C_{p1}. The detailed calculation methods for these terms can be found in the NREL WTDC&S Model [12].

b) Economy of scale cost reduction

The term $(\frac{2}{3}+\frac{1}{3}e^{-0.00174\,N(X)^2})$ in Equation (3.17) assumes there is an economy of scale for the initial capital cost of a large wind farm with $N(X)$ turbines, reducing the price of all turbines purchased based on the volume purchased. This cost-reduction term was

first introduced by Mosetti et al., and is widely-used in the literature [22, 23, 58, 60]. The maximum cost reduction is set at $r_{fc} \times C_{ic1} \times N(X) \times \frac{1}{3}$.

c) Fixed charge rate

The fixed charge rate (r_{fc}) is defined as "the annual amount per dollar of initial capital cost needed to cover the capital cost, a return on debt and equity, and various other fixed charges" [12]. It is set to be 0.1158 per year.

3.1.4. Energy model

The farm's total annual energy in MWh can be calculated by:

$$AEP_{tot}(X) = \sum_{i=1}^{N(X)} AEP_i(X) = \sum_{i=1}^{N(X)} \int_{0^o}^{360^o} \int_0^{u_{0\max}} P_i(u_i(u_0,\theta)) \times p(u_0,\theta) \times t \, du_0 d\theta \tag{3.20}$$

Where $AEP_{tot}(X)$ is the farm's total annual energy in MWh; $AEP_i(X)$ is the annual energy for turbine i in MWh; u_0 is the ambient wind speed for turbine i; $u_{0\max}$ is the maximum ambient wind speed for turbine i; θ is the wind direction; t is the total hours in a year; $p(u_0,\theta)$ is the probability of occurrence for ambient wind speed u_0 in direction θ; $u_i(u_0,\theta)$ is the effective wind speed of turbine i for an ambient wind speed u_0 and wind direction θ, detailed in the background introduction for wake loss model in Section 2.3.2. $P_i(u_i(u_0,\theta))$ is the power output of turbine i as a function of the effective wind speed of turbine i, calculated using the power curve of the GE1.5sle as shown below [109].

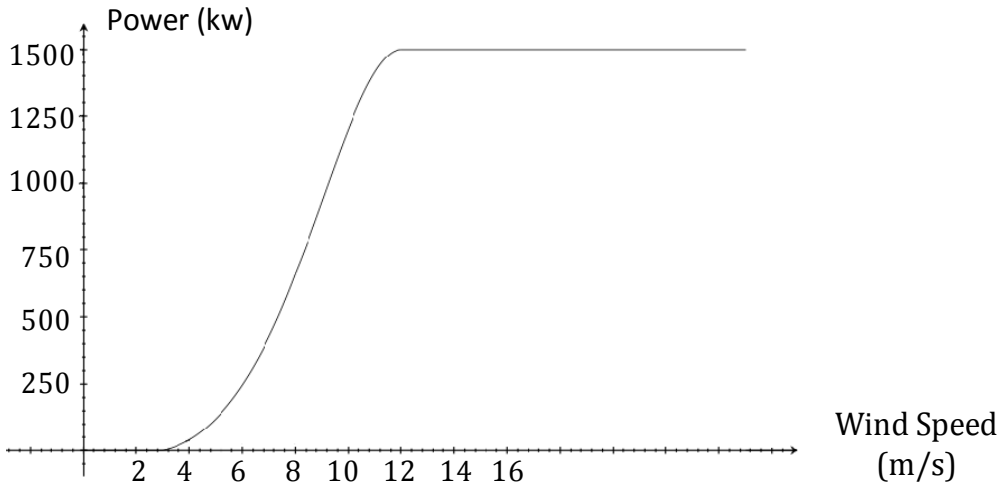

Figure 3.8 Power curve for GE1.5sle [109].

When a turbine is transforming wind energy into electricity, it will produce a turbulent wake that decreases the downstream wind speed [22]. A wake loss model is therefore introduced to determine the effective downstream wind speed with known ambient wind speed and wind direction. As discussed in Section 2.3.2, the author selected from various wake models and decided to use the Jensen wake model [64], which is frequently used by researchers [2, 22, 23, 58] and straight-forward to implement.

As introduced in Section 2.3.2, the downstream wind speed u_{ij} of turbine i affected by the wake of upstream turbine j is determined by [22, 64]:

$$u_{ij} = u_0\left(1 - \frac{2}{3}\left(\frac{r_r}{r_1}\right)^2\right) \tag{3.21}$$

Where r_r is the rotor radius, r_1 is the effective downstream radius of the wake, and u_{ij} is the effective downstream wind speed of turbine i in the wake of upstream turbine j at distance x [22]. To solve for u_{ij}, Jensen's wake model further assumes that [22, 64]:

$$r_1 = r_r + ax \tag{3.22}$$

$$a = \frac{0.5}{\ln(h_h / z_0)} \tag{3.23}$$

Where z is hub height (80m), z_0 is surface roughness, and a is the entrainment constraint.

In the case that a downstream turbine is placed in the wakes of several upstream turbines, we determine the resulting effective downstream wind speed u_i for turbine i in the wake of n upstream turbines by:

$$u_i = u_0\left[1 - \sqrt{\sum_{j=1}^{n}(1 - \frac{u_{ij}}{u_0})^2}\right] \tag{3.24}$$

3.2. **Solution and Results**

3.2.1. Optimization method

GAlib, a C++ library of genetic algorithms (GAs), is used to solve the non-linear constrained optimization problem [114]. Table 3.2 summarizes the detailed parameters. A GA mimics the mechanics of natural selection and survival of the fittest individuals in a heuristic probabilistic search algorithm [58]. GAs have advantages over traditional numerical optimization methods, e.g., GAs do not need to have a differentiable objective function and are less likely to get trapped in a local optimum [115, 116]. As the design variable is a 153-bit binary string, the objective function is non-differentiable and it is possible to have more than one optimal layout (multi-modal). Therefore, using a GA is the most suitable optimization approach.

Table 3.2 Parameters using within GAlib.

Genetic Algorithm Type	GASteadyStateGA
Genome Type	GA1DBinaryStringGenome
Population Size	3000
Generation Number	10000
Crossover Probability	0.9
Mutation Probability	0.01
Replacement Rate	0.5

The GA uses a fitness function to solve optimization problem. It includes two parts: the objective function— $COE(X)$ as in Equation (3.1), and a penalty function $\phi(X)$ for constraints $h_0(X)$ and $h_c(X)$ as in Equations (3.2) and (3.3):

$$\begin{aligned} Fitness &= COE(X) + q \cdot \phi(X) \\ &= COE(X) + q \cdot \left\{ [h_0(X)]^2 + \sum_{c=1}^{144} [h_c(X)]^2 \right\} \end{aligned} \tag{3.25}$$

Where q is a parameter that represents the magnitude of penalty [117]. When q is small, the fitness function is easily minimized, but may result in serious constraint violations; when it is large, all constraints can be easily satisfied, but may yield sub-optimal optimization results. This problem formulation uses a very small q , and the code verifies feasibility after each run; infeasible results are discarded.

3.2.2. Optimization results

For the square land-plot cases, the optimization program is applied to two wind conditions and three landowner participation rates. For the unequal rectangle land-plot cases, one case with the multidirectional non-uniform wind condition and six landowners' participation was investigated. For each of the seven cases, the optimization program ran

more than ten times with 10000 iterations each time, to ensure convergence. The best results for each case are recorded in Table 3.3:

Table 3.3 Results summarized from optimization program.

	Square Land: Unidirectional Uniform Wind			Square Land: Multidirectional Non-uniform Wind			Unequal Rectangle Land: Multidirectional Non-uniform Wind
Case #	Case (i,1,a)	Case (i,1,b)	Case (i,1,c)	Case (i,2,a)	Case (i,2,b)	Case (i,2,c)	Case (ii,2,c)
Landowner Participation	4	5	6	4	5	6	6
COE ($/MWh)	56.72	54.63	52.78	45.95	45.27	44.76	44.40
Energy Output (MWh/yr)	89733	103420	87130	126487	137991	143016	144421
Turbines #	28	32	24	32	35	36	36
Optimal Layouts #	18	9	1	1	1	1	1

For the square land-plot cases with 7m/s unidirectional wind [Cases (i,1,a), (i,1,b), and (i,1,c)], the COE decreases from $56.72 per MWH to $52.78 per MWH when 6 landowners are willing to participate instead of 4. This trend can also be found for the square land-plot cases with multidirectional non-uniform wind [Cases (i,2,a), (i,2,b), and (i,2,c)]—the COE decreases slightly from $45.95 per MWH to $44.76 per MWH with more landowners participating. Across the same participation rates, e.g. Case (i,2,a) compared to Case (i,1,a), the multidirectional non-uniform wind cases have much lower COEs than the unidirectional uniform wind cases as the former have more optimistic wind conditions. The unequal rectangle land-plot Case (ii,2,c) has similar COE, energy output, and number of turbines as the comparable equal-land Case (i,2,c). All cases have unique optimal layouts except for Cases (i,1,a) and (i,1,b). Figures 3.9 through 3.13 represent the example optimal

layouts for the various cases. The unused land plots are represented by grey squares, and the optimized turbine locations are represented by in the figures below:

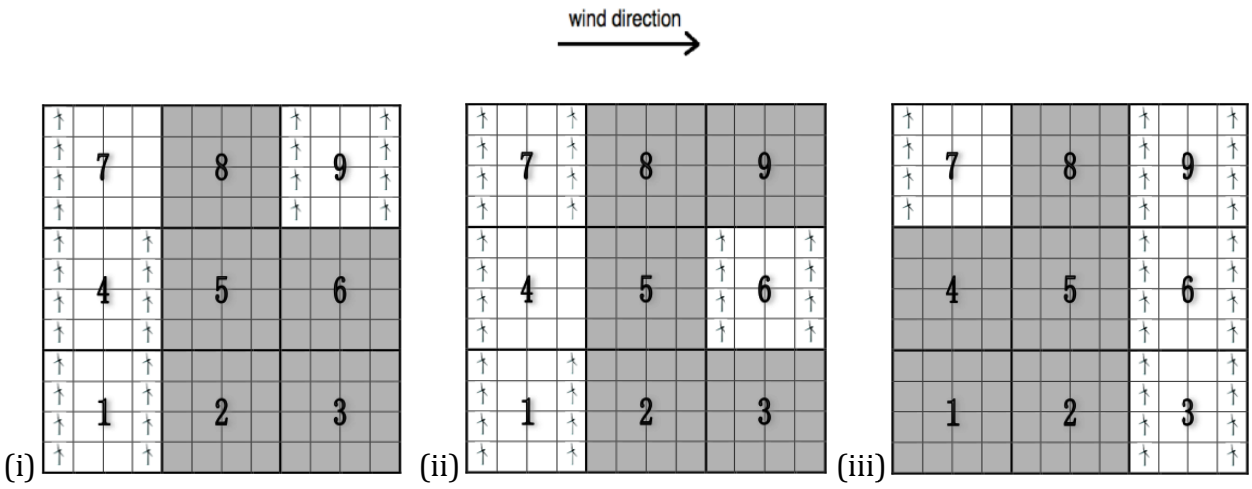

Figure 3.9 Square land, unidirectional uniform wind case (i,1,a) has multiple optimal layouts (example layouts).

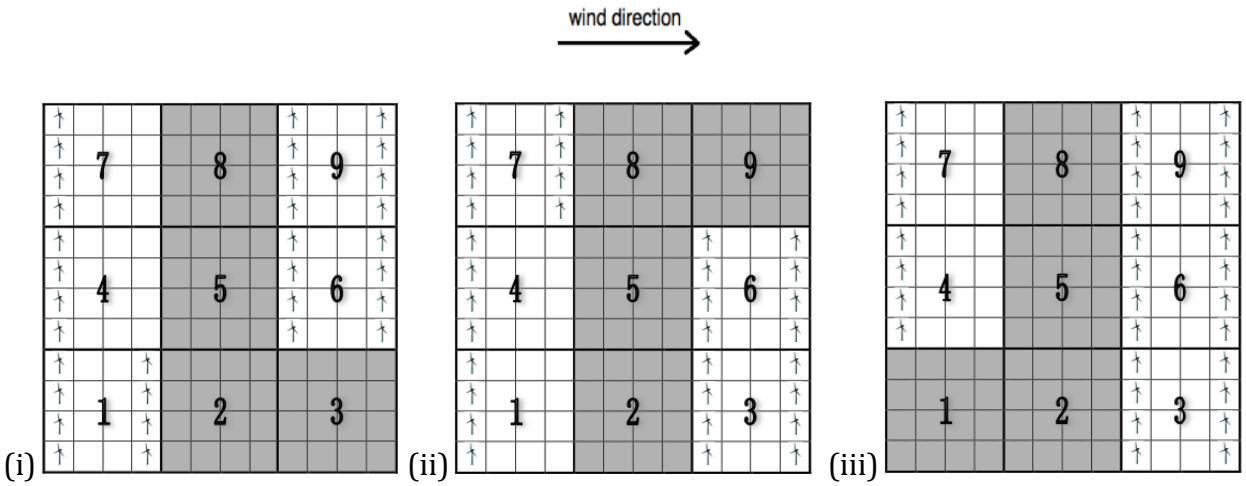

Figure 3.10 Square land, unidirectional uniform wind case (i,1,b) has multiple optimal layouts (example layouts).

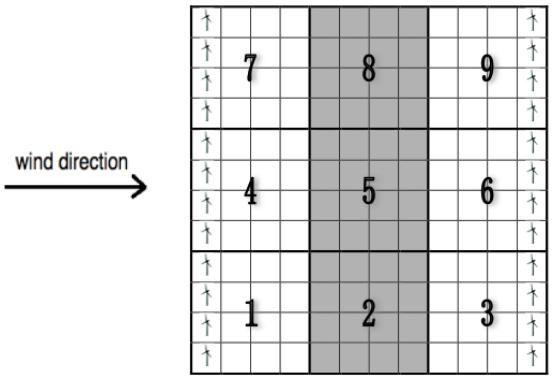

Figure 3.11 Square land, unidirectional uniform wind case (i,1,c) has a unique optimal layout.

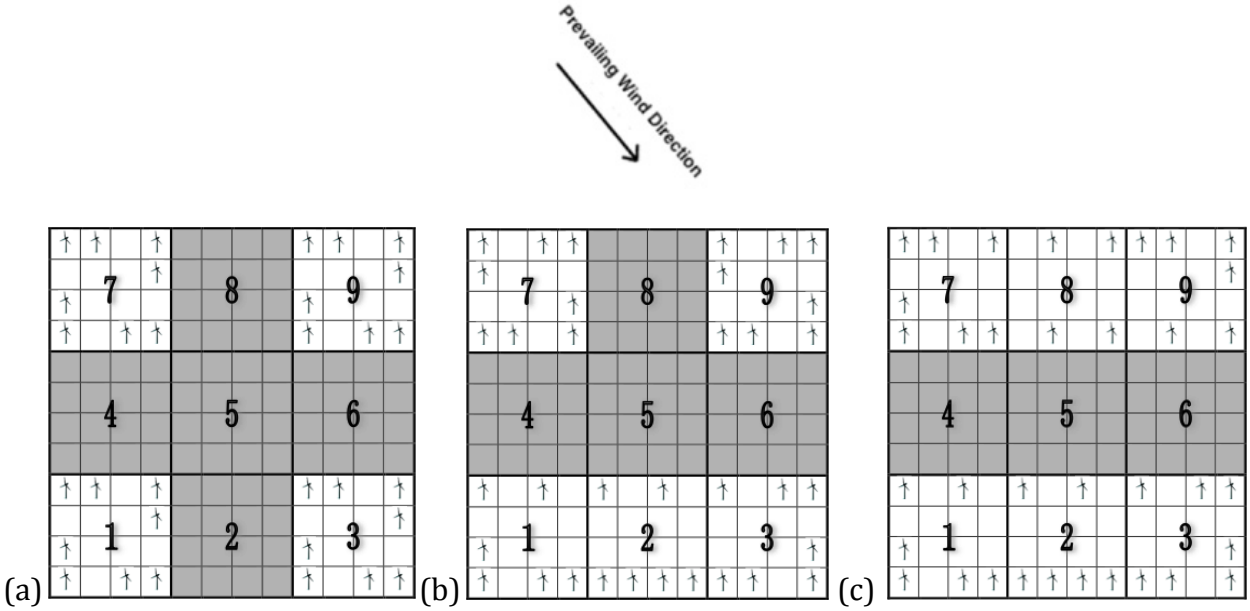

Figure 3.12 Square land, multidirectional non-uniform wind cases (i,2,a), (i,2,b), and (i,2,c) have unique optimal layouts.

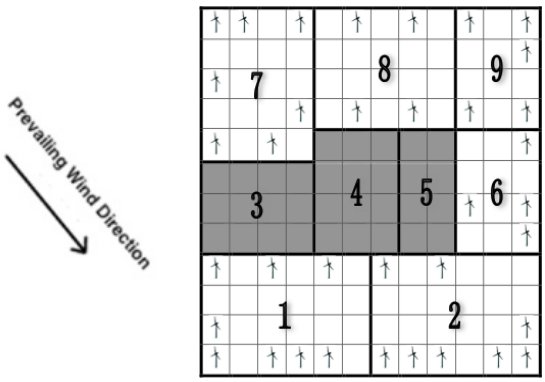

Figure 3.13 Unequal rectangle land, multidirectional non-uniform wind case (ii,2,c) has a unique optimal layout.

Table 3.4 summarizes the detailed cost of each category for the optimization results. The newly-added remittance fees are approximately 2% of the total cost, and 10% of the total operation expenses. Throughout the reporting and discussion of results, the author uses "cost impact" to refer to the percentage of total cost that is comprised by a sub-cost, such as the remittance fees. Although the cost impact of remittance fees is smaller than most other cost categories, it has great impact on the operating expenses, for example, the remittance fee accounts for approximately 10% of the operating expenses in Case (i,1,a).

Table 3.4 Detailed cost summarized for the optimization results. Percent figures rounded to nearest full percent, dollars shown in thousands.

Wind scenarios	Unidirectional uniform			Multidirectional non-uniform			
Case #	Case (i,1,a)	Case (i,1,b)	Case (i,1,c)	Case (i,2,a)	Case (i,2,b)	Case (i,2,c)	Case (ii,2,c)
Land plot scenario	Equal square	Equal square	Equal square	Equal square	Equal square	Equal square	Unequal rect.
Landowner participation	4	5	6	4	5	6	6
Remittance fees ($k (thousands)/yr) (% of total cost)	116 (2%)	132 (2%)	99 (2%)	132 (2%)	145 (2%)	149 (2%)	149 (2%)
Maintenance cost ($k /yr) (% of total cost)	628 (12%)	724 (13%)	610 (13%)	885 (15%)	966 (15%)	1001 (16%)	1011 (16%)
Replacement/overhaul cost ($k/yr) (% of total cost)	449 (9%)	514 (9%)	385 (8%)	514 (9%)	562 (9%)	578 (9%)	578 (9%)
Turbine system cost ($k/yr) (% of total cost)	2925 (57%)	3214 (57%)	2631 (57%)	3214 (55%)	3435 (55%)	3510 (55%)	3510 (55%)
Balance of station cost ($k/yr) (% of total cost)	970 (19%)	1066 (19%)	873 (19%)	1066 (18%)	1139 (18%)	1164 (18%)	1164 (18%)
Total operating expenses ($k/yr) (% of total cost)	1193 (23%)	1370 (24%)	1094 (24%)	1531 (26%)	1672 (27%)	1728 (27%)	1738 (27%)
Total initial capital cost ($k/yr) (% of total cost)	3896 (77%)	4280 (76%)	3504 (76%)	4280 (74%)	4574 (73%)	4674 (73%)	4674 (73%)
Total Cost ($k/yr)	5089	5650	4599	5812	6247	6402	6412

In the multidirectional non-uniform wind scenario, the cost impact of remittance fees increases slightly when more landowners are willing to participate and are thus included in the project, e.g. 2.327% for Case (i,2,c) compared to 2.271% for Case (i,2,a). However, in the unidirectional uniform wind scenario, the cost impact of remittance fees is the smallest when the number of participating landowners is the biggest, e.g. 2.152% for Case (i,2,c). This is because in Case (i,2,c), the optimal number of turbines is only 24, which is the smallest, and thus requires the lowest remittance fees. The cost impact of maintenance in the multidirectional non-uniform wind cases is greater than in the unidirectional uniform wind cases, e.g. 15% for Case (i,2,a) compared to 12% for Case (i,1,a). This is because the maintenance cost is directly related to the annual energy output, and the multidirectional non-uniform wind cases produce more energy due to capturing more wind resource.

In the unidirectional uniform wind scenario, the participating landowners can obtain remittance fees of either \$17k or \$33k per year, depending on the number of turbines on their land. In the multidirectional non-uniform wind scenario, the remittance fees for different participating landowners can vary from \$17k to \$33k per year. Table 3.5 summarizes the remittance fees for each landowner in the multidirectional non-uniform wind scenario. In Cases (i,2,a) and (i,2,b), the differences in the remittance fees for different participating landowners are not obvious. However, in Cases (i,2,c) and (ii,2,c), landowner 8 receives a much lower remittance fee than the others. The reason is that fewer turbines are placed on plot 8 due to its unfavorable location. Turbines on plot 8 are placed at upwind locations in the prevailing wind direction, and thus can bring wake losses to all downstream turbines. Also, turbines on plot 8 are placed in the middle of land plots 7 and

9, and thus can receive wake losses from turbines on plot 7 and bring wake losses to turbines on plot 9. Therefore, plot 8 cannot have many turbines, even though it has a relatively large size as shown in Figure 3.13 for unequal rectangle Case (ii,2,c). As a result, landowner 8 receives a lower remittance fee compared to other participating landowners. Also in this Case, landowner 6 has a low remittance fee. This is due to its small size of rectangle plot as shown in Figure 3.13. Landowners 1, 3, 7 and 9 obtain remittance fees in all the three cases for equally-sized square land-plot shape, indicating their importance for the wind project.

Table 3.5 Remittance Fees summarized for each Landowner in multidirectional non-uniform wind scenario. Dollars shown in thousands.

Case #	Case (i,2,a)	Case (i,2,b)	Case (i,2,c)	Case (ii,2,c)
Landowner Participation	4	5	6	6
Remittance Fees for Landowner 1 ($k/yr)	33	25	25	33
Remittance Fees for Landowner 2 ($k/yr)	0	25	25	33
Remittance Fees for Landowner 3 ($k/yr)	33	29	29	0
Remittance Fees for Landowner 4 ($k/yr)	0	0	0	0
Remittance Fees for Landowner 5 ($k/yr)	0	0	0	0
Remittance Fees for Landowner 6 ($k/yr)	0	0	0	17
Remittance Fees for Landowner 7 ($k/yr)	33	33	29	29
Remittance Fees for Landowner 8 ($k/yr)	0	0	17	17
Remittance Fees for Landowner 9 ($k/yr)	33	33	25	21

3.3. **Discussion and Conclusion**

In Table 3.3, the optimal COEs range from $44.40 to $56.72 per MWH. These values are in line with COEs reported by NREL, which range from $40 to $90 per MWH for a 2002-03 comparison [72]. In Table 3.5, the remittance fee paid to participating landowners ranges from $17,000 to $33,000, annually. Landowners receive an annual compensation amount of $4250 per turbine.

For the unidirectional uniform wind case (i,1,a), in which 4 out of 9 landowners are willing to participate, there are eighteen equally optimal layouts, as partially presented in Figure 3.9. For the unidirectional uniform wind case (i,1,a), in which 4 out of 9 landowners are willing to participate, there are eighteen equally optimal layouts, as partially presented in Figure 3.10. The multiple optimal layouts available in these two cases are beneficial to the developers. It indicates that if a particular landowner does not want to participate, the site developer can choose a different optimal layout. While the cases here include many assumptions and only a small number of landowners, the idea of switching layouts without sacrificing performance is scalable, and can help to improve the success rate of the wind farm projects—saving effort, time and money.

The unidirectional uniform wind case (i,1,c) and the multidirectional non-uniform wind cases (i,2,a), (i,2,b), (i,2,c), and (ii,2,c) each have a unique optimal layout, as presented in figures 3.11 through 3.13. When the wind is blowing from west to east, as shown in Figure 3.11, land plots 2, 5 and 8 were not selected, offering enough space to separate the downstream turbines from the ones upstream. When the wind is blowing from 36 directions (for the equal square land-plot shape), no matter what the landowner participation rate is, land plots 1, 3, 7 and 9 are selected and land plots 4, 5, and 6 are not selected, as shown in Figure 3.12. This indicates that some land parcels may be more important to the success of project than others. Using this information, developers can expend more effort and money on negotiating for the most crucial plots of land.

The unequal rectangle land case (ii,2,c) has similar findings as Case (i,2,c). It includes all the land plots in the upstream and downstream locations of the prevailing wind direction (e.g. land plots 1 and 2 in downstream locations, and land plots 7, 8, and 9 in

upstream locations), and excludes three land plots in the middle row to offer enough space to minimize the wake loss impact (e.g. land plots 3, 4, and 5). Note that land plot 6 is selected even though it is located in the middle row. This is because Case (ii,2,c) must select six land plots, and plot 6 has the smallest wake loss for downstream turbines in the prevailing wind direction.

There are costs not accounted for in this study, which are open to future work. For example, figures 3.9 through 3.12 indicate that optimal layouts use discontinuous pieces of land to reduce wake losses between adjacent turbines. However, this will increase installation and O&M costs not accounted for explicitly here, and make road planning for installation and maintenance of turbines more complicated. This impact on cost could be analyzed with a more detailed cost model. Note that land plots in Iowa are typically used for agricultural purposes, e.g. producing soybean and corn. The construction and maintenance of wind farms has a negative impact on crop productions. The Appendix in this dissertation analyzes and calculates the agricultural losses due to wind farm construction and maintenance. According to the analysis in Appendix, the annual temporary and permanent agricultural losses range from $594.34 to $698.07 per turbine construction for corn following soybean land in Iowa. These values are much lower than the annual remittance fee paid to participating landowners, which is $4250 per turbine. Therefore, although the participating landowners might suffer some monetary losses due to reduced crop productions, the losses should be compensated for by the remittance fee. Yet this purely economic analysis does not include perceived risk of crop damage which may manifest as hindrance to accepting the developer's contract. In Chapter 4, landowners will each be given different willingness-to-accept values for remittance fees.

This chapter incorporates a realistic levelized cost model into a wind farm layout optimization system model together with a model of landowner participation rates. The system-level COE optimization model is tested under two land-plot shapes: equally-sized square land plots and unequal rectangle land plots. The resulting predicted COEs are in line with NREL costs reported from wind farms. It proves that it is important to include landowners in the WFLO problem: to identify crucial plots of land; to identify alternate optimal layout scenarios; and, ultimately, to increase the accuracy of predictions of financial viability.

Note that the wind and land conditions used in this chapter are based on assumptions. In Chapter 4 and Chapter 5, real wind and land data will be taken into account to further validate the conclusions. In addition, due to the uncertainty in the nature of wind projects, environmental parameters such as wind, surface roughness, etc., will be addressed as uncertain in the following chapters, along with landowner decisions. An optimization-under-uncertainty system model will be developed, as introduced in Chapter 4. Moreover, instead of representing landowner participation scenarios as a binary string variable, a more realistic landowner decision model will be developed in Chapter 4.

CHAPTER 4. MODEL 2: WIND FARM LAYOUT OPTIMIZATION UNDER UNCERTAINTY WITH REALISTIC LANDOWNER DECISIONS

As discussed in Section 1.2, there is much uncertainty in the overall viability of wind projects during the early development stages. However, developers and landowners must make many important decisions with high levels of risk. Studying the wind farm layout optimization problem under uncertainty can mitigate this risk. Therefore, Chapter 4 advances the system model developed in Chapter 3, and develops an optimization-under-uncertainty system model for the Wind Farm Layout Optimization (WFLO) problem, including uncertainty in landowner decisions.

First in this chapter, a sensitivity analysis is conducted among three epistemic uncertain parameters and finds two influential parameters: wind shear and the economies-of-scale cost-reduction factor for purchasing multiple turbines, which are subsquently modeled in the optimization as uncertain. Landowner decisions are represented using a novel Willingness-to-Accept (WTA) utility function with heterogeneous, uncertain parameters. Additionally, yearly wind data is modeled as aleatory uncertainty using a Weibull distribution.

Probability theory is used to model the epistemic uncertain parameters in the optimization-under-uncertainty system model. The optimization problem is formed as a robust design problem with two objectives: minimize the normalized mean value and the normalized standard deviation of the Cost-of Energy (COE) for the farm. Compromise programming is used to search for an optimal solution that satisfies the two objectives. The work demonstrates that a quantitative approach to uncertainty can help the developer

predict the viability of the project with an estimated COE and give landowners an idea of where turbines are likely to be placed on their land.

This chapter proceeds as follows: Section 4.1 introduces the sensitivity analysis method and results, while Section 4.2 models one aleatory uncertain parameter and three epistemic uncertain parameters. The propagation of uncertainty is discussed in Section 4.3, and Section 4.4 introduces the test problem formulation. Section 4.5 provides the results and analysis, while Section 4.6 offers the conclusion.

4.1. **Sensitivity Analysis**

During the early development stages of a wind farm project, a variety of environmental and model parameters are uncertain. Instead of modeling single source of uncertainty, the sensitivity analysis takes into account diversified sources of uncertainty, including surface roughness, wind shear exponent, and cost-reduction coefficient. The analysis aims to identify the most important uncertain parameters for the WFLO from the three candidates, i.e. the ones that have the greatest impact on the wind farm COE. There are other uncertain variables that have a highly predictable effect on wind farm COE: for example, an inaccurate turbine power curve decreases performance across the board, but does not influence where or how many turbines will be placed (unless in the presence of a cost constraint). In addition, there are some other important sources of uncertainty, such as the cost of repair and replacement when turbines break, that are addressed within the Wind Turbine Design Cost and Scaling Model from National Renewable Energy Laboratory (NREL) [12]. These sources of uncertainty are therefore already addressed within this dissertation's cost model by using a levelized expected yearly cost value.

This section first identifies candidate parameters to represent as uncertain. Then, the Tornado Diagram method, explained later, is used to conduct a sensitivity analysis among the three candidates to identify the influential ones. An irregular piece of land from Story County Wind Farm in central Iowa is selected to implement the analysis, as detailed in Section 4.1.1.

To begin the sensitivity analysis, the author first analyzes all the parameters of interest in the system model of the WFLO problem, as introduced in Chapter 3, and classifies them into different categories as shown in Table 4.1. The candidates for the sensitivity analysis must meet three requirements: (1) can affect the wind farm COE; (2) can affect the wind farm layout; and (3) are not addressed by other models. Based on the analysis results of Table 4.1, the author identifies three candidate parameters likely to affect placement and number of turbines as well as COE: surface roughness, wind shear exponent, and the cost-reduction coefficient for buying multiple turbines.

Table 4.1 Classification of uncertain parameters.

Uncertain Parameters	Affect COE?	Affect Layout?	Addressed by other Models?	Candidates?
Surface Roughness	Yes	Yes	No	Yes
Wind Shear Exponent	Yes	Yes	No	Yes
Wind Scenario	Yes	Yes	Yes, by the Weibull distribution (modeled as aleatory uncertainty in Section 4.2.1).	No
Power Curve Coefficients	Yes	No	No	No
Cost-reduction Coefficient	Yes	Yes	No	Yes
Land Lease Cost	Yes	Yes	Yes, by the author's enhanced cost model (modeled as an expected value using the data from Windustry [118, 119])	No

Table 4.1 continued

Turbine System Cost	Yes	Yes	Yes, by the author's enhanced cost model (modeled as an expected value using the data from Berkeley Lab [111, 118])	No
Repair/Replacement and other Costs	Yes	Yes	Yes, by NREL's cost model [12, 118] (modeled as expected values)	No

1) Surface Roughness Length

The surface roughness length of a terrain, which is determined by the size and distribution of the roughness elements it contains [120], varies with the time of season due to crops. Table 4.2 shows the surface roughness length for several typical terrains [108]:

Table 4.2 Typical Surface Roughness lengths are classified into nine categories [108].

Classification of the Terrain	Surface Roughness Length (m)
Offshore and water areas	0.0002
Mixed water and land	0.0024
Very open farmland	0.0300
Open farmland	0.0550
Mixed farmland	0.1000
Trees and farmland	0.2000
Forests and villages	0.4000
Large towns and cities	0.8000
Large build up cities	1.6000

In the sensitivity analysis, the surface roughness of the potential site is modeled as an uncertain parameter. According to Table 4.2, the reasonable surface roughness length for a farmland is between 0.03m and 0.2m.

2) Wind Shear Exponent

The wind data used for sensitivity analysis was collected at 10-meter-high anemometers. Wind shear, "the variation of wind speed with elevation" [121], allows for the

translation of this data to wind-turbine-height, 80 meters at the hub. An empirical wind shear model calculates the wind speed at the turbine hub height:

$$u_0 = u_r\left(\frac{h_h}{h_r}\right)^{\alpha} \tag{4.1}$$

Where u_0 is the ambient wind speed at the hub height of a turbine h_h; u_r is the wind speed at a reference height h_r; α is the wind shear exponent, which varies a lot during different time of day or season [37]. Table 4.3 summarizes typical wind shear exponents for different types of terrain [121], which agrees with NREL estimates of shear from 0.143 to 0.250 in Iowa [122]. Therefore, in this analysis, the wind shear exponent of the potential site, α, is modeled as an uncertain parameter and varies between 0.143 and 0.25.

Table 4.3 Wind Shear exponent varies with different types of terrains [121].

Classification of the Terrain	Wind Shear Exponent
Smooth, hard ground, water areas	0.10
Untilled ground with short grass	0.14
Country with foot-high grass and occasional tree	0.16
Tall crops, hedges, and a few trees	0.20
Occasional buildings, many trees	0.22-0.24
Small towns and suburbs	0.28-0.30
Urban areas	0.4

3) Cost-Reduction Coefficient

In the sensitivity analysis, an advanced levelized cost model is used to calculate the levelized cost per year of the wind farm project. More details of this cost model can be found in Section 3.1.3 of Chapter 3. The model takes into account a coefficient c_r to represent the cost reduction for the initial capital cost of a large wind farm with $N(X)$ turbines, and assumes the maximum cost reduction for the wind farm is

$c_r \times C_{ic1} \times N(X) \times r_{fc}$. Where C_{ic1} is the initial capital cost for a single turbine in dollars; r_{fc} is the fixed charge rate. A variety of factors can affect the value of c_r, including market supply and demand, place of purchase or construction, and etc. In the literature, the most commonly used cost-reduction coefficient is a constant of 0.33 [22, 23, 58, 60]. In this analysis, the cost-reduction coefficient is modeled as an uncertain parameter with a reasonable range from 0.1 to 0.5.

The Tornado Diagram method is used to conduct the sensitivity analysis. The general steps for this method are [123]:

(1) Define the base-case value, upper limit, and lower limit for each uncertain parameter;

(2) Once at a time, each parameter is set to its upper and lower limits with the other parameters remain at their base-case values; then run the optimization program to find out the corresponding optimal wind farm COE;

(3) Construct the tornado diagram using the data from Step (2); the uncertain parameter whose limits have the widest optimal COE range is placed on the top bar of the diagram; the other parameters are placed in descending order of effect on the optimal wind farm COE.

In this analysis, the base-case values, upper and lower limits selected for each uncertain parameter are summarized in Table 4.4. The upper and lower limits are selected based on the discussion above. The base-case values are selected for the surface roughness length of an open farmland, the wind shear exponent of a terrain classified as "Tall crops,

hedges, and a few trees", and the most commonly used cost-reduction coefficient in the literature (0.33).

Table 4.4 Base-case values, upper and lower limits selected for the uncertain candidates.

Uncertain Candidate	Base-Case Value	Lower Limit	Upper Limit
Surface Roughness Length	0.055	0.03	0.2
Wind Shear Exponent	0.2	0.143	0.25
Cost-Reduction Coefficient	0.33	0.1	0.5

4.1.1. Problem formulation for sensitivity analysis

An irregular piece of land from Story County Wind Farm [124] in central Iowa is selected to implement the sensitivity analysis. The author aims to identify the influential uncertain parameters for a real Iowa wind farm. The land is 13440 acres (54.4 square kilometers), which is selected based on the average land size for 161 wind projects (54.5 square kilometers) summarized by National Renewable Energy Laboratory (NREL) [125]. The area investigated for the sensitivity analysis is larger by 124% than the area represented in the subsequent system optimization model in Section 4.4. This is because the accuracy of parameter sensitivity at a real-scale is crucial, while the usefulness and success of the optimization model can be demonstrated on a smaller-scale that is less computationally intensive.

The selected wind farm is located approximately 20 miles east of the Iowa State University campus, and is operated by NextEra Energy [126]. Figure 4.1 is a representation of the land with bold blue line indicating the land boundary. The entire land is divided into 566 cells with a width of four rotor diameters. For more details on the model and assumptions refer to Assumption 2 in Section 3.1.1 of Chapter 3.

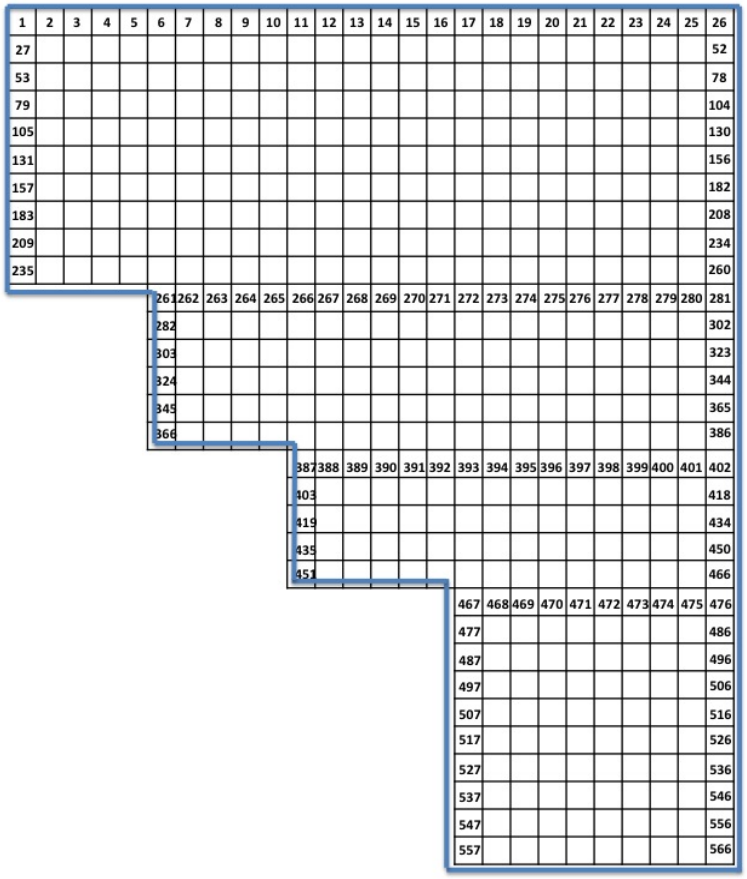

Figure 4.1 The land is divided by 566 cells.

Given the value of the three uncertain parameters, the optimization model aims to help site developers identify the optimal turbine locations in order to obtain the optimal COE of a real Iowa wind farm. The objective function, minimizing COE, is defined as:

Minimize:

$$COE(X) = \frac{C(X)}{AEP_{tot}(X)} \tag{4.2}$$

Where $COE(X)$ is the levelized cost of energy of the wind farm in \$/MWh; $C(X)$ is the levelized cost per year of a wind farm in dollar; $AEP_{tot}(X)$ is the farm's total annual energy in MWh; X is a 566-bit binary string design variable to indicate the potential

turbine locations, where "1" means a wind turbine is placed in the center of the corresponding cell, "0" means no wind turbines is placed in the corresponding cell. More details of this optimization model can be found in Chapter 3.

4.1.2. Sensitivity analysis results

A genetic algorithm (GA), which facilitates the binary design variable and non-differentiable objective function, was used to solve the optimization problem. The optimization program was developed using C++, and has incorporated a C++ library GAlib developed by Wall [114], as introduced in Section 3.2.1. The program investigated seven cases with different combinations of uncertain parameters: one case for the base-case values, and six cases for the lower and upper limits of the three uncertain parameters respectively. Each case was set to run over ten times with 10000 iterations each time. Table 4.5 summarizes the best results of the ten runs for each combination.

Table 4.5 Optimization results, summarized for seven cases.

Case #	Cases Description	COE ($/MWh)	Number of Turbines
(1)	Base Case	37.27	52
(2)	Lower Surface Roughness (0.03 m)	37.35	51
(3)	Upper Surface Roughness Length (0.2 m)	37.12	54
(4)	Lower Wind Shear Component (0.143)	45.38	52
(5)	Upper Wind Shear Component (0.25)	32.36	51
(6)	Lower Cost-Reduction Coefficient (0.1)	46.14	44
(7)	Upper Cost-Reduction Coefficient (0.5)	30.81	56

Based on the results summarized in Table 4.5, a Tornado Diagram for the three uncertain parameters can be generated as in Figure 4.2. Among the three candidates, cost-reduction coefficient and wind shear exponent can influence the COE by 24% and 22% compared to the base case, while surface roughness length can only influence the COE by

0.4%. It indicates as long as the surface roughness length is within the assumed reasonable range, the optimization model can always find an optimal layout that lead to a COE around $37 per MWh.

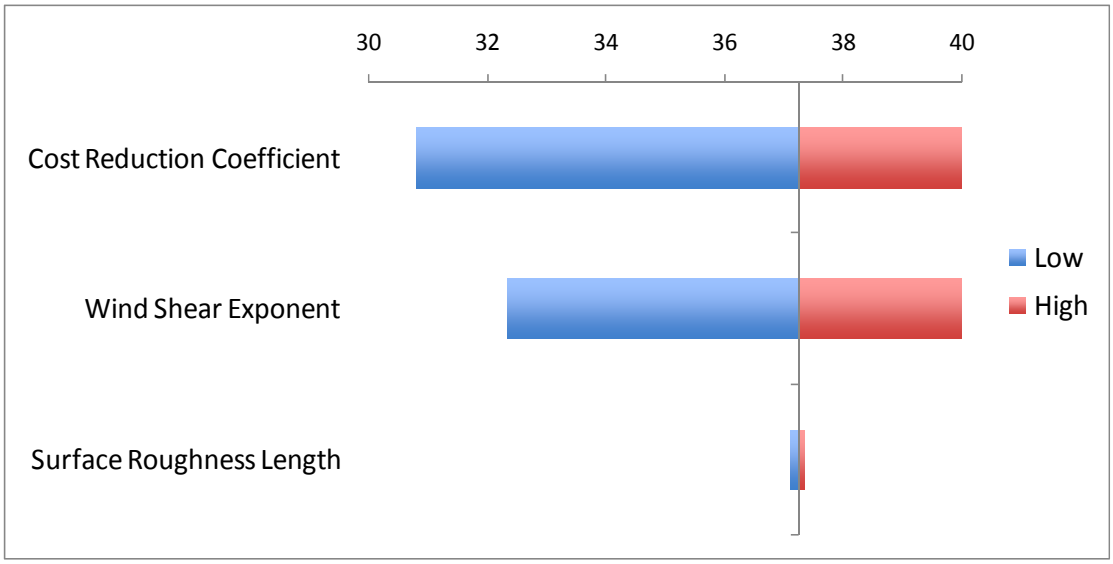

Figure 4.2 Tornado Diagram, represented for the three uncertain parameters.

The final optimal turbine layouts for the seven cases are presented in Figures 4.3 through 4.6, with solid black squares indicating the optimal locations of turbines.

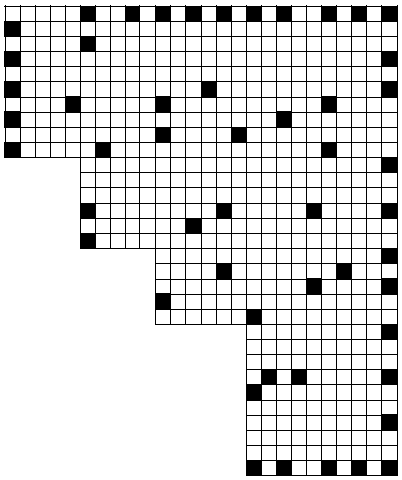

Figure 4.3 Optimal layout for Case (1) – Based Case (52 turbines).

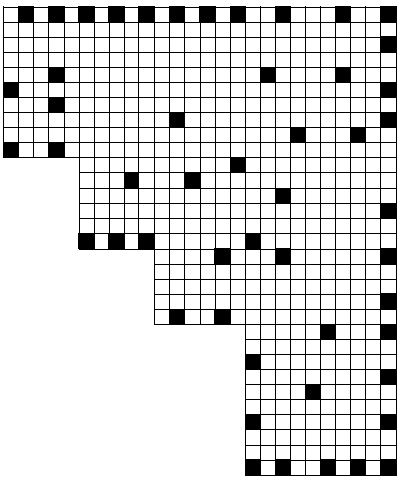

(i) Surface roughness = 0.03 (51 Turbines)

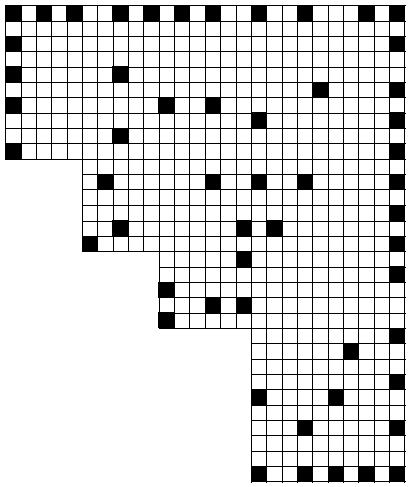

(ii) Surface roughness = 0.2 (54 Turbines)

Figure 4.4 Optimal layouts for Cases (2, 3).

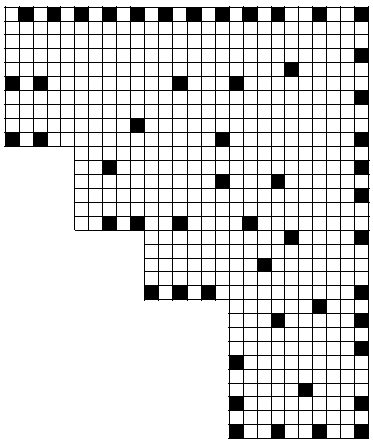

(i) Wind shear = 0.143 (52 Turbines)

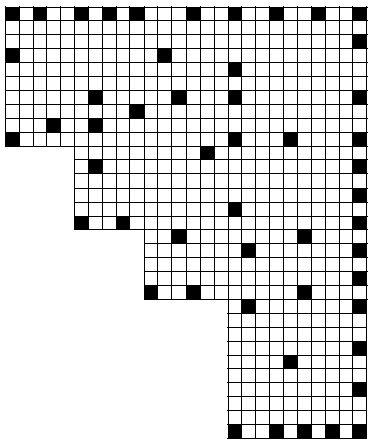

(ii) Wind shear = 0.25 (51 Turbines)

Figure 4.5 Optimal layouts for Cases (4, 5).

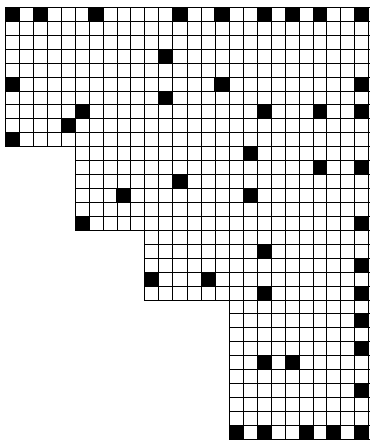

(i) Cost reduction = 0.1 (44 Turbines)

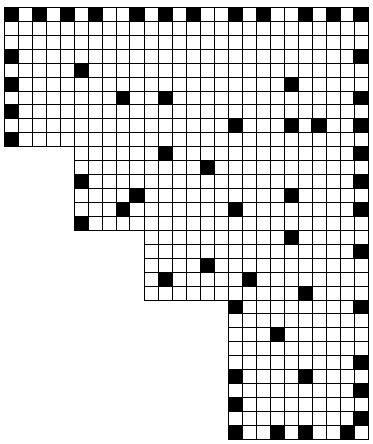

(ii) Cost reduction = 0.5 (56 Turbines)

Figure 4.6 Optimal layouts for Cases (6, 7).

The optimal layouts for the seven cases share similar pattern with more than half of the turbines located at the boundary of the land to reduce wake loss. Most cases have more than 51 turbines, while case (6) has only 44 turbines. This is because case (6) has the smallest cost-reduction coefficient, which means the average cost per turbine does not reduce greatly with the installation of more turbines.

Based on the sensitivity analysis results, surface roughness has very little impact on the COE and is therefore treated as certain going forward, with a value of 0.055m—a reasonable surface roughness for open farmland [108]. Wind shear has the greatest impact on the COE, and can influence the results by 24% compared to the base case where all the uncertain parameters are set at typical values. Cost-reduction coefficient also has great impact on the COE, and can influence the results by 22% compared to the base case. Therefore, uncertainty models will be developed for both the wind shear exponent and cost-reduction coefficient.

4.2. **Uncertainty Modeling**

Figure 4.7 presents the propagation of uncertainty through the system model to calculate the COE. Four sub-models were used here: a wind shear model, a cost model, a turbine power model, and Jensen's wake loss model [64]. Two types of uncertainty are modeled: aleatory and epistemic. Section 4.2.1 provides the uncertain modeling for aleatory wind data, while Sections 4.2.2 to 4.2.4 introduce three important epistemic uncertain parameters.

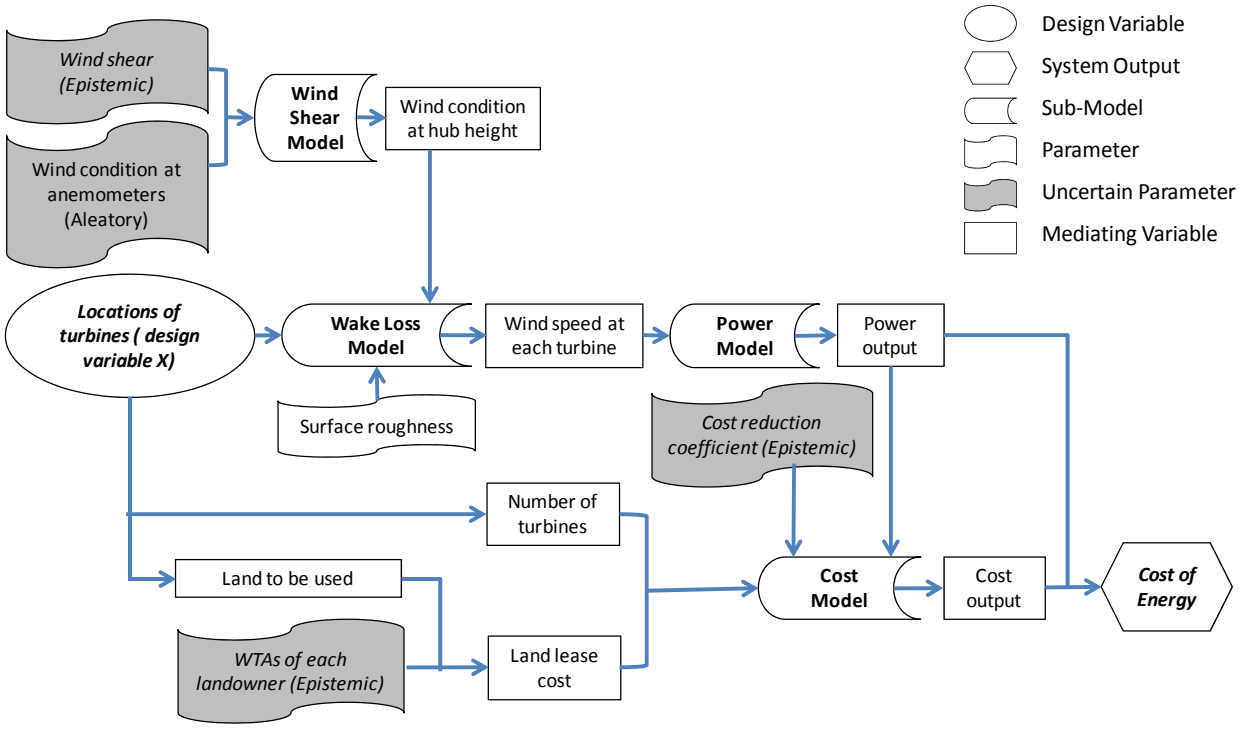

Figure 4.7 Propagation of uncertainty through the system model to calculate the COE.

4.2.1. Aleatory uncertainty: modeling yearly wind data

The wind data is modeled as a specific type of uncertainty, aleatory, which means the uncertainty is due to the inherent variability that does not revolve as development progresses. To model the wind scenario of the selected site, actual one-year wind data from the Iowa Environment Mesonet (IEM) for 2011 is modeled [127]. The wind data, which ranges from 3 knots to 38 knots with a mean value of 9 knots, is collected at 10-meter-high anemometers. Figure 4.8 provides the wind rose plot of year 2011 generated from IEM website [128].

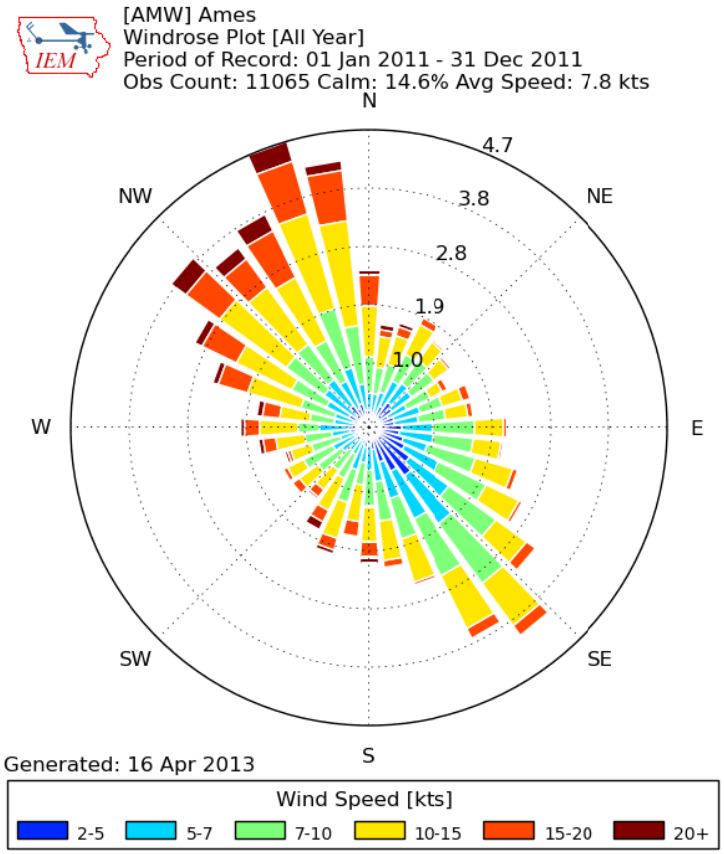

Figure 4.8. Wind rose of year 2011 generated from IEM website [128].

Weibull distribution, one of the most widely used wind models [75, 76], is used to model the wind data. The probability density function (PDF) of Weibull distribution for wind speed v is a function depending on the shape factor k and the scale factor λ [77]:

$$PDF(v) = \frac{k}{\lambda}\left(\frac{v}{\lambda}\right)^{k-1} e^{-\left(\frac{v}{\lambda}\right)^{k}} \tag{4.3}$$

The fittest results for the one year wind data is summarized in Table 4.6 for 36 wind directions with corresponding occurrence probability for each direction. Note that, the correlation coefficients R^2 summarized in Table 4.6 for all 36 directions vary from 0.97 to 1.00, with only one exception of 0.93 for wind direction 250 degree. Therefore, the Weibull distribution fits well for the IEM wind data.

Table 4.6 Weibull distribution highly correlated with IEM wind data.

Wind Direction (degree)	Shape Factor k	Scale Factor λ	Correlation Coefficient R^2	Occurrence Probability for Each Direction
0	2.42	11.95	0.99	0.03
10	2.14	10.54	0.99	0.02
20	2.15	10.42	0.99	0.02
30	2.12	9.12	0.99	0.02
40	2.19	7.82	0.97	0.02
50	2.12	8.03	0.97	0.02
60	2.14	8.69	0.98	0.02
70	2.05	8.61	0.98	0.02
80	2.20	8.51	0.99	0.02
90	2.34	8.30	0.99	0.02
100	2.53	8.18	0.99	0.03
110	2.39	8.71	0.99	0.03
120	2.38	8.33	0.99	0.03
130	2.12	8.48	0.98	0.04
140	2.13	8.51	0.97	0.05
150	2.33	8.71	0.99	0.04
160	2.31	8.74	0.98	0.03
170	2.37	9.28	0.99	0.03
180	2.18	10.71	0.99	0.03
190	2.29	10.48	0.99	0.02
200	2.23	10.29	0.99	0.02
210	2.02	11.67	0.98	0.02
220	2.03	10.41	0.98	0.02
230	2.15	10.20	0.98	0.02
240	2.06	9.18	0.97	0.02
250	1.94	9.73	0.93	0.02
260	2.04	10.77	0.99	0.02
270	2.03	10.53	0.99	0.02
280	2.19	11.54	0.99	0.02
290	2.45	12.00	0.99	0.03
300	2.31	12.07	0.99	0.04
310	2.24	12.62	0.99	0.04
320	2.17	11.89	1.00	0.04
330	2.27	12.78	1.00	0.04
340	2.36	12.69	1.00	0.05
350	2.60	12.54	0.99	0.05

4.2.2. Epistemic uncertainty: landowner participation

During wind farm development stages, many other sources of uncertainty are epistemic due to the lack-of-knowledge of parameters. In this work, Probability Theory is used to model the important epistemic uncertain parameters as random variables. Due to the lack-of-knowledge in early wind farm development, sufficient data are not available to quantify the uncertain parameters as probabilistic distributions. Therefore, the reasonable range of each uncertain parameter is divided into three intervals with assigned probabilities (probability distribution uniform within each interval), as discussed below.

An important source of uncertainty is landowner participation, as demonstrated in Chapter 3. When a wind farm is placed on a plot of land, the landowner will be approached by developers for permission to build. In this situation, landowners are sellers and developers are buyers. Landowner participation decisions are modeled as utility functions. In order for the landowner to be willing-to-accept (WTA) the developer's monetary lease agreement (remittance), the utility of having turbines plus their associated monetary compensation must be greater than or equal to the utility of not having turbines and not having monetary compensation. A basic background on the concept of WTA is provided in Section 2.5. Here, the WTA is a minimum annual compensation amount per MW installed that satisfies the following equation:

$$U(m_0 + WTA, 1) \geq U(m_0, 0) \tag{4.4}$$

Where U is a landowner's utility function; m_0 is the landowner's initial wealth; "1" represents the presence of wind turbines on his/her land; and "0" represents the absence of wind turbines on his/her land.

Through experiment, conversations, and other interactions, site developers gain an initial estimation of landowners' WTAs. These estimations are initially uncertain. As the project proceeds to land acquisition negotiations, these estimations will become more precise. In this research, the vector of WTAs for each landowner, w_{WTA}, are modeled as uncertain parameters, to represent early-stage development conditions. For landowners, the annual compensation per MW installed can range from \$1000 to \$5000 with an average of \$2757, as summarized in Table 3.1 of Section 3.1.3. In this section, the range of WTAs is set to be between \$1000 and \$50000. When a landowner has a WTA higher than \$5000, it indicates the landowner is not in favor of the wind project, and will only participate when the compensation is very high. Note that the upper bound of WTAs is \$50000, which approximates the entire property value, assuming multiple turbines are placed.

The range of WTAs is further divided into three intervals as shown in Table 4.7, where [1000, 2500) represents a low WTA, [2500, 5000) represents a moderate WTA, and [5000, 50000) represents a high WTA. Landowners are divided into four groups, each with their own uncertain WTA, for a total of four uncertain parameters associated with WTA/remittance fees. Table 5 summarizes the assumed estimations from a hypothetical site developer for each landowner group. (1) Type-A landowners will accept moderate compensation. The minimum WTA is much more likely to be between \$2500 and \$5000 (Probability=0.7) than between \$1000 and \$2500 (Probability=0.2) or between \$5000 and \$50000 (Probability =0.1); (2) Type-B landowners will accept low compensation due to enthusiasm for other aspects of the project, such as environmental benefits. The minimum WTA is most likely to be between \$2500 and \$5000 (Probability =0.5) and between \$1000

and $2500 (Probability=0.4); (3) Type-C landowners will accept high or moderate compensation. The minimum WTA is most likely to be between $5000 and $50000 (Probability=0.5) and $2500 and $5000 (Probability=0.4); (4) Type-D landowners do not like wind projects, and are unlikely to participate without high compensation. The minimum WTA is much more likely to be between $5000 and $50000 (Probability=0.7).

Table 4.7 Intervals and probabilities, assumed for four WTAs.

Willingness to Accept for type-A Landowners ($/yr per MW installed)			
Intervals	[1000,2500)	[2500,5000)	[5000, 50000]
Probabilities	0.2	0.7	0.1
Willingness to Accept for type-B Landowners ($/yr per MW installed)			
Intervals	[1000,2500)	[2500,5000)	[5000, 50000]
Probabilities	0.4	0.5	0.1
Willingness to Accept for type-C Landowners ($/yr per MW installed)			
Intervals	[1000,2500)	[2500,5000)	[5000, 50000]
Probabilities	0.1	0.4	0.5
Willingness to Accept for type-D Landowners ($/yr per MW installed)			
Intervals	[1000,2500)	[2500,5000)	[5000, 50000]
Probabilities	0.1	0.2	0.7

It is important to note that the probabilities are assumed in the example problem. When this research is applied to actual development projects, these assignments must be made with input from the developers and other sources.

Currently, in actual lease agreements, developers offer all landowners the same remittance. This is in order to decrease the possibility for individual negotiations, which would increase the project timeline. “Riders” are offered to cover additional cost burdens on an as-needed basis. But the model here assumes the developers pay landowners the exact compensation that they are willing to accept (not, for example, a higher value), and

that these are different values for different types of landowners. The reason for this is to explore and identify plots of land that are worth paying extra to purchase. A constraint could easily be added stating that all landowners must be willing to accept the same remittance, or a remittance level based mathematically on the total energy output of the farm. This is explored in Chapter 5.

4.2.3. Epistemic uncertainty: wind condition

The details of the wind data representation can be found in Section 4.2.1, and the uncertain wind shear exponent in section 4.1. The uncertain wind shear exponent is varied between 0.143 and 0.25. The range of wind shear exponent is further divided into three intervals with the assumption that the wind shear exponent is most likely to be within the middle range [0.18, 0.22) (probability=0.5), as shown in Table 4.8.

Table 4.8 Intervals and probabilities, assumed for wind shear exponent.

Wind Shear Exponent			
Intervals	[0.143, 0.18)	[0.18, 0.22)	[0.22,0.25)
Probabilities	0.3	0.5	0.2

4.2.4. Epistemic uncertainty: cost model

The levelized cost per year of a wind farm project is defined as:

$$\mathrm{C}(X) = r_{fc} \times C_{ic1} \times N(X) \times (1 - c_r + c_r \times e^{-0.00174\, N(X)^2}) + C_{aot}(X) \tag{4.5}$$

Where $\mathrm{C}(X)$ is the levelized cost per year of a wind farm project in dollars; r_{fc} is the fixed charge rate; C_{ic1} is the initial capital cost for a single turbine; and $N(X)$ is the number of turbines in a wind farm. The cost-reduction coefficient c_r represents the economies-of-scale cost reduction for the initial capital cost of a large wind farm with $N(X)$ turbines; the

maximum cost reduction is $r_{fc} \times C_{ic1} \times N(X) \times c_r$. The remainder of Equation (4.5) is, $C_{aot}(X)$, annual operating expense for the farm:

$$\begin{aligned} C_{aot}(X) &= C_{llt}(X) + C_{omt}(X) + C_{rot}(X) \\ &= \sum_{i=1}^{N_{LO}} WTA_i \times P_{MWi} + C_{omt}(X) + C_{rot}(X) \end{aligned} \tag{4.6}$$

Where $C_{llt}(X)$ is the land lease cost per year; WTA_i is the WTA for landowner i; P_{MWi} is the total megawatts installed on the land of landowner i; N_{LO} is the total number of landowners; $C_{omt}(X)$ is the levelized maintenance cost per year; $C_{rot}(X)$ is the levelized replacement and overhaul cost per year. All dollar values in the model are based on 2002 dollars, and a detailed formulation of this cost model can be found in Section 3.1.3.

In this optimization formulation, the cost-reduction coefficient c_r is modeled as an uncertain parameter. This cost coefficient depends on the timing of the turbine of purchase, place of purchase/construction, market supply and demand, and other factors. The most widely used cost-reduction coefficient is a certain value of 0.33 in the literature [22, 23, 58, 60]. In this optimization formulation, the coefficient range is 0.1 to 0.5, based on the typical value of 0.33 used in other papers [22, 23, 58, 60]. The sensitivity analysis showed this assumed range can influence the COE by 22% compared to the base case. This range is further divided into three intervals with the assumption that the cost-reduction coefficient is most likely to be between 0.25 and 0.4 (probability=0.5), as shown in Table 4.9.

Table 4.9. Intervals and probabilities, assumed for cost-reduction coefficient.

Cost-Reduction Coefficient			
Intervals	[0.1,0.25)	[0.25,0.4)	[0.4,0.5]
Probabilities	0.4	0.5	0.1

4.3. **Uncertainty Propagation**

In this Chapter, three epistemic sources of uncertainty with six uncertain parameters are modeled as discussed above: WTAs for type-A, type-B, type-C, and type-D landowners, wind shear exponent, and cost-reduction coefficient. Latin Hypercube Sampling, a compromise method that incorporates the benefits of Monte Carlo Sampling and Importance Sampling [93], was used to draw n_s samples of the six uncertain parameters. n_s was set to be 100 to obtain a ratio of 17 between sample size and random parameters (100/6=17). Matala [129] discusses that this ratio is sufficient for Latin Hypercube Sampling. Once the system outputs $COE_i, i = 1,2,\ldots,n_s$ were obtained, the mean value μ_{COE} and the standard deviation σ_{COE} of the COE were estimated by:

$$\mu_{COE} = \frac{1}{n_s}\sum_{i=1}^{n_s} COE_i \tag{4.7}$$

$$\sigma_{COE} = \sqrt{\frac{1}{n_s - 1}\sum_{i=1}^{n_s}\left(COE_i - \mu_{COE}\right)^2} \tag{4.8}$$

The robust design problem was formed as a multi-objective optimization problem with two objectives: minimize the normalized mean value of the COE ($f_1 = \frac{\mu_{COE}}{\mu^*_{COE}}$) and the normalized standard deviation of the COE ($f_2 = \frac{\sigma_{COE}}{\sigma^*_{COE}}$). μ^*_{COE} is the optimal mean value if optimizing μ_{COE} individually, and σ^*_{COE} is the optimal standard deviation if optimizing σ_{COE} individually.

Compromise programming was used to search for the solution on the efficient frontier closest to the utopia point [130]. The utopia point, also called the ideal point, is the point where each objective achieves its optimal value. Compromise programming identifies the closest obtainable point to the utopia point [131]. For this problem, when minimizing each objective individually over the design space, following equations can be obtained:

$$f_1^* = \min\left\{\frac{\mu_{COE}}{\mu_{COE}^*}\right\} = \frac{\mu_{COE}^*}{\mu_{COE}^*} = 1 \tag{4.9}$$

$$f_2^* = \min\left\{\frac{\sigma_{COE}}{\sigma_{COE}^*}\right\} = \frac{\sigma_{COE}^*}{\sigma_{COE}^*} = 1 \tag{4.10}$$

Then, the compromise programming problem was formulated as [131]:

$$\text{minimize } \left\| f - f^* \right\| \tag{4.11}$$

Where $f = [f_1, f_2] = \left[\frac{\mu_{COE}}{\mu_{COE}^*}, \frac{\sigma_{COE}}{\sigma_{COE}^*}\right]$; $f^* = [f_1^*, f_2^*] = [1,1]$; $\|\cdot\|$ is the metric of choice. When using a weighted L_p-metric, the distance between f and f^* is calculated by [131]:

$$\left\| f - f^* \right\|_p^w = \left(\sum_{i=1}^{2} \left(w_i \left| f_i - f_i^* \right| \right)^p \right)^{\frac{1}{p}} \tag{4.12}$$

Where $w_i \geq 0, i = 1 \text{ or } 2$ are the importance weightings of the objectives (equal at 0.5 here). $p = \{1,2,\ldots\}$ defines the metric [131]: 1) when $p = 1$, L_1 is the Manhattan metric, which is equivalent to the weighted sum formulation; 2) when $p = 2$, L_2 is the Euclidean metric; 3) when $2 < p < \infty$, the objective function of Compromise Programming is nonlinear and difficult to handle; 4) when $p = \infty$, L_∞ is the Chebyshev metric with the objective function defined as:

$$\min \max_{i=1,2} \left\{ w_i \left(f_i - f_i^* \right) \right\} \tag{4.13}$$

The Chebyshev metric, which is able to search for solutions located both in the convex and non-convex parts of the Pareto front [132], is used to form the objective function. The general procedures for the optimization program are shown in Figure 4.9. Note that equal importance weights are assigned to the two objectives: the normalized mean value and the normalized standard deviation of the COE. In practice, users of the approach presented here can set their own weights, or explore a spectrum of weights to form a Pareto frontier.

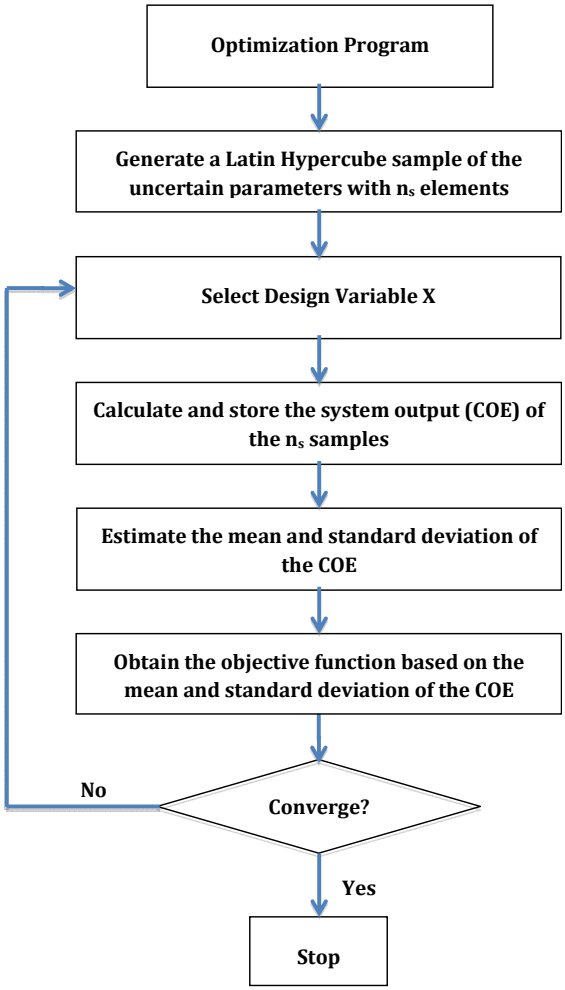

Figure 4.9 General Procedures for Optimization Program has six steps.

4.4. **Test Problem Formulation**

The robust optimization problem tests an assumed plot of land 4928 by 4928 meters, owned by 16 landowners. Each landowner (marked by a bold number in Figure 4.10) owns a square plot, divided into 16 cells. Wind turbines can only be placed in the center of each cell. Each cell can have 2 possible states: containing a turbine or not. The width of each cell is equal to four rotor diameters (308m for GE1.5sle) to reduce wake interactions. The author further classifies the sixteen landowners into four types as discussed in Section 4.2.2. Figure 4.10 represents the assumed locations of the four types of landowners, each type with a different behavior regarding the acceptance of wind farm remittances.

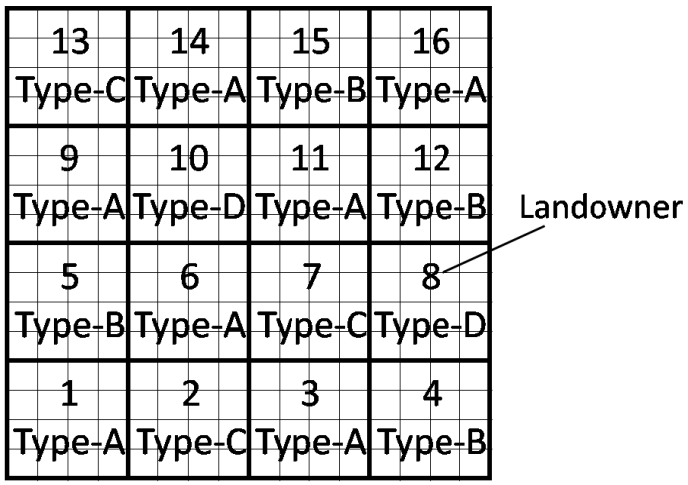

Figure 4.10 Four landowner types distributed among 16 plots.

The WTA behavior for the four types is detailed in Table 4.7. Note that the plot of land tested here is smaller than that used in the sensitivity analysis, as introduced in Section 4.1.1. In the sensitivity analysis, a real piece of land in Iowa is used, aiming to identify the influential uncertain parameters for general Iowa wind farms. However, the objective of this chapter is developing an optimization-under-uncertainty system model for

the WFLO problem and proving the feasibility of this model. Therefore, in order to save computational cost and facilitate results interpretation, a reduced-size assumed plot of land in this section is used, as shown in Figure 4.10, to test the proposed optimization-under-uncertainty system model.

The objective for the deterministic system model is minimizing COE given environmental and model parameters P, defined as:

$$COE(X,P)=\frac{C(X,P)}{AEP_{tot}(X,P)} \tag{4.14}$$

Where $COE(X,P)$ is the cost of energy of the farm in \$/MWh; $C(X,P)$ is the levelized cost per year of a wind farm in dollars; and $AEP_{tot}(X,P)$ is the farm's total annual energy in MWh. X is a 256-bit binary string design variable representing the potential turbine locations. Note that the optimization system model applies no constraint on the total energy output or the total number of turbines on the farm. The only constraint of the model is that turbines must be placed at the center of each cell, resulting in a minimum of four-rotor diameter separation between any two turbines to reduce wake interactions [78, 79].

4.5. **Results and Analysis**

GAlib, was again used to solve the optimization problem. The parameters of the GA are summarized in Table 4.10. Note that the optimization program ran in three different scenarios: (1) minimize the mean value of COE; (2) minimize the standard deviation of COE; and (3) compromise programming with two minimization objectives: the normalized mean value and standard deviation of COE. For each scenario, the program ran over ten

times with 10000 iterations each time. All three scenarios have very similar convergence histories in the optimization program. Figure 4.11 provides an example of the convergence history for Scenario 2.

Table 4.10 Parameters for Genetic Algorithm using GAlib.

Genetic Algorithm Type	GASteadyStateGA
Genome Type	GA1DBinaryStringGenome
Population Size	200
Generation Number	10000
Crossover Probability	0.9
Mutation Probability	0.01
Replacement Rate	0.5

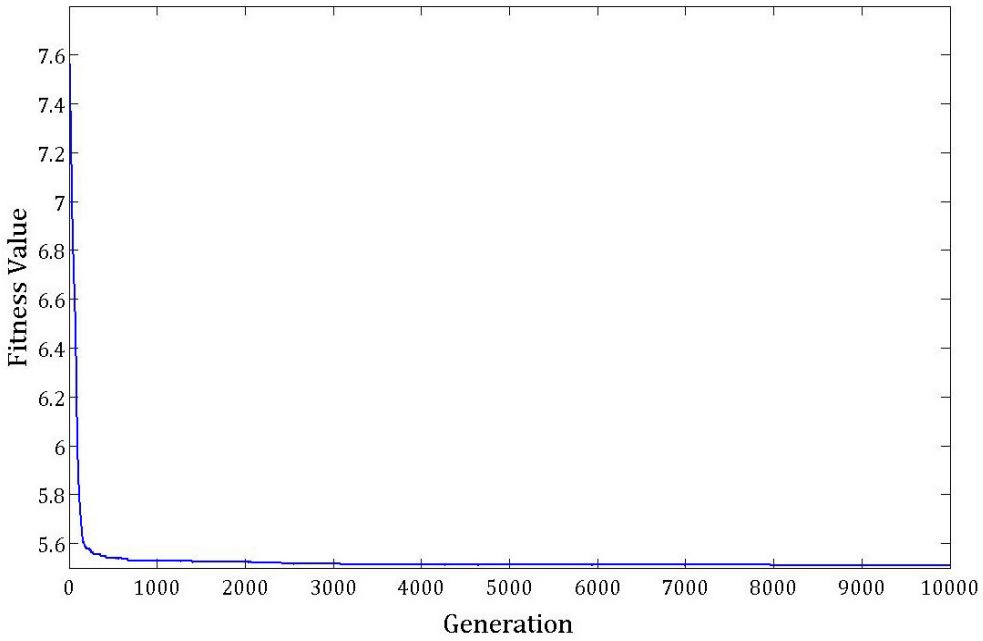

Figure 4.11. Convergence history generated for minimizing σ_{COE} individually.

The best results of the ten runs are recorded in Table 4.11. μ_{COE} ranges from \$42 to \$48 per megawatt hour, as shown in Table 4.11. This range is in line with the \$40 to \$90 range estimated by NREL for 2002-03 standard technology [Equation (4.5) is based on

2002 costs] [72]. There are several interesting findings in Table 4.11. For example, for μ_{COE}, the result of Scenario 3 is closer to Scenario 1 than Scenario 2. However, for number of turbines, the result of Scenario 3 is closer to Scenario 2 than Scenario 1. The uncertain cost-reduction coefficient, which reduces turbine cost based on the number purchased, implies that Scenarios 1 and 3 will have a lower μ_{COE}. Combined with the uncertain wind shear exponent, this further implies that Scenarios 2 and 3 will have less uncertainty in production and cost, and thus a smaller standard deviation.

Table 4.11 Results summarized from the optimization program.

Scenarios	1	2	3
Objectives	Minimize μ_{COE} Individually	Minimize σ_{COE} Individually	Minimize $\left[\frac{\mu_{COE}}{\mu^*_{COE}}, \frac{\sigma_{COE}}{\sigma^*_{COE}}\right]$
μ_{COE} ($/MWh)	42.42	47.21	44.05
σ_{COE} ($/MWh)	6.13	5.51	5.71
μ Energy Output (MWh/yr)	192751	85686	131467
μ Cost Output ($k/yr)	8,090	4,002	5,730
Number of Turbines	42	18	28

Figures 4.12 though 4.14 present the optimal layouts for the three scenarios, with  representing the optimized turbine locations. Unused, non-leased land plots are indicated in grey. Figure 4.12 presents the optimal layout for Scenario 1 (minimize μ_{COE}). Forty-two turbines are placed on eleven land plots. Of the five land plots unused, plots 8 and 10 are owned by type-D landowners, and plots 2, 7 and 13 are owned by type-C landowners. As discussed in Section 4, types C and D landowners have high monetary compensation requirements (WTAs). The optimization program avoids placing turbines on the land of such landowners to keep remittance fees down.

Scenario 2 (minimize σ_{COE}) has only eighteen turbines placed on twelve land plots, as indicated in Figure 4.13. Some of the type-C landowners, e.g. plots 2 and 13, are selected even though they have high WTAs. This is because it is not necessary to avoid placing turbines on expensive land in Scenario 2, as minimizing mean COE is not its objective. Note that the optimal layout in Fig. 8 only has eighteen turbines. When there are fewer turbines in the farm, the variance of the cost output is reduced due to the reduced variance of uncertain WTAs, and the variance of the energy output is also reduced as the variance of turbines' effective wind speeds (due to an uncertain wind shear exponent) is reduced. This ultimately reduces the σ_{COE}.

Similar trends can be found for Scenario 3 (minimize μ_{COE} and σ_{COE}) as indicated in Figure 4.14: all type-D landowners are not selected and some of the type-C landowners are not selected, which is consistent with the fact that type-D landowners have the highest WTAs. In Figure 4.14, plot 13 is selected although it has a type-C landowner. This is because plot 13 is located in a corner, with access to strong, stable wind.

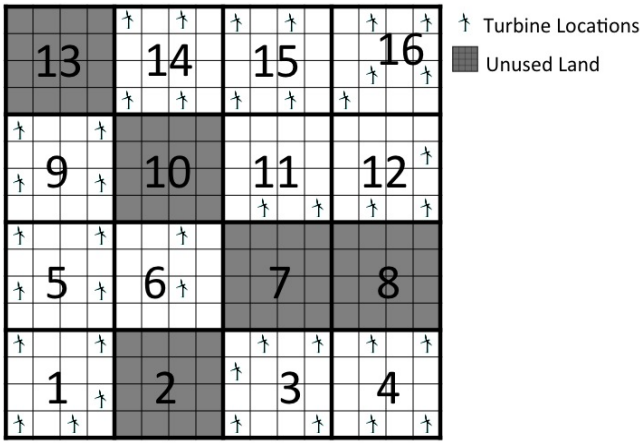

Figure 4.12 Optimal layout minimizing μ_{COE}.

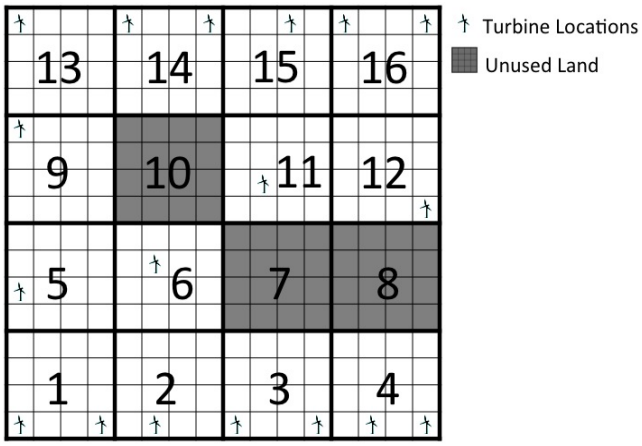

Figure 4.13 Optimal layout minimizing σ_{COE}.

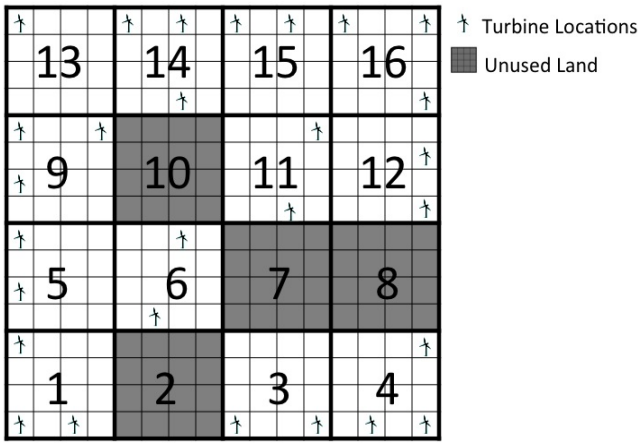

Figure 4.14 Optimal layout minimizing μ_{COE} and σ_{COE}.

4.6. **Conclusion**

Chapter 4 develops an optimization-under-uncertainty system model for a wind farm layout optimization problem. A sensitivity analysis is conducted first to rule out unimportant uncertain parameters. Yearly wind data is modeled as uncertainty using a Weibull distribution. Three epistemic sources of uncertainty are modeled in the proposed system model: landowner participation (willingness-to-accept), wind condition (wind shear), and cost model (economies-of-scale cost reduction). Probability Theory is used to

model the uncertain parameters, and Latin Hypercube Sampling to propagate the uncertainty throughout the system. Compromise programming is used to search for the non-dominated solution that best satisfies the two objectives: minimize the normalized mean value and standard deviation of the COE. The results demonstrate that even in an uncertain environment, developers can predict the viability of the project with an estimated COE and give landowners an idea of where turbines are likely to be placed on their land.

Although this system model is specifically designed for the early development stages in a wind project, it can be used in all stages. During the very early development stages before the negotiation process, the estimations of uncertain parameters (e.g. WTAs for all the landowners) could be replaced by typical values (e.g. $1000-$5000 for WTAs). Then the optimization model can be used to identify the most crucial landowners for negotiations. During negotiations, the estimations of uncertain WTAs could be updated iteratively. When the uncertain parameters become relatively certain, they can be updated again and the final layout determined.

The optimal layout results in Figures 4.12 though 4.14 indicate a range of landowner importances in determining project success. In Scenario 1, as the objective is minimizing μ_{COE}, all type-C and type-D landowners are excluded to keep remittance fees down. In Scenario 2, fewer turbines are placed to reduce the variance of uncertain WTAs and the variance of turbines' effective wind speeds due to uncertain wind shear exponent, which ultimately reduces the σ_{COE}. In Scenario 3, although landowner 13 requests more compensation, their land's wind-resource benefit outweighs the additional cost. It indicates

that evaluating the land of reluctant landowners individually can be important to the project.

Therefore, this system model has the potential to substantially change the land acquisition process. Developers typically offer landowners all the same remittance fee, as they are unsure whose land will be most crucial, and they do not want to enter into negotiations with each individual landowner. The model can help developers identify plots of land that are worth the extra investment. Also, it can help landowners adjust their compensation expectations, either higher or lower, without pricing themselves out of participation.

The work has a number of directions for expansion. The optimization-under-uncertainty system model is tested on an assumed plot of land with 16 landowners. In Chapter 5, real land will be used to further validate the results. In addition, this work only focuses on the costs and profitability of wind farms without addressing the noise impact. In Chapter 5, the optimization-under-uncertainty system model will be further advanced with landowners' noise concern. Chapter 5 will also provide a realistic approach of offering all landowners the same compensation package.

CHAPTER 5. MODEL 3: MODELING NOISE IMPACT AND EQUAL COMPENSATION FOR LANDOWNERS IN WIND FARM LAYOUT OPTIMIZATION UNDER UNCERTAINTY

When placing wind turbines within an available land area close to residential locations, noise impact becomes a primary concern for the Wind Farm Layout Optimization (WFLO) problem, as discussed in Section 1.3. People do not like to hear wind turbine noise, and different people may have different perceptions on it [21]. Developers receive complaints and lawsuits about excessive noise and its associated adverse health impacts [19]. For example, an Oregon landowner claims he is suffering "emotional distress, deteriorating physical and emotional health, dizziness, inability to sleep, drowsiness, fatIgue, headaches, difficulty thinking, irritation and lethargy" due to the wind turbine noise [20]. As a result, he files a $5 million suit over turbine noise recently.

According to a study conducted by Ambrose and Rand, a community would have a strong desire to stop noise if the noise level is above 43dB at their homes (about as loud as a refrigerator), and have vigorous community action if the noise level is above 49.5dB (about as loud as a moderate rainfall) [19]. Developers typically offer landowners a separate contract with an annual payment up to $1500 for compensating the noise disturbance [133, 134]. If developers can guarantee the noise level is below a certain limit or give landowners an idea of the likely auditory impact, the landowners will accept the contract more easily. Therefore, it is important to model noise impact in the WFLO problem. This chapter further advances the optimization-under-uncertainty system model developed

in Chapter 4 with a model of noise impact and associated fees that landowners are willing to accept for different levels of noise.

The noise generation of a farm is typically set as a constraint or an objective function in current WFLO research [135, 136]. No existing WFLO research models monetary compensation offers to compensate landowners for noise disturbance. This chapter addresses this limitation by developing a novel uncertain willingness-to-accept (WTA) model for noise. The proposed system model is tested on a real piece of farm land in Iowa with 22 landowners and 12 noise receivers (houses). It can help developers identify plots of land that are worth the extra investment, and provide developers a robust wind farm design that is not only profitable but also has minimal noise disturbance for landowners. It can also give landowners an idea of where turbines are likely to be placed on their land, and the likely auditory impacts.

The chapter proceeds as follows: Section 5.1 provides the introduction, while Section 5.2 introduces the noise propagation model. Section 5.3 presents the improved cost model, and the uncertain Willingness-to-Accept model for noise is introduced in Section 5.4. The detailed problem formulation is presented in Section 5.5, while Sections 5.6 to 5.8 offer the results, discussion and conclusion.

5.1. **Introduction**

Figure 5.1 represents the overview of the COE system model with models of noise propagation and equal compensation for landowners. Five models are used to calculate the COE: a noise propagation model (introduced in Section 5.2), a cost model (similar as the model in Section 4.2.4 with the addition of equal compensation for landowners for

participation and noise), a wind shear model (discussed in Section 4.1), Jensen's wake loss model (discussed in Section 2.3.2), and a power model (discussed in Section 3.1.4).

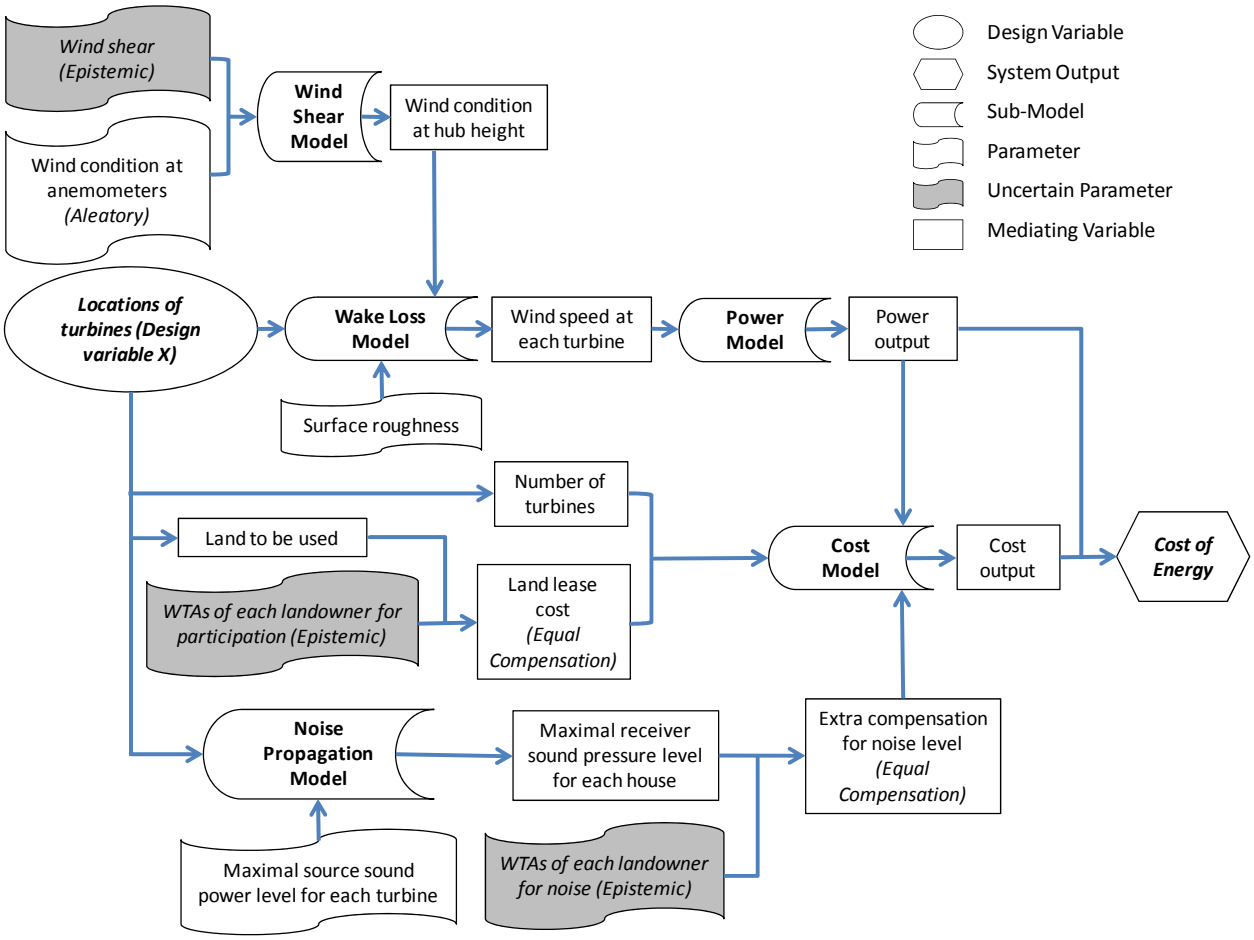

Figure 5.1 Overview of the COE model with a noise model.

Similar as the COE system model in Chapter 4, wind condition is modeled as aleatory uncertainty using a Weibull Distribution, Three epistemic sources of uncertainty are modeled in this chapter. Landowner participation and wind shear are modeled as in Chapter 4. The economies-of-scale cost reduction coefficient is excluded because the number of turbines is fixed, as explained later in Section 5.3. The third source of uncertainty modeled is the monetary compensation required for a given noise impact, as discussed later in Section 5.4. Note that there are some other important sources of uncertainty, such as the

atmospheric attenuation coefficient in the noise propagation model, as introduced in Section 5.2. This source of uncertainty is address by using an expected value, which represents the average temperature and relative humidity for Ames in 2011.

An important improvement of the COE system model is the modeling of equal compensation for landowners. In Chapter 4, the author assumes the developers pay each landowner the exact compensation that they are personally willing to accept. However, in actual lease agreements, develops offer all landowners the same compensation package. This is in order to decrease the possibility for individual negotiations, which would increase the project timeline and cost. To address this limitation, Chapter 5 develops an equal compensation model for landowners, as shown in Figure 5.1 and detailed below.

For each sample of the uncertain WTA_p (for participation), the maximum WTA_p among all the participating landowners will be used to calculate the final, shared compensation value offered to each landowner. This simulates the real situation, where each landowner has different WTA_p but all are offered the same compensation for participation. Therefore, in order to get the permission of all the important landowners identified by the optimization algorithm, developers need to offer to pay the maximum WTA_p for these landowners to everyone. As compared to Chapter 4, this rule gives the optimization algorithm more incentive to avoid costly landowners for participation, as it then needs to pay all participants that much for their participation.

5.2. **Noise Propagation Model**

The noise propagation model used here is based on ISO 9613-2:1996(E) [137]:

$$L_{AT} = 10\lg\left\{\sum_{i=1}^{n}\left[\sum_{j=1}^{8}10^{0.1\left[L_{fT}(ij)+A_f(j)\right]}\right]\right\} \tag{5.1}$$

Where L_{AT} is the A-weighted downwind sound power level at a receiver location (landowner's house); n is the number of noise sources (number of turbines); i is an index representing the noise sources; j is an index representing the eight standard octave-band midband frequencies; $A_f(j)$ is the standard A-weighting (IEC 651 or IEC 61672); and $L_{fT}(ij)$ is sound pressure level at a receiver location for noise source i and octave-band j :

$$L_{fT}(ij) = L_W + D_C + A \tag{5.2}$$

Here L_W represents the octave-band sound pressure level for the noise source (turbine); D_C is the directivity correction, assumed to be 0dB in the work ; and the octave-band attenuation A is defined as:

$$A = A_{div} + A_{atm} + A_{gr} + A_{bar} + A_{misc} \tag{5.3}$$

Where A_{div} is the attenuation due to the geometrical divergence, defined as:

$$A_{div} = [20\lg(d/d_0) + 11] \text{ dB} \tag{5.4}$$

Here d is the distance from the source to receiver; and d_0 is the reference distance (1m).

A_{atm} is the attenuation due to atmospheric absorption, defined as:

$$A_{atm} = a_c d/1000 \tag{5.5}$$

a_c is the atmospheric attenuation coefficient. In this research, the coefficient a_c for temperature 10° and relative humidity 70% is selected, as the average temperature and

relative humidity for Ames in 2011 are 9.2 and 77% according to the real data obtained from Iowa Environmental Mesonet [127].

A_{gr} is the attenuation due to the ground effect, defined as:

$$A_{gr} = A_s + A_r + A_m \tag{5.6}$$

The detailed method for calculating A_s, A_r, A_m is in [137]. The author assumes the ground is porous ground for source region, middle region, and receiver region (G=1). The source (turbine) height is 80m, and the receiver height is 2m.

A_{bar} is the attenuation due to barriers, assumed to be 0; and A_{misc} is the attenuation due to miscellaneous, assumed to be 0.

5.3. **Improving the Cost Model to be In-line with Industry Data**

According to the conversations with wind farm developers in industry, the Cost-of-Energy (COE) for their farms typically ranges from $51 to $57 per MWh. However, in the author's previous work, the optimal COE from Chapter 3 ranges from $44 to $46 per MWh in the multidirectional wind scenario, and the optimal COE from Chapter 4 ranges from $42 to $48 per MWh. These ranges are about $10 per MWh lower than real industry data because the work has included an economies-of-scale cost reduction coefficient, which is commonly used in academic research, but rarely used in industry. To investigate the impact of cost reduction coefficient on optimal COE for the system model of Chapter 5, the author first conducts an analysis for a certain WFLO problem with a noise model in this section.

Figure 5.2 presents the real piece of land tested in this chapter, which is part of the Story County Wind Farm [124]. There are 16 real turbines placed on the land, marked by

white stars as shown in Figure 5.2. In this section, the author optimizes the layout of 16 turbines for the selected piece of land with all environmental parameters certain using two system models: (1) one with cost reduction coefficient; and (2) one without cost reduction coefficient. Table 5.1 summarizes the optimal results for these two models. The author also conducts a comparative case for the layout of 28 turbines, as shown in Table 5.1.

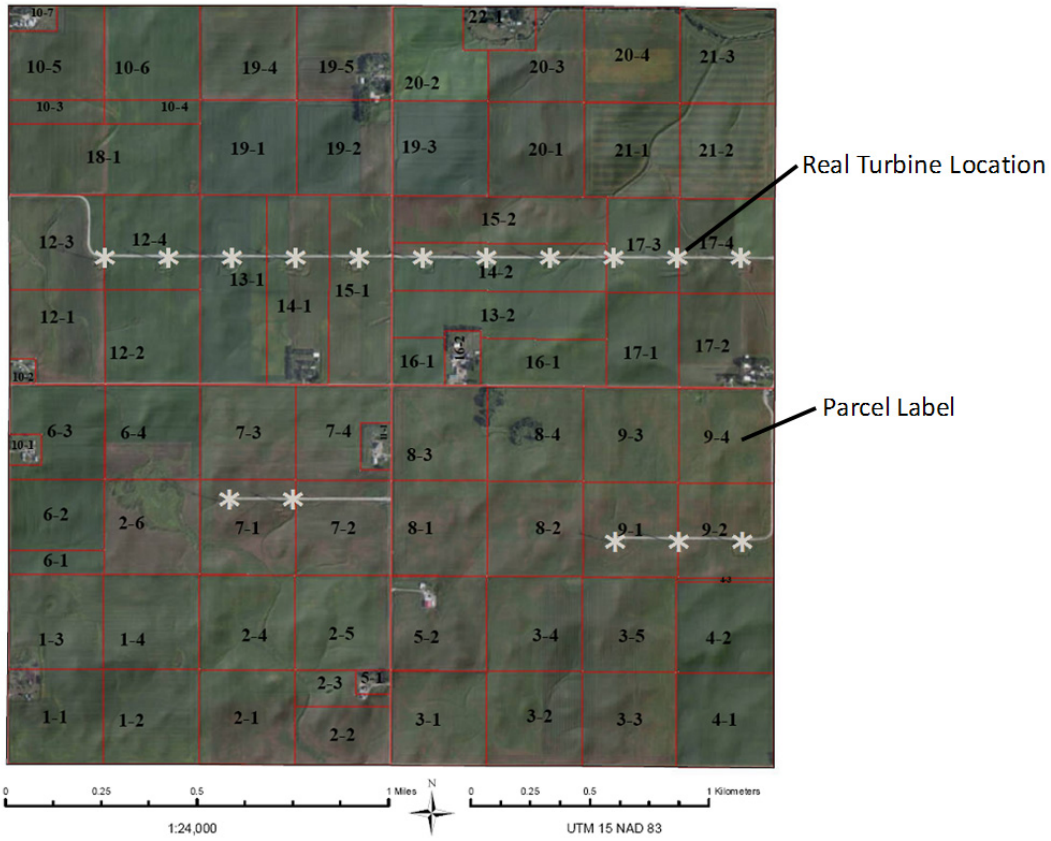

Figure 5.2 The selected piece of land has sixteen wind turbines.

Table 5.1 Optimal COE for a certain WFLO problem with a noise model.

Turbine numbers	Optimal COE with cost reduction coefficient ($/MWh)	Optimal COE without cost reduction coefficient ($/MWh)
16	45.68	50.34
28	42.51	52.70

Table 5.1 shows the optimal COE without including cost reduction is more in line with the real industry data, which ranges from $51 to $57 per MWh, compared to the one with cost reduction. In addition, when the number of turbines increases from 16 to 28, the advantage of removing cost reduction is more obvious, as the optimal COE for 28 turbines with cost reduction is further away from the industry data. The author thus decides to use the system model without a cost reduction term to investigate the optimal COE for number of turbines from 10 to 40, and analyze whether the results are in line with the industry data. Figure 5.3 summarizes the optimal COE for different number of turbines.

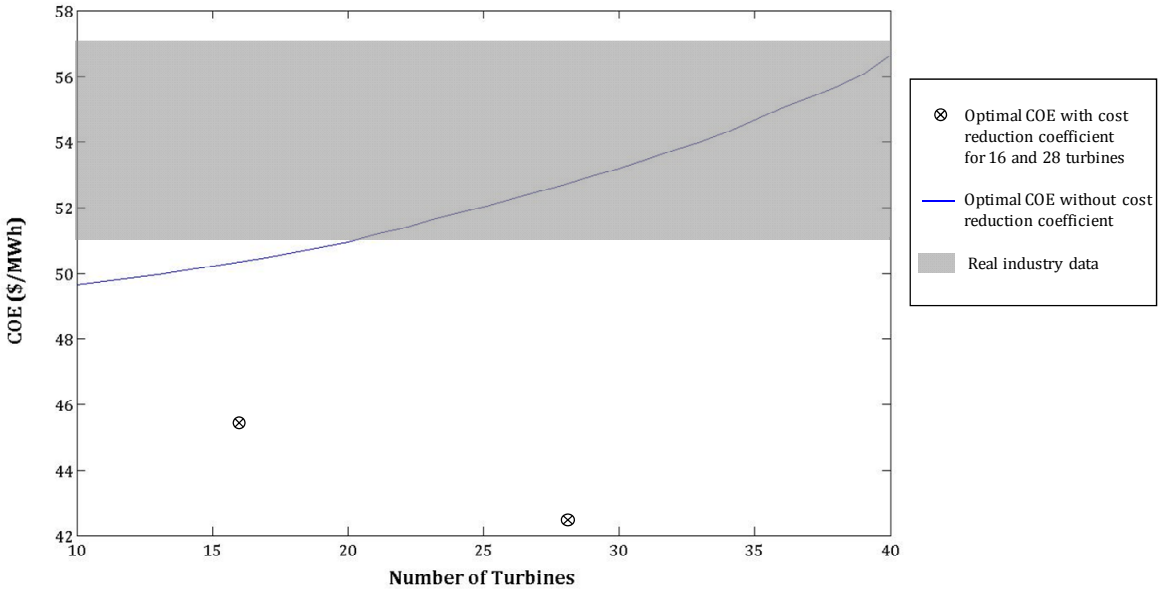

Figure 5.3 Relationship between the optimal COE and the number of turbines.

According to Figure 5.3, the optimal COE ranges from $49.65 to $56.63 per MWh, which is in line with the real industry data. Therefore, the author decides to remove the cost reduction formulation for the system model in this chapter. There are several interesting findings from the above results:

(1) When the number of turbines increases, the COE will also increase. This is because with more turbines placed in the farm, the wake losses will become

more serious. Then the energy output of turbines with wake losses will decrease slightly.

(2) When the number of turbines is relatively small, the COE increases slowly with the number of turbines. For example, the COE only increases 0.11 $/MWh when the number of turbines changes from 10 to 11. However, when the number of turbines changes from 39 to 40, the COE increases 0.56 $/MWh. This trend can also be found in the figure: the slope at the beginning of the curve is much smaller than that at the end of the curve. This is because when the number of turbines is small, the wind resource is not fully used. The optimization algorithm can easily find an optimal layout that adds one more turbine without introducing obvious wake losses. But when the number of turbines is large, adding one more turbine introduces more wake losses.

5.4. **Uncertain Willingness-to-Accept Model for Noise**

The noise disturbance that a landowner hears depends on the distance between their homes and the surrounding turbines. If the noise they hear is above a certain dB level, they will receive an annual compensation amount of up to $1500 in total from developers [133, 134]. In this section, an uncertain willingness-to-accept model for noise is developed to represent the minimum amount of annual payment that a landowner is willing to accept to compensate for a certain noise level.

5.4.1. Community reaction for different noise levels

Ambrose and Rand investigate the community reaction to different noise levels, as show in Table 5.2 [19]. According to this table, people will have no reaction if the noise level

is below 29dB, but will have a strong desire to stop noise if the noise level is above 43dB. Therefore, the work sets 43dB as a hard constraint for the optimization program, i.e. the program guarantees the noise levels for all the residential locations at 2m height are less than 43dB. The model proposes: (1) If the noise level is below 29dB, landowners will not receive any compensation; and (2) If the noise level is between 29dB and 43dB, landowners will receive compensation amounts up to $1500 per year.

Table 5.2 Community Reaction for Different Noise Levels [19]

Community Reaction	Noise Level (dB)
No Reaction	<29
Sporadic Complaints	29-33.5
Widespread Complaints	33.5-43
Strong Appeals to Stop Noise	43-49.5
Vigorous Community Action	>49.5

5.4.2. Landowner noise perception types

Landowners are further divided to three groups according to their perception of noise at 43dB: (1) Type-1 landowners: cannot notice the turbine noise of 43dB (10%); (2) Type-2 landowners: can notice the turbine noise of 43dB, but do not feel annoyed (75%); and (3) Type-3 landowners: feel annoyed at turbine noise of 43dB (15%). The percentage for each landowner type is based on the study conducted by Pedersen and Waye [21], which evaluates the perception and annoyance of wind turbine noise among people living near the turbines. Note that the landowner types for noise in this section are different from the landowner types for participation, as discussed before in Section 4.2.2. Each landowner will have a different profile for noise perception and participation willingness.

5.4.3. Willingness-to-Accept utility model for noise

The author defines $WTA_{n,43}$ as the minimum annual payment that a landowner is willing to accept to compensate for the noise level of 43dB:

$$U\left(m_0 + WTA_{n,43}, 1\right) \geq U\left(m_0, 0\right) \tag{5.7}$$

Where U is a landowner's utility function; m_0 is the landowner's initial wealth; $WTA_{n,43}$ is the landowner's minimum WTA dollar amount for a 43dB noise; "1" represents the presence of a 43dB turbine noise at the landowner's house; and "0" represents the absence of turbine noise at the landowner's house.

In this chapter, $WTA_{n,43}$ is modeled as an epistemic uncertainty. The reasonable range of $WTA_{n,43}$ is set to be between \$0 and \$1500, which is the typical compensation range offered by developers [133, 134]. Landowners are classified into three types, each with their own uncertain $WTA_{n,43}$, as shown in Table 5.3. (1) Type-1 landowners, as discussed above, cannot notice the turbine noise of 43dB. Therefore, the $WTA_{n,43}$ is most likely to be between \$0 and \$500 (Probability=0.7) and between \$500 and \$1000 (Probability=0.3); (2) Type-B landowners can notice the turbine noise of 43dB, but do not feel annoyed. Therefore, the $WTA_{n,43}$ is equally likely to be between \$0 and \$500 (Probability =0.5) and between \$500 and \$1000 (Probability=0.5); (3) Type-C landowners feel annoyed at turbine noise of 43dB. Therefore, the $WTA_{n,43}$ is most likely to be between \$1000 and \$1500 (Probability=0.7) and \$500 and \$1000 (Probability=0.3).

Table 5.3 Intervals and probabilities, assumed for the $WTA_{n,43}$.

$WTA_{n,43}$ for type-1 Landowners ($/yr)			
Intervals	[0,500]	[500,1000]	[1000, 1500]
Probabilities	0.7	0.3	0
$WTA_{n,43}$ for type-2 Landowners ($/yr)			
Intervals	[0,500]	[500,1000]	[1000, 1500]
Probabilities	0.5	0.5	0
$WTA_{n,43}$ for type-3 Landowners ($/yr)			
Intervals	[0,500]	[500,1000]	[1000, 1500]
Probabilities	0	0.3	0.7

Given the $WTA_{n,43}$ amount ($/yr) of a landowner, the author assumes that the landowner's minimum WTA amount for a noise level of L_{AT} follows a linear relationship:

$$WTA_n(L_{AT}) = \begin{cases} 0 & L_{AT} \le 29\,\text{dB} \\ \dfrac{(L_{AT}-29)\times WTA_{n,43}}{43-29} & 29\,\text{dB} < L_{AT} < 43\,\text{dB} \\ WTA_{n,43} & L_{AT} = 43\,\text{dB} \\ \text{inf} & L_{AT} > 43\,\text{dB} \end{cases} \tag{5.8}$$

Where $WTA_n(L_{AT})$ is the landowner's minimum WTA amount in $/yr for a noise level of L_{AT}; L_{AT} is real receiver noise level in dB at the landowner's house, calculated through Equation (5.1); $WTA_{n,43}$ is the given WTA amount ($/yr) of the landowner for a 43dB noise.

As discussed above, when the noise level is below 29dB, landowners will have no reaction according to a study conducted by Ambrose and Rand [19]. Therefore, $WTA_n(L_{AT})$ is set to be 0 when L_{AT} is below 29dB, indicating landowners are willing to accept a noise

level below 29dB without compensation. However, when the noise level is above 43dB, landowners will have strong appeals to stop noise [19]. Therefore, $WTA_n(L_{AT})$ is set to be infinite when L_{AT} is above 43dB, indicating landowners are not willing to accept a noise level above 43dB no matter how much compensation they receive from the developers.

Similar as the equal compensation model for participation, as discussed in Section 5.1, the author develops an equal compensation model for noise in this section to mimic the real world situation. In wind farm practices, if develops pay a certain annual amount for a landowner who hears a certain noise level, they need to pay everyone else the same compensation as long as they hear the same noise level. Therefore, the author uses the maximum WTA_n for a 43dB noise among all the landowners to replace the $WTA_{n,43}$ in Equation (5.8), and calculate the final noise compensation for each landowner.

5.5. **Problem Formulation**

5.5.1. Land and location introduction

A square piece of land from Story County Wind Farm [124] in central Iowa is selected to test the proposed system model in this chapter. The wind farm is located approximately 20 miles east of the Iowa State University campus, and is operated by NextEra Energy [126]. Figure 5.4 is a representation of the land with red lines indicating the boundary of each individual land parcel. The two by two miles square land is owned by 22 landowners. Most landowners own multiple land parcels. Each parcel is marked by a unique black label, as shown in Figure 5.4. For example, the label “9-4” indicating the

corresponding parcel is the fourth parcel owned by landowner 9. Note that all parcels owned by the same landowner will have same WTA profiles for participation and noise.

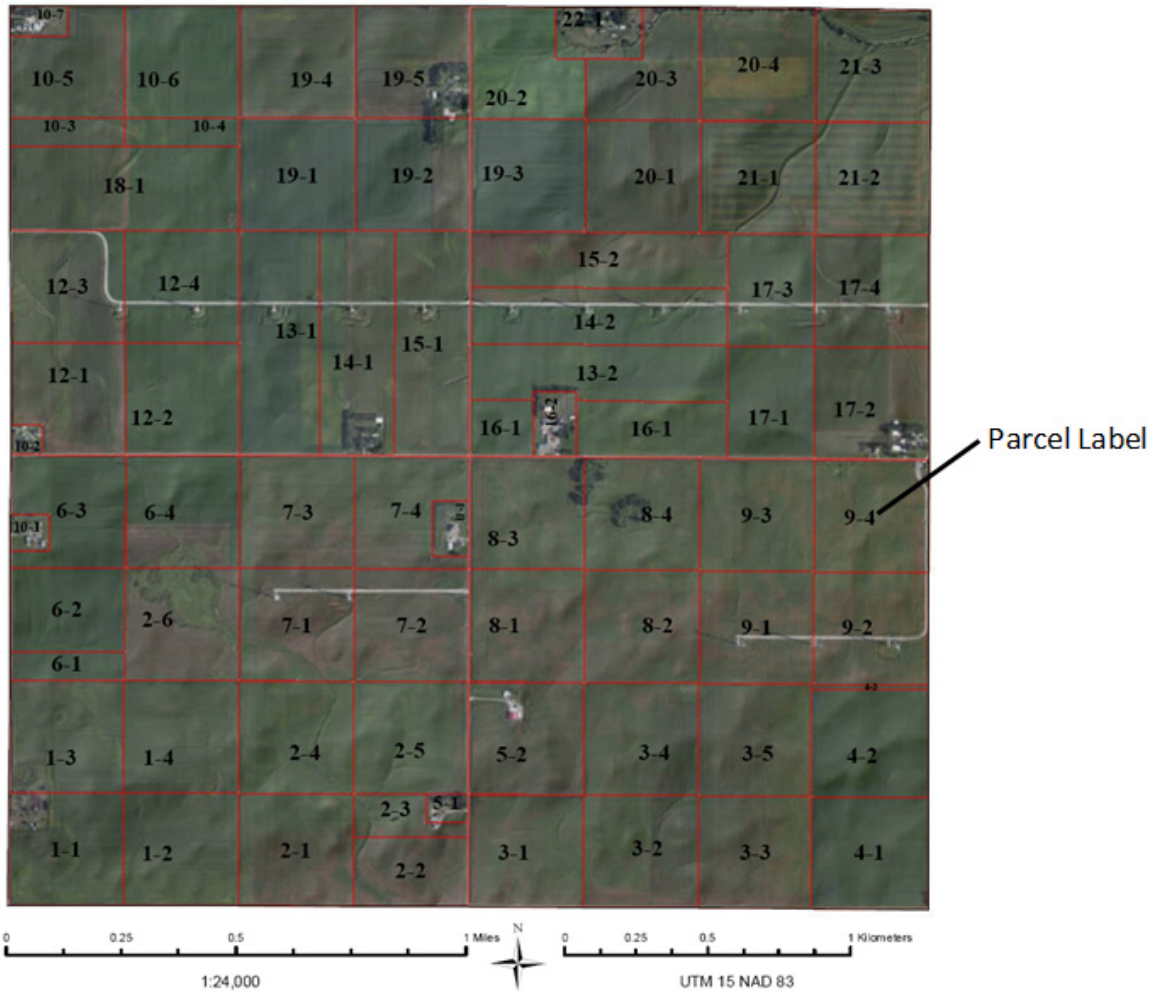

Figure 5.4 The selected piece of land has 22 landowners.

The model allows for 100 potential locations for turbines, as indicated by the white circles in Figure 5.5. The distance between any two potential locations is set to be more than four rotor diameters to reduce wake interactions. Future work will modify the formulation with more potential locations to investigate a wider solution space.

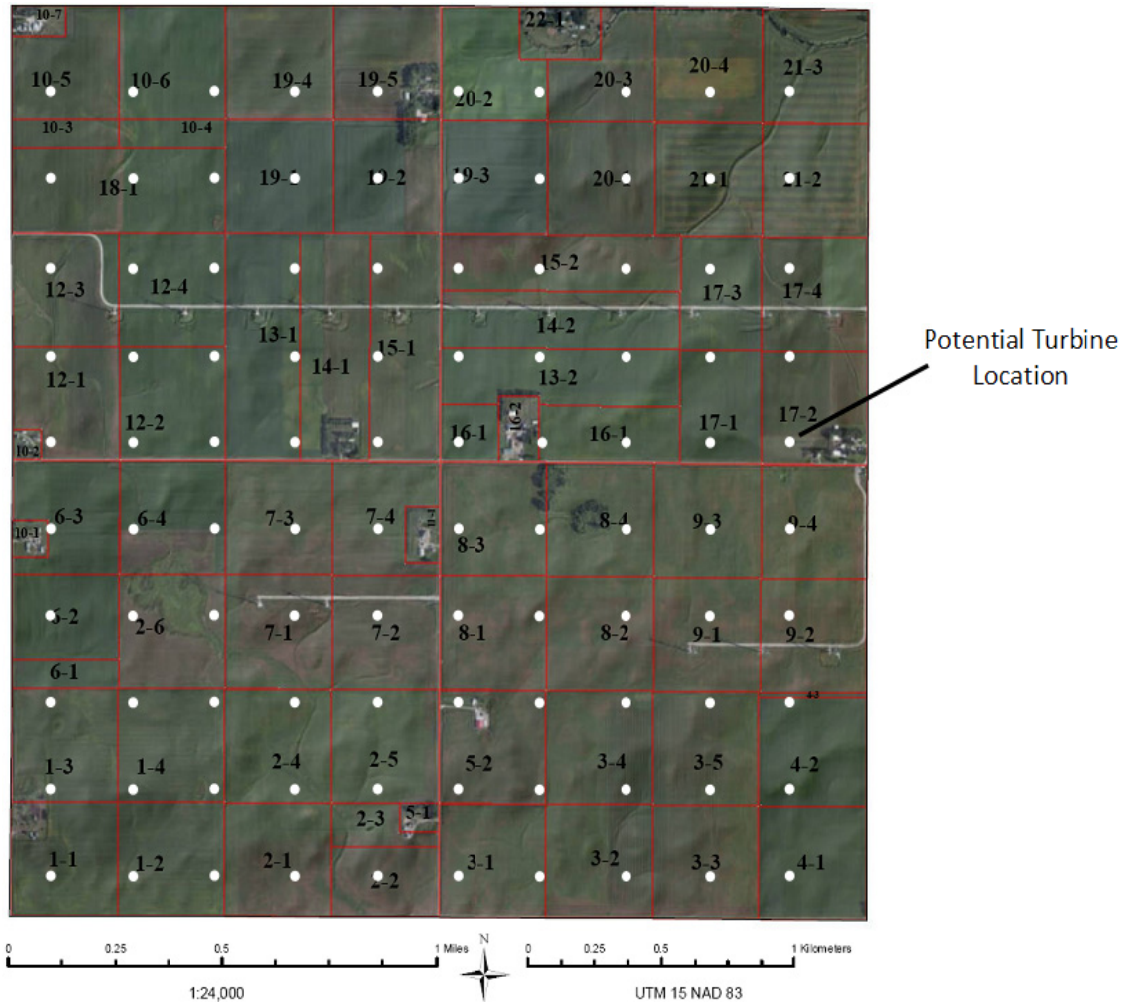

Figure 5.5 The selected piece of land has 100 potential turbine locations.

5.5.2. Distribution of landowner types for participation willingness and noise perception

Four types of landowners are modeled with different participation willingness, as detailed in Section 4.2.2 of Chapter 4. Classifications are shown in Table 5.4:

Table 5.4 Landowner type for participation willingness, assumed for 22 landowners.

Landowner type for participation willingness	Landowner #
Type-A	Landowners 1, 3, 6, 9, 11, 14, 16, and 22
Type-B	Landowners 2, 7, 13, 17, and 21
Type-C	Landowners 4, 5, 12,15, 18, and 19
Type-D	Landowners 8, 10, and 20

Twelve houses, determined as the noise receivers in this chapter, are located at the selected piece of land, as shown in Figure 5.6. The houses are owned by nine landowners. Figure 5.6 represents the location and ownership of these houses (each house is marked by a yellow number with a yellow point indicating its central location). Three types of landowners with different noise perception are modeled. Based on the study conducted by Pedersen and Waye [21], as discussed in Section 5.4.2, the percentages for Type-1, Type-2, and Type-3 landowners are 10%, 75%, and 15% respectively. Therefore, the formulation assumes one type-1 landowner, seven type-2 landowners, and one type-3 landowner, summarized in Table 5.5..

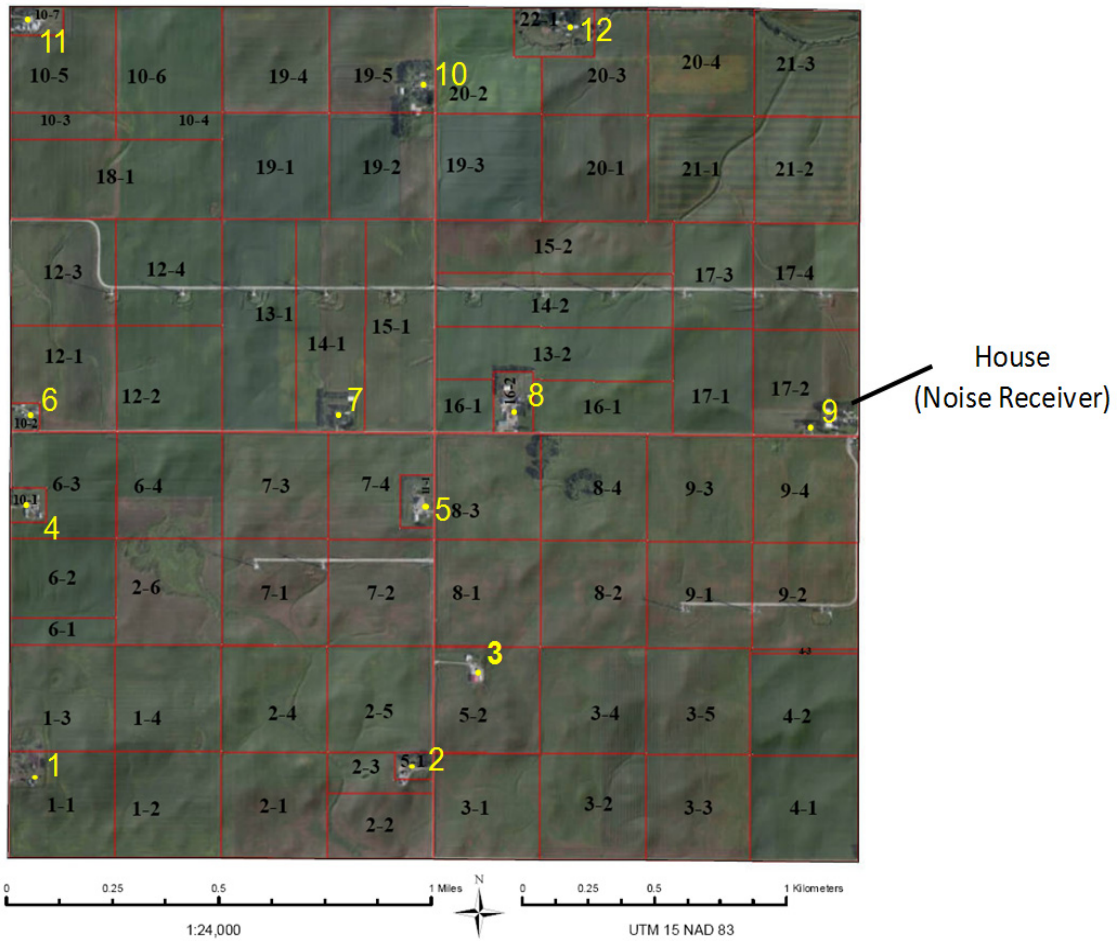

Figure 5.6 Twelve houses, owned by nine landowners.

Table 5.5 Noise-perception type, assumed for each landowner with a house.

House #	Landowner #	Noise-perception type
1	1	Type-2
2	5	Type-3
3	5	Type-3
4	10	Type-2
5	11	Type-2
6	10	Type-2
7	14	Type-2
8	16	Type-2
9	17	Type-1
10	19	Type-2
11	10	Type-2
12	22	Type-2

5.5.3. Objective function

The objective for the deterministic system model is minimizing COE given environmental parameters P for a fixed number of turbines (16 turbines for the selected piece of land), defined as:

Minimize:

$$COE(X,P)=\frac{C(X,P)}{AEP_{tot}(X,P)} \tag{5.9}$$

Subject to:

$$h(X)=N(X)=16 \tag{5.10}$$

Where $COE(X,P)$ is the cost of energy of the farm in \$/MWh, as detailed in Section 5.1; $C(X,P)$ is the levelized cost per year of a wind farm in dollars; $AEP_{tot}(X,P)$ is the farm's total annual energy in MWh; $h(X)$ is the equality constraint; and $N(X)$ is the total number of turbines in the farm. X is a 100-bit binary string design variable representing the potential turbine locations. The equality constraint $h(X)$ indicates the total number of

turbines selected by the optimization program will be fixed at 16. This number is selected based on the real number of turbines within the selected land, as shown in Figure 5.2. In implementation, it is straight-forward to modify this number to meet developers' expectation.

5.6. **Results**

GAlib was used to solve the optimization problem. A penalty function for constraint violation, as introduced in Section 3.2.1, was used to address the equality constraint of Equation (5.10). The optimization program ran in three different scenarios: (1) minimize the mean value of COE; (2) minimize the standard deviation of COE; and (3) compromise programming with two minimization objectives: the normalized mean value and standard deviation of COE. For each scenario, the program ran over ten times with 10000 iterations each time. The best results of the ten runs are recorded in Table 5.6. The noise levels for the 12 noise receivers (houses) are summarized in Table 5.7. Note that the convergence histories of the three scenarios are not presented here, as they are all similar to Figure 4.11 in Chapter 4.

Table 5.6 Results summarized from the optimization program for 16 turbines.

Scenarios	1	2	3
Objectives	Minimize μ_{COE} Individually	Minimize σ_{COE} Individually	Minimize $\left[\frac{\mu_{COE}}{\mu^*_{COE}}, \frac{\sigma_{COE}}{\sigma^*_{COE}}\right]$
μ_{COE} ($/MWh)	52.44	52.51	52.44
σ_{COE} ($/MWh)	5.08	5.08	5.08
μ Energy Output (MWh/yr)	73838.4	73707.1	73837.7
μ Cost Output ($k/yr)	3831.60	3829.90	3831.64

Table 5.7 Noise levels, summarized for the 12 noise receivers (houses).

Scenarios	1	2	3
Objectives	Minimize μ_{COE} Individually	Minimize σ_{COE} Individually	Minimize $\left[\frac{\mu_{COE}}{\mu^*_{COE}}, \frac{\sigma_{COE}}{\sigma^*_{COE}}\right]$
Noise Level for House 1 (dB)	39.48	40.52	39.45
Noise Level for House 2 (dB)	42.91	39.44	42.89
Noise Level for House 3 (dB)	38.49	38.36	38.37
Noise Level for House 4 (dB)	42.84	42.80	42.81
Noise Level for House 5 (dB)	38.66	37.29	37.80
Noise Level for House 6 (dB)	42.29	42.12	42.24
Noise Level for House 7 (dB)	42.43	39.52	39.73
Noise Level for House 8 (dB)	41.23	38.16	40.74
Noise Level for House 9 (dB)	42.67	42.34	42.67
Noise Level for House 10 (dB)	38.78	39.24	41.92
Noise Level for House 11 (dB)	37.31	37.14	37.32
Noise Level for House 12 (dB)	34.63	34.88	36.30
Average Noise Level (dB)	40.14	39.32	40.19

Figures 5.7 through 5.9 present the optimal layouts for the three scenarios, with representing the optimized turbine locations.

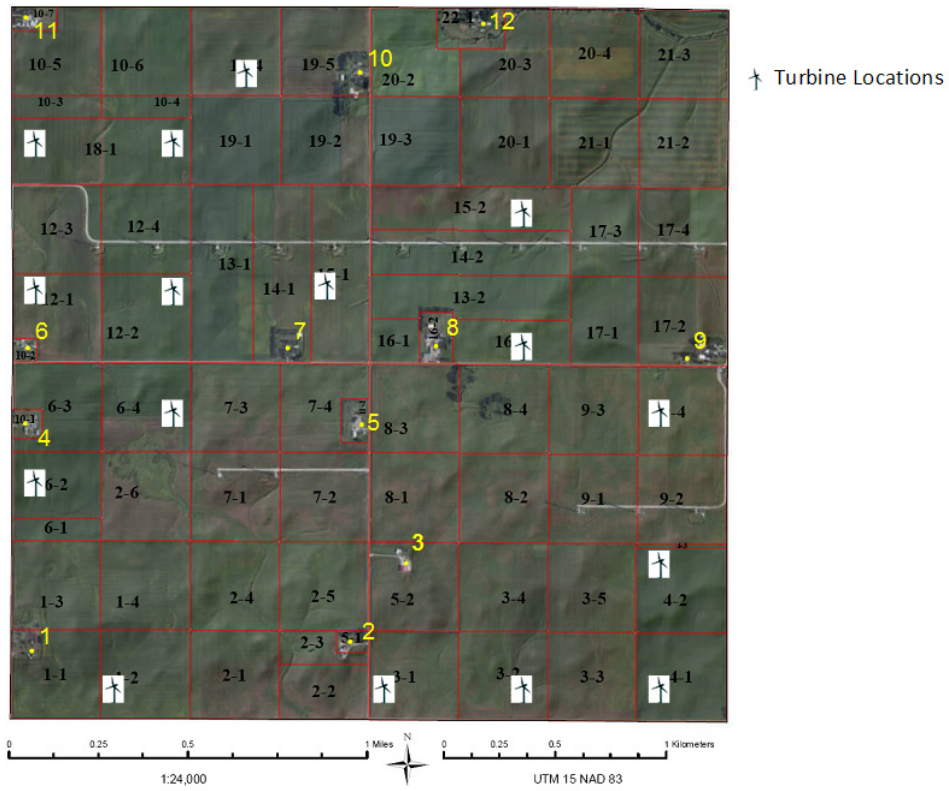

Figure 5.7 Optimal layout minimizing μ_{COE} .

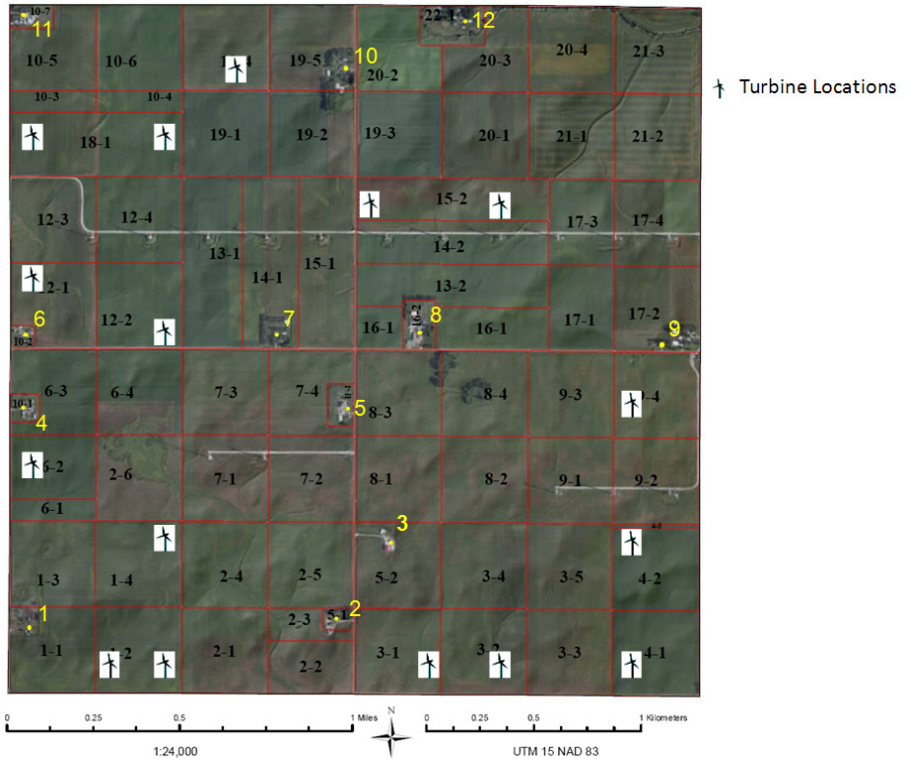

Figure 5.8 Optimal layout minimizing σ_{COE} .

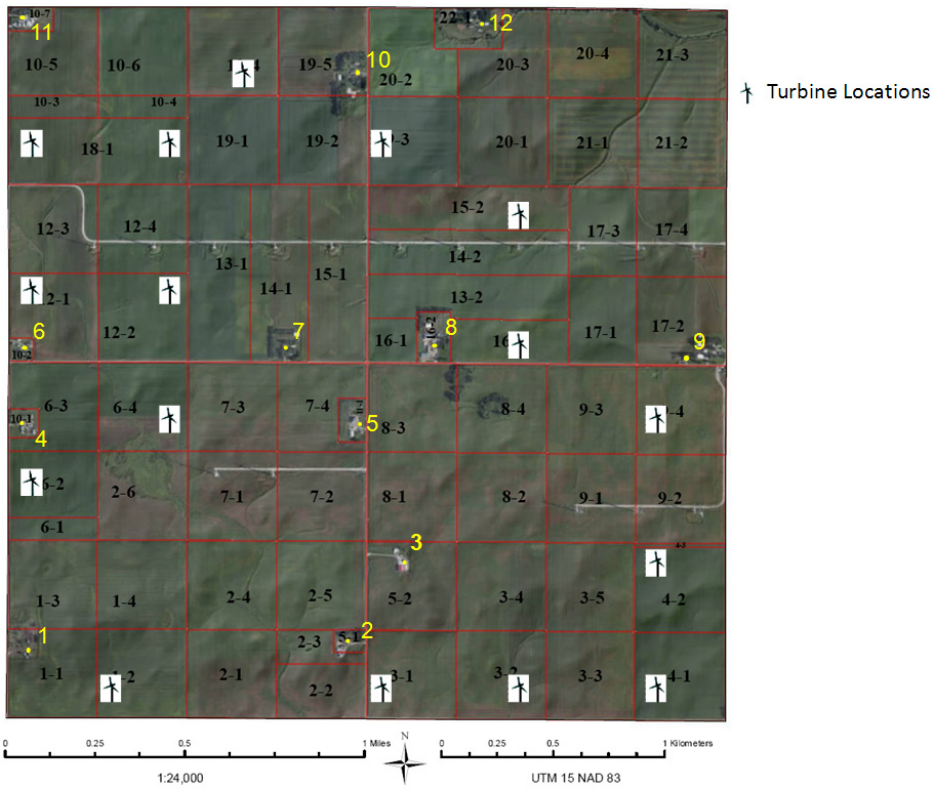

Figure 5.9 Optimal layout minimizing μ_{COE} and σ_{COE}.

5.7. **Discussion**

As shown in Table 5.6, all the three scenarios have the same σ_{COE} to significant digits. It indicates that the variance of COE does not vary when the number of turbines in the farm is fixed. A similar finding has been discussed before in Section 4.5 of Chapter 4. It indicates the variance of COE is correlated with the number of turbines. Scenarios (1) and (3) have very similar results, including μ_{COE}, σ_{COE}, mean energy output and mean cost output, as summarized in Table 5.6. This is because minimizing μ_{COE} individually will not be obviously different from minimizing both μ_{COE} and σ_{COE}, as the σ_{COE} will basically not vary when the number of turbines is fixed. Therefore, in order to save calculation expenses,

running only one scenario to minimize the mean value of COE will be sufficient for the robust optimization problem when the number of turbines in the farm is predetermined.

Table 5.7 shows that scenarios (1) and (3) have very similar noise outputs for the 12 houses. In Table 5.7, houses 2 and 9 receive the highest noise level for scenarios (1) and (3), while house 12 receives the lowest. As discussed in Section 5.4.3 and Table 5.5, house 9 is owned by a Type-1 landowner, who does not hear the turbine noise of 43dB. Therefore, the noise level for this house is one of the highest. However, house 2 is owned by a Type-3 landowner, who will feel annoyed at turbine noise of 43dB. To save the compensation cost for noise, the noise level of house 2 should be minimized. But house 2 is located at the boundary of the entire land plot, which is favored by the optimization program to reduce wake losses. Therefore, the optimization program does not avoid placing turbines around house 2, as its location benefit outweighs the extra compensation for noise. On the other hand, house 12, which is also located at the boundary of the entire land plot as house 2, receives the lowest noise level. This is because house 12 is surrounded by landowner 20, who is a Type-D landowner with the highest remittance requirement for participating in the project, as discussed in Table 5.4. If turbines are placed on the land of owner 20, all the other landowners will receive the same remittance fees, which would be set to landowner 20's level. Therefore, to save the remittance fees for participation, no turbines are placed around house 12, which results in the lowest noise level of house 12.

Scenarios (1) and (3) also have quite similar optimal layouts, as shown in Figures 5.7 and 5.9. Note that no turbines are placed on the land of type-D landowners (landowners 8, 10 and 20) for the three scenarios. As discussed in Section 4.2.2, type-D landowners request

the highest remittance fees for participation. Therefore, the optimization program avoids placing turbines on the land of such landowners to keep remittance fees down.

5.8. **Conclusion**

This chapter addresses the limitation of previous research and develops an uncertain willingness-to-accept model for noise, which represents the minimum amount of annual payment in dollar that a landowner is willing to accept to compensate for a certain noise level. The uncertain WTA model, together with a noise propagation model and two other important sources of uncertainty, is then incorporated into the previous-developed optimization-under-uncertainty system model. The proposed system model is tested on a real piece of land in Iowa with 22 landowners and 12 noise receivers (houses).

In Table 5.6, the optimal mean value of COE ranges from \$52 to \$53 per MWh, which is in line with the real COE data in industry. Scenarios (1) and (3) have very similar optimization results, which indicate minimizing μ_{COE} individually will not be obviously different from minimizing both μ_{COE} and σ_{COE}, as the σ_{COE} will basically not vary when the number of turbines is fixed. This finding can be beneficial for developers: it means, if the developers can predetermine the number of turbines in the farm, running only one scenario to minimize the mean value of COE will be sufficient to obtain a robust optimal farm layout. This will save considerable time and calculation expenses for a real wind farm project.

The noise outputs summarized in Table 5.7 and the optimal layouts in Figures 5.7 though 5.9 indicate a range of landowner importances in determining project success. The crucial landowners are identified by the optimization program based on many conflicting factors, such as their location benefits, their WTAs for participation in the project, and their

noise perception types. The WTA for participation in the project, which has an uncertain range from $1000 to $50000 per MW installed, plays an important role in determining crucial landowners, as proved in the optimal layouts in figures 5.7 though 5.9—all type-D landowners who request the highest WTAs are not included in the layouts. However, the annual monetary compensation for noise, which has a small uncertain range from $0 to $1500, plays a less important role in determining crucial landowners, as proved in Table 5.7—the noise level of house 2 is the highest although it is owned by a landowner with a high noise compensation request. It indicates the location benefit of house 2 outweighs the additional noise compensation. Therefore, determining the importance of a landowner is not a straightforward work for developers. The proposed optimization-under-uncertainty system model can help developers identify plots of land that are worth the extra investment.

This work has a few limitations. As the estimations of uncertain parameters are all based on assumptions in this chapter, it would be best to conduct interviews with real developers and landowners to improve accuracy. This could be accomplished through an anonymous survey, with results distributed to all interested parties. Additionally, different types and sources of uncertainty can be added, such as those associated with turbine failure. Moreover, the optimization program only tests 100 potential turbine locations in this chapter. In the future, it would be best to investigate a wider solution space with more potential turbine locations. The noise propagation model used in the work is a basic one based on ISO 9613-2:1996. A more complicated noise model could be included to further validate the results.

CHAPTER 6. CONCLUSION

6.1. **Contributions**

This research addresses the limitations of current wind farm layout optimization research, and develops an optimization-under-uncertainty system model with landowners' financial and noise concerns. Unlike NREL's model that uses arbitrary constants to estimate costs, this work adds realism to the wind farm layout optimization problem to improve predictions. The optimal COE results found in the research are closer to the actual industry data than NREL's Model. The system model aims to help wind farm developers and landowners make wise decisions during the early development stages of a wind farm project. It would give landowners an idea of where turbines are likely to be placed on their land, and the likely auditory impacts. It would also give developers the ability to predict land plots that are crucial to the success of the project, and those that are less crucial, and realistic estimates of costs and profitability. The transparency of information during the early farm development stages would facilitate the negotiation process between developers and landowners, and ultimately improve the success rates of wind projects.

Chapter 3 first incorporates the landowner issues into the wind farm layout optimization research. It relaxes the assumption that a continuous piece of land is available, developing a novel approach that represents landowner participation scenarios as a binary string variable. In addition, unlike other research that uses a pseudo-COE formulation, Chapter 3 develops a realistic COE model and incorporates it into a wind farm layout optimization system model. The system model is tested under two land–plot shapes: equally-sized square land plots and unequal rectangle land plots. It can help site developers

identify the most crucial land plots for project success and the optimal position of turbines, with realistic estimates of costs and profitability prior to the negotiation process with landowners. Using this approach, a site developer can spend more resources on persuading these most-important landowners to take part in the project, or approach them in a personalized manner. This will ultimately increase the efficiency of wind farm projects, saving time and money in the development stages.

Chapter 4 advances the system model developed in Chapter 3 using an optimization-under-uncertainty approach. An optimization-under-uncertainty system model is developed in this chapter to assist in early-stage wind farm development. A wind farm layout is optimized under multiple sources of uncertainty. Yearly wind data is modeled as aleatory uncertainty using a Weibull distribution. Landowner participation is represented with a novel uncertain model of willingness-to-accept monetary compensation. An uncertain wind shear parameter and economies-of-scale cost reduction parameter, which are identified as important through a sensitivity analysis, are also included. Probability Theory is used to model the epistemic uncertain parameters, and Latin Hypercube Sampling to propagate the uncertainty throughout the system. Compromise programming is used to search for the non-dominated solution that best satisfies the two objectives: minimize the normalized mean value and the standard deviation of the COE. The results suggest that some landowners that will only accept high levels of compensation are worth pursuing, while others are not. The proposed optimization-under-uncertainty system model can mitigate risks for both wind farm developers and landowners. It demonstrates that even in the uncertain development environment, the work can still help developers

predict the viability of the project with an estimated COE and give landowners an idea of where turbines are likely to be placed on their land.

Chapter 5 further advances the optimization-under-uncertainty system model with landowners' noise concern. Unlike previous research which typically sets the noise generation of a wind farm as a constraint or an objective function, Chapter 5 takes into account the monetary compensation related to noise disturbance and develops an uncertain willingness-to-accept model for noise, which represents the minimum amount of annual payment in dollar that a landowner is willing to accept to compensate for a certain noise level. The uncertain willingness-to-accept model, together with a noise propagation model and two other important sources of uncertainty, is then incorporated into the optimization-under-uncertainty system model. The advanced system model is tested on a real piece of land in Iowa with 22 landowners and 12 noise receivers (houses). The crucial landowners are identified by the optimization program based on many conflicting factors, such as their location benefits, their WTAs for participation in the project, and their noise perception types. The proposed system model can help developers identify plots of land that are worth the extra investment, and provide developers a robust wind farm design that is not only profitable but also has minimal noise disturbance for landowners. It can also give landowners an idea of where turbines are likely to be placed on their land, and the likely auditory impacts.

6.2. **Benefits for Developers and Landowners**

The system model proposed in this research is beneficial for both developers and landowners. The optimal results in Chapter 5 indicate a range of landowner importances in

determining project success. The crucial landowners are identified by the optimization program based on many conflicting factors, such as their location benefits, their WTAs for participation in the project, and their noise perception types. The results show some landowners that will only accept high levels of compensation are worth pursuing, which indicates evaluating the land of reluctant landowners individually can be important to the project. Therefore, the system model has the potential to substantially change the land acquisition process. Developers typically offer landowners all the same remittance fee, as they are unsure whose land will be most crucial, and they do not want to enter into negotiations with each individual landowner. The model can help developers identify plots of land that are worth the extra investment with realistic estimations of costs and profitability. Also, it can help landowners adjust their compensation expectations, either higher or lower, without pricing themselves out of participation.

In addition, the system model can mitigate risks for landowners. In wind farm practices, landowners are offered a contract for access to the entire plot of land, with no guarantee on the noise impact, visual impact, construction impact on crops, or inconvenience during turbine installation and maintenance. It is very difficult for landowners to value the compensation package, as they are given incomplete information on how the turbines will impact their lifestyle and land. The proposed system model in this research can provide landowners an idea of where turbines are likely to be placed on their land and the likely auditory impacts. This will help landowners make wise participation decisions and mitigate their risks.

Although the proposed system model is specifically designed for the early development stages in a wind project, it can be used in all stages. During the very early

development stages before the negotiation process, the estimations of uncertain parameters (e.g. WTAs for all the landowners) could be replaced by typical values (e.g. $1000-$5000 for WTAs). Then the optimization model can be used to identify the most crucial landowners for negotiations. During negotiations, the estimations of uncertain WTAs could be updated iteratively. When the uncertain parameters become relatively certain, they can be updated again and the final layout determined.

To implement the proposed system model to actual wind practices, a few extensions are needed. First, developers should be able to obtain the basic wind and land condition of the potential wind farm site, e.g. the yearly wind data from nearby station, the ownership of each land parcel, the boundary of each land parcel, and etc. Then, developers are expected to have basic estimations of landowners' WTAs through their communications and negotiations. Finally, developers should have access to machines with high computationally efficiency, as the running time of the optimization program highly depends on the machines' computation capability. There are also extensive programming needs if the potential site is large with considerable land parcels.

6.3. **Limitations**

This work has a few limitations. There are costs not accounted for, which are open to future work. For example, the optimal layouts found in this study use discontinuous pieces of land to reduce wake losses between adjacent turbines. However, this will increase installation and O&M costs not accounted for explicitly here, and make road planning for installation and maintenance of turbines more complicated. This impact on cost could be analyzed with a more detailed cost model.

Land plots in Iowa are typically used for agricultural purposes, e.g. producing soybean and corn. The construction and maintenance of wind farms has a negative impact on crop productions. This work has a purely economic analysis for the agricultural losses due to wind farm construction and maintenance, as introduced in Appendix, but does not include perceived risk of crop damage which may manifest as hindrance to accepting the developer's contract. Similarly, landowners' concern of shadow flicker is also not addressed in this research.

The work only models three sources of uncertainty. Wind farms also have uncertainty in mechanical system performance, which could be address through reliability-based design, but has not been addressed in the work. Additionally, the estimations of uncertain parameters are all based on assumptions, it would be best to conduct interviews with real developers and landowners to improve accuracy. This could be accomplished through an anonymous survey, with results distributed to all interested parties.

In Chapter 5, the optimization program only tests 100 potential turbine locations. In the future, the author would like to investigate a wider solution space with more potential turbine locations, and test whether the wider solution space will lead to a better optimization results.

In addition, the noise propagation model used in the work is a basic one based on ISO 9613-2:1996. The model calculates the worst receiver noise levels for the 12 houses using the maximum source noise level, e.g. the maximum noise level emitted from the rotor blades. In reality, the source noise level varies a lot during different times of day and by season, depending on the wind resource. Landowners might have different WTA requests for noise during different times of day, e.g. a higher WTA request for noise during night time

due to sleep disturbance. In the future, a more nuanced models of noise and noise perception and acceptance could be included to further enhance the results.

The wake loss model used in the study is a basic one based on Jensen's model. More complicated wake loss models are available in the literature [61, 65, 66]. Gaumond et al. compared three wake models and found out that the Jensen model might underestimate wake losses for a large wind farm [69]. To address this limitation, a further experiment could be conducted to determine which, if any, wake loss model is best in terms of accuracy for Iowa wind farms. Then the most appropriate wake model could be incorporated into the proposed system model to provide more realistic results.

This research can be extended in several ways. First, the optimization program could be improved with a wider solution space and better optimization algorithm. In addition, the COE system model could be enhanced with more complex models, e.g. noise propagation model, installation and maintenance cost model, wake loss model, and etc. Other important concerns of landowners, such as crop damage and shadow flicker, could also be included. Finally, the author could cooperate with developers to work on actual wind projects. The real inputs from developers and landowners could be used to further test the feasibility of the proposed system model.

APPENDIX: AGRICULTURAL LOSSES DUE TO WIND FARM CONSTRUCTION AND MAINTENANCE

During the wind farm construction period, temporary service roads and a disturbed land area near the turbines take some land out of crop productions [138]. The transportation of large and heavy equipment can damage the soil and drainage tiling, and result in a temporary crop yield loss that can last up to 5 years. Once wind farm construction is completed, the width of service roads is usually reduced, and some are permanently used for maintaining the wind farm.

Arvidsson and Håkansson develop a crop yield loss model for soil compaction based on experimental results on Swedish fields [139]. The empirical model estimates the crop yield loss based on traffic intensity, soil moisture content, tire pressure and clay content. The author applies this model to Story County Wind Farm in Iowa, estimating the traffic intensity during wind farm construction. As the crop yield loss model is based on Swedish fields, the accuracy of predictions for Iowa may have unknown limitations.

For the land temporarily damaged during construction, the annual crop yield loss is calculated at 42.57% based on the model in [139]. The author assumes that the area of temporarily damaged land per turbine construction is 1 hectare. The annual temporary monetary losses per turbine construction for corn following soybean land in Iowa were estimated as detailed in . Note that the crop profit margin per hectare is obtained from a study conducted by Johnson for corn following soybean land in Iowa, as detailed in [140]. also summarizes the annual permanent monetary losses per turbine construction for corn following soybean land in Iowa, with the assumption that a land area of 0.5 hectare is

permanently used per turbine construction for putting up turbine base and building the narrowed service roads.

Table 6.1 Annual monetary loss per turbine due to wind farm construction and maintenance for corn following soybean land in Iowa

Crop Type	Corn Following Soybean
Crop Profit Margin Per Hectare ($/ha) [140]	1396.15
Temporarily Damaged Land Area Per Turbine Construction (ha)	1
Temporary Monetary Loss Calculation	0.4257 x 1 x 1396.15
Temporary Monetary Loss Per Turbine Construction ($/yr)	594.34
Permanently Used Land Area Per Turbine Construction (ha)	0.5
Permanent Monetary Loss Calculation	0.5 x 1396.15
Permanent Monetary Loss Per Turbine Construction ($/yr)	698.07
Total Monetary Loss Per Turbine Construction ($/yr)	1292.41

REFERENCES

[1] United States Department of Energy, 2008, "20% Wind by 2030," Increasing Wind Energy's Contribution to U.S. Electricity Supply, available at http://www.nrel.gov/docs/fy08osti/41869.pdf, accessed on Oct. 28, 2013.

[2] Samorani, M., 2010, "The Wind Farm Layout Optimization Problem," Technical Report, Leeds School of Business, University of Colorado at Boudler.

[3] Burkholder, J., 2008, "Trade Wind Reps Host Public Dinner and Presentation," available at http://www.clintondailyjournal.com/V2_news_articles.php?heading=0&story_id=1763&page=, accessed on Oct. 28, 2013.

[4] Wüstenhagen, R., Wolsink, M., and Bürer, M., 2007, "Social Acceptance of Renewable Energy Innovation: An Introduction to the Concept," *Energy Policy*, 35(5), pp. 2683-2691.

[5] Hoen, B., Wiser, R., Cappers, P., Thayer, M., and Sethi, G., 2009, "The Impact of Wind Power Projects on Residential Property Values in the United States: A Multi-Site Hedonic Analysis," Technical Report: LBNL-2829E, Ernest Orlando Lawrence Berkeley National Laboratory.

[6] Macalester College, 2011, "Wind Energy – Visual Impacts and Public Perception: Cascade Wind," available at http://www.macalester.edu/windvisual/cascadeinfo.html, accessed on Jan. 5 2013.

[7] Community Energy, 2008, "Jordanville Wind," available at http://www.macalester.edu/windvisual/JordanvilleWind2p.pdf, accessed on Jan. 5 2013.

[8] Iberdrola Renewables, 2008, "Elk River Wind," available at http://www.macalester.edu/windvisual/ElkRiver2p.pdf, accessed on Jan. 5 2013.

[9] FPL Energy, 2008, "Horse Hollow," available at http://www.macalester.edu/windvisual/HorseHollow2p.pdf, accessed on Jan. 5 2013.

[10] Highland New Wind Development, 2008, "Highland New Wind," available at http://www.macalester.edu/windvisual/HighlandNewWind2p.pdf, accessed on Jan. 5 2013.

[11] Windustry, 2009, "Wind Energy Easement and Leases: Compensation Packages," Windustry's Wind Easement Work Group, available at http://saline.unl.edu/c/document_library/get_file?folderId=294039&name=DLFE-18538.pdf, accessed on Oct. 28 2013.

[12] Fingersh, L., Hand, M., and Laxson, A., 2006, "Wind Turbine Design Cost and Scaling Model," Technical Report: NREL/TP-500-40566, National Renewable Energy Laboratory.

[13] Kost, C., Schlegl, T., Thomsen, J., Nold, S., and Mayer, J., 2012, "Study Levelized Cost of Electricity Renewable Energies," Fraunhofer ISE, availble at http://www.ise.fraunhofer.de/en/publications/veroeffentlichungen-pdf-dateien-en/studien-und-konzeptpapiere/study-levelized-cost-of-electricity-renewable-energies.pdf, accessed on Oct. 28 2013.

[14] Wind Energy TechnoCentre, 2011, "Wind Farm Development Stages," available at http://www.eolien.qc.ca/?id=32&titre=Wind_farm_development_stages&em=6387, accessed on Jan. 5 2013.

[15] Pedersen, E., and PerssonWaye, K., 2008, "Wind Turbines-Low Level Noise Sources Interfering with Restoration?," *Environmental Research Letters*, 3(2008), pp. 015002 - 015005.

[16] Laumann, K., Gärling, T., and Stormark, K., "Selective Attention and Heart Rate Responses to Natural and Urban Environments," *Journal of Environmental Psychology*, 23(2), pp. 125-134.

[17] Hartig, T., and Staats, H., 2003, "Guest Editors' Introduction: Restorative Environments," *Journal of Environmental Psychology*, 23(2), pp. 103-107.

[18] Wallenius, M., 2004, "The Interaction of Noise Stress and Personal Project Stress on Subjective Health," *Journal of Environmental Psychology*, 24(2), pp. 167-177.

[19] Ambrose, S., and Rand, R., 2013, "Wind Turbine Noise Complaint Predictions Made Easy," available at http://www.windaction.org/documents/37241, accessed on Oct. 28 2013.

[20] The Associated Press, 2013, "Oregon Man Files $5 Million Suit over Wind Farm Noise," available at http://www.oregonlive.com/pacific-northwest-news/index.ssf/2013/08/post_133.html, accessed on Oct. 28 2013.

[21] Pedersen, E., and Waye, K., 2007, "Wind Turbine Noise, Annoyance and Self-Reported Health and Well-Being in Different Living Environments," *Occupational and Environmental Medicine*, 64(7), pp. 480-486.

[22] DuPont, B., and Cagan, J., 2012, "An Extended Pattern Search Approach to Wind Farm Layout Optimization," *Journal of Mechanical Design*, 134(8), pp. 081002-081018.

[23] Mosetti, G., Poloni, C., and Diviacco, B., 1994, "Optimization of Wind Turbine Positioning in Large Windfarms by Means of a Genetic Algorithm," *Journal of Wind Engineering and Industrial Aerodynamics*, 51(1), pp. 105-116.

[24] Grady, S., Hussaini, M., and Abdulah, M., 2005, "Placement of Wind Turbines using Genetic Algorithms," *Renewable Energy*, 30(2), pp. 259-270.

[25] Şişbot, S., Turgut, Ö., Tunç, M., and Çamdalı, Ü., 2010, "Optimal Positioning of Wind Turbines on Gökçeada using Multi-Objective Genetic Algorithm," *Wind Energy*, 13(4), pp. 297-306.

[26] Wang, F., Liu, D., and Zeng, L., 2009, "Study on Computational Grids in Placement of Wind Turbines Using Genetic Algorithm," World Non-Grid-Connected Wind Power and Energy Conference Proceedings, Sep. 24-26, 2009, Nanjing, China.

[27] Bilbao, M., and Alba, E., 2009, "GA and PSO Applied to Wind Energy Optimization," CACIC Conference Proceedings, Jujuy, Argentina.

[28] Bilbao, M., and Alba, E., "Simulated Annealing for Optimization of Wind Farm Annual Profit,"2nd International Symposium on Logistics and Industrial Informatics , Linz, Austria .

[29] Ozturk, U., and Norman, B., 2004, "Heuristic Methods for Wind Energy Conversion System Positioning," *Electric Power Systems Research*, 70(3), pp. 179-185.

[30] Marmidis, G., Lazarou, S., and Pyrgioti, E., 2008, "Optimal Placement of Wind Turbines in a Wind Park using Monte Carlo Simulation," *Renewable Energy*, 33(7), pp. 1455-1460.

[31] Samorani, M., 2010, "The Wind Farm Layout Optimization Problem," Technical Report, Leeds School of Business, University of Colorado at Boudler.

[32] Chowdhury, S.,Messac, A., Zhang, J., Castillo, L., and Lebron, J. ., 2010, "Optimizing the Unrestricted Placement of Turbines of Differing Rotor Diameters in a Wind Farm for Maximum Power Generation," ASME IDETC Conference Proceedings, Montreal, Canada.

[33] Frandsen, S., 1991, "Uncertainty On Wind Turbine Power Curve Measurements," *Wind Energy Conversion*, pp. 169-174.

[34] Ravey, I., and Derrick, A., 1995, "Investigations into the Use of Site Calibration to Reduce the Uncertainty in Power Performance Verification of Wind Turbines in Complex Terrain," *Wind Energy Conversion*, pp. 179-182.

[35] Kwon, S., 2010, "Uncertainty Analysis of Wind Energy Potential Assessment," *Applied Energy*, 87(3), p. 856.

[36] Messac, A., Chowdhury, S., and Zhang, J., 2012, "Characterizing and Mitigating the Wind Resouce-based Uncertainty in Farm Performance," *Journal of Turbulence*, 13(13), pp. 1-26.

[37] DuPont, B., Cagan, J., and Moriarty, P., 2012, "Optimization of Wind Farm Layout and Wind Turbine Geometry Using a Multi-Level Extended Pattern Search Algorithm that Accounts for Variation in Wind Shear Profile Shape," ASME 2012 International Design Engineering Technical Conferences & Computers and Information in Engineering Conference, August 12-15, Chicago, IL, USA.

[38] Veers, P., 1996, "Fatigue Reliability of Wind Turbine Fleets: The Effect of Uncertainty on Projected Costs," *Journal of Solar Energy Engineering*, 118(4), p. 222.

[39] Walford, C., 2006, "Wind Turbine Reliability: Understanding and Minimizing Wind Turbine Operation and Maintenance Costs," SANDIA Report, SAND2006-1100.

[40] Veers, P., 1995, "All Wind Farm Uncertainty is Not the Same: the Economics of Common Versus Independent Causes," Proc. Windpower 95, AWEA.

[41] Friedman, P., 2010, "Evaluating Economic Uncertainty of Municipal Wind Turbine Projects," *Renewable Energy*, 35(2), p. 484.

[42] Gomez-Quiles, C., 2011, "Price and Resource-Related Uncertainty in the Estimation of the Revenue of a Wind Farm," *IEEE Transactions on Power Systems*, 26(4), pp. 2074-2083.

[43] Usaola, J., and Angarita, J., "Bidding Wind Energy Under Uncertainty," Proc. International Conference on Clean Electrical Power, pp. 754-759.

[44] Pinson, P., Chevallier, C., and Kariniotakis, G., 2007, "Trading Wind Generation From Short-Term Probabilistic Forecasts of Wind Power," IEEE *Transactions* on Power Systems, 22(3), p. 1148.

[45] Sloth, C., Esbensen, T., Niss, M., Stoustrup, J., and Odgaard, P., "Robust LMI-Based Control of Wind Turbines with Parametric Uncertainties," Proc. Control Applications, (CCA) & Intelligent Control, (ISIC), 2009 IEEE, pp. 776-781.

[46] Guo, Y., Hosseini, S., Jiang, J., Tang, C., and Ramakumar, R., 2012, "Voltage/Pitch Control for Maximisation and Regulation of Active/Reactive Powers in Wind Turbines with Uncertainties," IET Renewable Power Generation, 6(2), p. 99.

[47] Luo, C., Banakar, H., Shen, B., and Ooi, B., 2007, "Strategies to Smooth Wind Power Fluctuations of Wind Turbine Generator," *IEEE Transactions on Energy Conversion*, 22(2), p. 341.

[48] Saranyasoontorn, K., and Manuel, L., 2008, "On the Propagation of Uncertainty in Inflow Turbulence to Wind Turbine Loads," *Journal of Wind Engineering and Industrial Aerodynamics*, 96(5), p. 503.

[49] Ju, Y., and Zhang, C., 2012, "Multi-Point Robust Design Optimization of Wind Turbine Airfoil Under Geometric Uncertainty," *Proceedings - Institution of Mechanical Engineers*, 226(2), p. 245.

[50] Karki, R., and Billinton, R., 2004, "Cost-Effective Wind Energy Utilization for Reliable Power Supply," *IEEE Transactions on Energy Conversion*, 19(2), p. 435.

[51] Usaola, J., 2009, "Probabilistic Load Flow with Wind Production Uncertainty Using Cumulants and Cornish–Fisher Expansion," *International Journal of Electrical Power & Energy Systems*, 31(9), p. 474.

[52] Ruiz, P., Philbrick, C., and Sauer, P., 2009, "Wind Power Day-Ahead Uncertainty Management Through Stochastic Unit Commitment Policies," Proc. Power Systems Conference and Exposition, pp. 1-9.

[53] Toh, G., and Gooi, H., 2011, "Incorporating Forecast Uncertainties into EENS for Wind Turbine Studies," *Electric Power Systems Research*, 81(2), pp. 430-439.

[54] Yu, H., Chung, C., Wong, K., and Zhang, J., 2009, "A Chance Constrained Transmission Network Expansion Planning Method with Consideration of Load and Wind Farm Uncertainties," *IEEE Transactions on Power Systems*, 24(3), p. 1568.

[55] Moehrlen, C., 2004, "Uncertainty in Wind Energy Forecasting," PhD thesis, University College Cork.

[56] Lange, M., 2005, "On the Uncertainty of Wind Power Predictions---Analysis of the Forecast Accuracy and Statistical Distribution of Errors," *Journal of Solar Energy Engineering*, 127(2), pp. 177-184.

[57] Venetsanos, K., Angelopoulou, P., and Tsoutsos, T., 2002, "Renewable Energy Sources Project Appraisal Under Uncertainty: the Case of Wind Energy Exploitation within a Changing Energy Market Environment," *Energy Policy*, 30(4), p. 293.

[58] Grady, S., Hussaini, M., and Abdullah, M., 2005, "Placement of Wind Turbines Using Genetic Algorithms," *Renewable Energy*, 30(2), pp. 259-270.

[59] Bilbao, M., and Alba, E., 2009, "GA and PSO Applied to Wind Energy Optimization," CACIC Conference Proceedings, Oct. 5-9, 2009, Jujuy, Argentina.

[60] Marmidis, G., Lazarou, S., and Pyrgioti, E., 2008, "Optimal Placement of Wind Turbines in a Wind Park Using Monte Carlo Simulation," *Renewable Energy*, 33(7), pp. 1455-1460.

[61] González, J., Rodríguez, A., Mora, J., Santos, J., and Payán, M., 2010, "Optimization of Wind Farm Turbines Layout Using an Evolutive Algorithm," *Renewable Energy*, 35 (2010), pp. 1671-1681.

[62] Zhang, J., Chowdhury, S., Messac, A., Castillo, L., and Lebron, J., 2010, "Response Surface Based Cost Model for Onshore Wind Farms Using Extended Radial Basis Functions," ASME 2010 International Design Engineering Technical Conference, Montreal, Canada.

[63] Tegen, S., Hand, M., Maples, B., Lantz, E., Schwabe, P., and Smith, A., 2012, "2010 Cost of Wind Energy Review," Technical Report: NREL/TP-5000-52920, National Renewable Energy Laboratory.

[64] Jensen, N., 1983, "A Note on Wind Generator Interaction," Risø National Laboratory, DK-4000 Roskilde, Denmark.

[65] Elkinton, C., Manwell, J., and McGowan, J., 2006, "Offshore Wind Farm Layout Optimization (OWFLO) Project: Priliminary Results," 44th AIAA Aerospace Sciences Meeting and Exhibit, AIAA, Reno, Nevada, USA.

[66] Mikkelsen, R., Sørensen, J., Øye, S., and Troldborg, N., 2007, "Analysis of Power Enhancement for a Row of Wind Turbines Using the Actuator Line Technique," *Journal of Physics: Conference Series*, 75 (2007), p. 012044.

[67] Barthelmie, J., Folkerts, L., Rados, K., Larsen, C., Pryor, C., Frandsen, T., Lange, B., and Schepers, G., 2006, "Comparison of wake model simulations with offshore wind turbine wake profiles measured by sodar," *Journal of Atmospheric and Oceanic Technology*, 23, pp. 888–901.

[68] Barthelmie, J., Rathmann, O., Frandsen, T., Hansen, K., Politis, E., Prospathopoulos, J., Rados, K., Cabezón, D., Schlez, W., Phillips, J., Neubert, A., Schepers, G., and van der Pijl, P., 2007, "Modelling and Measurements of Wakes in Large Wind Farms," *Journal of Physics*: Conference Series 2007, 75, p. 012049.

[69] Gaumond, M., Réthoré, P.-E., Bechmann, A., Ott, S., Larsen, G. C., Pena Diaz, A., and Hansen, K. S., 2013, "Benchmarking of Wind Turbine Wake Models in Large Offshore Wind Farms. available at: http://www.eera-dtoc.eu/wp-content/uploads/files/Gaumond-et-al-Benchmarking-of-wind-turbine-wake-models-in-large-offshore-wind-farms.pdf, accessed on Oct. 28, 2013.

[70] Chen, L., and MacDonald, E., 2012, "Considering Landowner Participation in Wind Farm Layout Optimization," Journal of Mechanical Design, 134(8), pp. 084506-084506.

[71] Bilbao, M., and Alba, E., "Simulated Annealing for Optimization of Wind Farm Annual Profit," Proc. 2nd International Symposium on Logistics and Industrial Informatics, Sep. 10-12, 2009, Linz, Austria.

[72] Lantz, E., Wiser, R., and Hand, M., 2012, "IEA Wind Task 26: The Past And Future Cost Of Wind Energy," Technical Report: NREL/TP-6A20-53510, National Renewable Energy Laboratory.

[73] Zhang, J., Chowdhury, S., Messac, A., and Castillo, L., 2011, "Multivariate and Multimodal Wind Distribution Model Based on Kernel Density Estimation," ASME 2011 5th International Conference on Energy SustainabilityWashington, DC, USA.

[74] Erdem, E., Shi, J., 2011, "Comparison of Bivariate Distribution Construction Approaches for Analysing Wind Speed and Direction Data," *Wind Energy*, 14 (2011), pp. 27-41.

[75] Morgan, E., Lackner, M., Vogel, R., and Baise, L., 2011, "Probability Distributions for Offshore Wind Speeds," *Energy Conversion and Management*, 52 (2011), pp. 15-26.

[76] Carta, J., Ramı´rez, P., and Vela´zquez, S., 2009, "A Review of Wind Speed Probability Distributions Used in Wind Energy Analysis Case Studies in the Canary Islands," *Renewable and Sustainable Energy Reviews*, 13 (2009), pp. 933-955.

[77] Lackner, M., and Elkinton, C., 2007, "An Analytical Framework for Offshore Wind Farm Layout Optimizaiton," *Wind Engineering* 31(1), pp. 17-31.

[78] Kusiak, A., and Song, Z., 2010, "Design of Wind Farm Layout for Maximum Wind Energy Capture," *Renewable Energy*, 35(3), pp. 685-694.

[79] Ozturk, A., and Norman, B., 2004, "Heuristic Methods for Wind Energy Conversion System Positioning," *Electric Power Systems Research*, 70(3), pp. 179-185.

[80] Şişbot, S., Turgut, Ö., Tunç, M., and Çamdalı, Ü., 2010, "Optimal Positioning of Wind Turbines on Gökçeada Using Multi-objective Genetic Algorithm," *Wind Energy*, 13(4), pp. 297-306.

[81] Nikolaidis, E., Mourelatos, Z., and Pandey, V., 2011, *Design Decisions under Uncertainty with Limited Information*, CRC Press/Balkema, Leiden, The Netherlands.

[82] Giunta, A., Eldred, M., Swiler, L., Trucano, T., and Wojtkiewicz, S., 2004, "Perspectives on Optimization under Uncertainty: Algorithms and Applications," 10th AIAA/ISSMO Multidisciplinary Analysis and Optimization Conference, Albany, New York.

[83] Yao, W., Chen, X., Luo, W., Tooren, M., and Guo, J., 2011, "Review of Uncertainty-based Multidisciplinary Design Optimization Methods for Aerospace Vehicles," *Progress in Aerospace Science*, 47, pp. 450-479.

[84] Du, X., and Chen, W., 2004, "Sequential Optimization and Reliability Assessment Method for Efficient Probabilistic Design," *Journal of Mechanical Design*, 126, pp. 225-233.

[85] Du, X., and Chen, W., 2002, "Efficient Uncertainty Analysis Methods for Multidisciplinary Robust Design," *AIAA Journal*, 40(3), pp. 545-552.

[86] Du, X., Sudjianto, A., and Chen, W., 2004, "An Integrated Framework for Optimization Under Uncertainty Using Inverse Reliability Strategy," *Journal of Mechanical Design*, 126, pp. 562-570.

[87] Phadke, M., 1989, *Quality Engineering using Robust Design*, Prentice Hall, Englewood Cliffs, New Jersey.

[88] Chen, W., Allen, J., Mistree, F., and Tsui, K., 1996, "A Procedure for Robust Design: Minimizing Variations Caused by Noise Factors and Control Factors," *Journal of Mechanical Design*, 118(4), pp. 478-485.

[89] Howard, R., 1988, "Decision Analysis: Practice and Promise," *Management Science* 34(6), pp. 679-695.

[90] Du, X., and Chen, W., 2001, "A Most Probable Point Based Method for Uncertainty Analysis," *Journal of Design and Manufacturing Automation*, 4(1), pp. 47-66.

[91] Jin, Y., and Branke, J., 2005, "Evolutionary Optimization in Uncertain Environments-A Survey," IEEE Transactions on Eevolutionary Computation, 9(3), pp. 303-317.

[92] Diwekar, U., 2008, "Optimization Under Uncertainty," *Introduction to Applied Optimization*, Springer, New York, USA, pp. 1-54.

[93] Helton, J., and Davis, F., 2003, "Latin Hypercube Sampling and the Propagation of Uncertainty in Analyses of Complex Systems," Reliability Engineering and Systems Safety, 81(1), pp. 23-69.

[94] Helton, J., Johnson, J., Sallaberry, C., and Storlie, C., 2006, "Survey of Sampling-based Methods for Uncertainty and Sensitivity Analysis," *Reliability Engineering and System Safety*, 91(10), pp. 1175-1209.

[95] Fishburn, P., 1968, "Utility Theory," *Management Science*, 14(5), pp. 335-378.

[96] Slovic, P., 1995, "The Construction of Preference," *American Psychologist*, 50(5), pp. 364-371.

[97] Bentham, J., 1879, *An Introduction to the Principles of Morals and Legislation*, Clarendon Press.

[98] Tversky, A., and Kahneman, D., 1991, "Loss Aversion in Riskless Choice: A Reference-Dependent Model," *Quarterly Journal of Economics*, 106(4), pp. 1039–1061.

[99] Bateman, L., Munro, A., Rhodes, B., Starmer, C., and Sugden, R., 1997, "A Test of the Theory of Reference-Dependent Preferences," *The Quarterly Journal of Economics*, 112(2), pp. 479-505.

[100] MacDonald, E., 2008, "The Construction of Preference in Engineering Design and Implications for Green Products," Ph.D thesis, University of Michigan, Ann Arbor.

[101] Hess, S., Rose, J., and Hensher, D., 2008, "Asymmetric Preference Formation in Willingness to Pay Estimates in Discrete Choice Models," *Transportation Research Part E*, 44(5), pp. 847-863.

[102] Loomis, J., Peterson, G., Champ, P., Brown, T., and Lucero, B., 1998, "Paired Comparison Estimates of Willingness to Accept Versus Contingent Valuation Estimates of Willingness to Pay," *Journal of Economic Behavior & Organiza*tion, 35, pp. 501-515.

[103] List, J., and Shogren, J., 2002, "Calibration of Willingness-to-Accept," *Journal of Environmental Economics and Management*, 43, pp. 219-233.

[104] Horowitz, J., and McConnell, K., 2002, "A Review of WTA/WTP Studies," *Journal of Environmental Economics and Management*, 44, pp. 426-447.

[105] Thaler, R., 1980, "Toward a Positive Theory of Consumer Choice," *Journal of Economic Behavior and Organization*, I (1980), pp. 39-60.

[106] Wickens, C. D., 2004, An introduction to human factors engineering.

[107] Kahle, C., 2009, "Average Size of Farms by County, Years 1890 to 1997," Census of Agriculture, National Agricultural Statistics Service, U.S. Department of Agriculture. available at http://www.recap.iastate.edu/atlas/farms/average-farm-size.php, accessed in 2009.

[108] Thørgersen, M., Sørensen, T., Nielsen, P., Grötzner, A., and Chun, S., 2005, "WindPRO/PARK: Introduction to Wind Turbine Wake Modelling and Wake Generated Turbulence," EMD International A/S, Aalborg, Denmark.

[109] Archer, C., and Jacobson, M., 2007, "Supplying Baseload Power and Reducing Transmission Requirements by Interconnecting Wind Farms," *Journal of Applied Meteorology and Climatology*, 46(11), pp. 1701-1717.

[110] McCracken, M., 2005, "Levelized Cost." available at http://www.teachmefinance.com/Scientific_Terms/Levelized_cost.html, accessed on Oct. 28, 2013.

[111] Bolinger, M., and Wiser, R., 2011, "Understanding Trends in Wind Turbine Prices Over the Past Decade," LBNL-5119E, Lawrence Berkeley National Laboratory.

[112] Bureau of Labor Statistics, 2012, "Producer Price Indexes,"available at http://www.bls.gov/ppi/, accessed on Oct. 28, 2013.

[113] NASA, 2012, "Gross Domestic Product Deflator Inflation Calculator,"available at http://cost.jsc.nasa.gov/inflateGDP.html, accessed in 2012.

[114] Wall, M., 1999, "GAlib: a C++ Library for Genetic Algorithm Components," Massachusetts Institute of Technology, available at http://lancet.mit.edu/ga/Copyright.html, accessed on Oct. 28, 2013.

[115] Houck, C., Joines, J., and Kay, M., 1995, "A Genetic Algorithm for Function Optimization: a Matlab Implementation," Technical Report: NCSU-IE-TR-95- 09, North Carolina State University, Raleigh, NC.

[116] Davis, L., 1991, *Handbook of Genetic Algorithms*, Van Nostrand Reinhold Co., New York, NY.

[117] Vanderplaats, G., 1984, *Numerical Optimization Techniques for Engineering Design: with Applications*, McGraw-Hill College, New York, NY.

[118] Chen, L., and MacDonald, E., 2014, "A System-level Cost-of-Energy Wind Farm Layout Optimization with Landowner Modeling," *Energy Conversion and Management,* 77, pp. 484-494.

[119] Windustry, 2009, "Wind Energy Easement and Leases: Compensation Packages," Windustry Wind Easement Work Group, available at http://saline.unl.edu/c/document_library/get_file?folderId=294039&name=DLFE-18538.pdf, accessed on Oct. 28, 2013.

[120] Khalfallah, M., and Koliub, A., 2007, "Wind Turbines Power Curve Variability," *Desalination*, 209(1), pp. 230-237.

[121] Ray, M., Rogers, A., and McGowan, J., 2006, "Analysis of Wind Shear Models and Trends in Different Terrain," Conference Proceeding: American Wind Energy Association Windpower, Pittsburgh, PA, June 2-7, 2006.

[122] Elliott, D., Schwartz, M., and Scott, G., 2008, "Wind Shear and Resources at Elevated Heights: Indiana and Iowa Case Studies," National Renewable Energy Laboratory, NREL/PO-500-43150.

[123] Eschenbach, T., 1992, "Spiderplots versus Tornado Diagrams for Sensitivity Analysis," *Interfaces*, 22(6), pp. 40-46.

[124] Wikipedia, 2013, "Story County Wind Farm," available at http://en.wikipedia.org/wiki/Story_County_Wind_Farm, accessed on Oct. 28, 2013.

[125] Denholm, P., Hand, M., Jackson, M., and Ong, S., 2009, "Land-Use Requirements of Modern Wind Power Plants in the United States," Technical Report NREL/TP-612-45834.

[126] Takle, E., and Lundquist, J., 2011, "Research Experience for Undergraduates: Crop-Wind-Energy-Experiment (C-WEX)," available at

http://www.eol.ucar.edu/system/files/files/field_project/CWEX/CWEX_Facility_Request.pdf, accessed on Oct. 28, 2013.

[127] Iowa Environmental Mesonet, 2013, "ASOS/AWOS Data Download," Iowa State University Department of Agronomy, available at http://mesonet.agron.iastate.edu/request/download.phtml?network=IA_ASOS, accessed on Oct. 28, 2013.

[128] Iowa Environmental Mesonet, 2013, "Custom Wind Roses," Iowa State University Department of Agronomy, available at http://mesonet.agron.iastate.edu/sites/dyn_windrose.phtml?station=AMW&network=IA_ASOS, accessed on Oct. 28, 2013.

[129] Matala, A., 2008, "Sample Size Requirement for Monte Carlo - Simulations using Latin Hypercube Sampling,"Helsinki University of Technology, Department of Engineering Physics and Mathematics, Systems Analysis Laboratory, Mat-2.4108 Independent Research Projects in Applied Mathematics.

[130] Marler, R., and Arora, J., 2004, "Survey of Multi-objective Optimization Methods for Engineering," *Structural and Multidisciplinary Optimization*, 26, pp. 369-395.

[131] Chen, W., Wiecek, M., and Zhang, J., 1999, "Quality Utility - A Compromise Programming Approach to Robust Design," *Journal of Mechanical Design*, 121(2), pp. 179-187.

[132] Erbas, S., and Erbas, C., 2003, "A Multiobjective Off-line Routing Model for MPLS Networks," Proc. The 18th International Teletraffic Congress (ITC-18). Elsevier, Amsterdam, pp. 471–480.

[133] Mosman, K., "Wind Farm A Good Neighbor?" available at http://www.windaction.org/posts/30655-wind-farm-a-good-neighbor#.Um8qmxDFaN4 , accessed on Oct. 28, 2013.

[134] Muschell, K., 2013, "BP Good Neighbor Recruiting Letter," available at http://pandorasboxofrocks.blogspot.com/2013/01/bp-good-neighbor-recruitment-letter.html, accessed on Oct. 28, 2013.

[135] Fagerfjäll, P., 2010, "Optimizing Wind Farm Layout: More Bang for the Buck Using Mixed Integer Linear Programming," *Chalmers University of Technology and Gothenburg University*.

[136] Kwong, W., Zhang, P., Romero, D., Moran, J., Morgenroth, M., and Amon, C., 2012, "Multi-objective Optimization of Wind Farm Layouts under Energy Generation and Noise Propagation," ASME 2012 International Design Engineering Technical Conferences & Computers and Information in Engineering Conference, Chicago.

[137] ISO 9613-2, 1996, "Acoustics – Attenuation of sound during propagation outdoors – Part 2: General method of calculation."

[138] Windustry, 2013, "Why Wind Energy," available at http://www.windustry.org/wind-basics/why-wind-energy, accessed on Oct. 28, 2013.

[139] Arvidsson, J., and Håkansson, I., 1991, "A Model for Estimating Crop Yield Losses Caused by Soil Compaction," *Soil & Tillage Rese*arch, 20(2), p. 319.

[140] Johnson, S., 2011, "2012 Crop Input Costs Increase, Along With Profit Margin Opportunities," AgDM Newsletter, available at http://www.extension.iastate.edu/agdm/articles/others/JohSept11.html, accessed on Oct. 28, 2013.